The petrological evolution of the Late Paleozoic A-type granites of the

Wentworth plutonic complex of the Cobequid Shear Zone

By

Angeliki Papoutsa

A thesis Submitted to
Saint Mary's University, Halifax, Nova Scotia
in Partial Fulfillment of the Requirements for
the Degree of Masters in Applied Science

December, 2011, Halifax, Nova Scotia

© Angeliki Papoutsa, 2011

Approved _____

Dr Georgia Pe-Piper

Professor

Approved _____

Dr Trevor MacHattie

Department of Natural Resourses

Approved _____

Dr Victor Owen

Professor

Approved _____

Dr David Piper

Geological Survey of Canada

Approved _____

Dr Cristian Suteanu

Professor

Approved _____

Dr Brendan Murphy

Professor

Date December 12, 2011

Library and Archives
Canada

Published Heritage
Branch

395 Wellington Street
Ottawa ON K1A 0N4
Canada

Bibliothèque et
Archives Canada

Direction du
Patrimoine de l'édition

395, rue Wellington
Ottawa ON K1A 0N4
Canada

Canada

TABLE OF CONTENTS

The petrological evolution of the Late Paleozoic A-type granites of the Wentworth
plutonic complex of the Cobequid Shear Zone

By

Angeliki Papoutsa

Abstract

The Wentworth Pluton is a bimodal intrusion which consists principally of a 362 Ma, A-type granite, part of which was remelted by a major gabbro intrusion, resulting in the formation of late granites REE- rare metal mineralization is widespread in and around the Wentworth Pluton The Wentworth granites were examined geochemically and petrographically in order to determine the geological processes responsible for their distinct geochemistry The granites were derived from partial melting of subduction-related trondhjemites, in the lower Avalonian crust, triggered by asthenospheric upwelling in the Late Paleozoic The parent, REE-enriched magma formed early granites with REE-magmatic minerals Anatexis of these granites resulted in the release of volatiles and rare metals in hydrothermal fluids, reflected by a variety of hydrothermal REE-rich minerals This study has introduced new evidence on the petrogenesis of A-type granites and demonstrated the genetic relationship between the REE mineralization and the granites of the Wentworth Pluton

December 12, 2011

ACKNOWLEDGEMENTS

I would like to start by thanking my supervisor Georgia Pe-Piper and David Piper for having me here in Canada and providing me with such an interesting project It was my privilege to have them as my mentors these two years, not only for their significant academic guidance but also for their dedicated care and support I'm very thankful to them for developing my scientific thought and expanding my horizons in igneous petrology

I would like to express my gratitude to Dr Victor Owen, Dr Trevor MacHattie and Dr Cristian Suteanu, members of my supervisory committee, for their informative conversations, and for the time they spent editing this thesis Sincere thanks to Dr Brendan Murphy for acting as my external examiner, and for his significant contribution to the improvement of this thesis

Thank you to Randolph Corney, for all the times I asked for your help and you provided with no complaint A special thanks to Dr Vassilis Tsikouras for introducing me to Georgia Pe-Piper, who he spoke very highly of, and for all his support during the time I had to make the decision to leave Greece For his friendship and continuous guidance since I got involved with geology, I am most grateful

To all my friends I met in Canada, I feel blessed to be surrounded by people like you Finally, I would like to thank my mother, for her support and for all the time she spent keeping me company on weekends while I was locating grains under the microscope Thanks for sharing my enthusiasm for geology and even though you didn't want me to leave, you let me come here to Canada and study the subject that I love the most

List of abbreviations

Abbreviation	Description
A1	rift-related anorogenic granites
A2	arc-related anorogenic granites
Aes-Y	Aeschynite-(Y)
AFM diagram	Alkalies-FeO-MgO diagram
Aln	Allanite
Amp	Amphibole
Ap	Apatite
Arf	Arfvedsonite
ASI	Aluminum Saturation Index
BSE image	Back Scattered Electron image
Bt	Biotite
c	calcic
CAG	Continental Arc granites
CCG	Continental Collision granites
CEUG	Continental Epeirogenic Uplift granites
Che	Chevkinite
Chl	Chlorite
CHUR	Chondritic Uniform Reservoir
cpx	Clinopyroxene
EDS	Energy Dispersive Spectroscopy
EMP	Electron Microprobe
Ep	Epidote
Fed	Ferro-edenite
Fers	Fersmite
Fl	Fluorite
Fsp	Feldspar
Fwn	Ferro-winchite
gbr	gabbro
H-bas	Hydroxylbastnasite
Hbl	Hornblende
HDEHP	Bis (2-ethylhexyl) phosphoric acid
Hem	Hematite
Hing	Hingganite
HLBL	Hart Lake-Byers Lake
HREE	Heavy Rare Earth Elements
IAG	Island Arc Granites
ICP-MS	Ion Coupled Plasma Mass Spectrometer
Ilm	Ilmenite
INAA	Instrumental Neutron Activation Analysi
Ktf	Katophorite

List of abbreviations

LIF	Lithium Fluoride crystal
LIFH	Lithium Fluoride- high intensity crystal
LP	Late Paleozoic
LREE	Light Rare Earth Elements
MALI	Modified alkali-lime index
Mgt	Magnetite
Nb-min	Niobium mineral
NP	Neoproterozoic
ORG	Orogenic granites
Opq	Opaque mineral
PETJ	Polyethylene terephthalate high reflectivity crystal
Pl	Plagioclase
POG	Post-orogenic granites
Py	Pyrite
Qz	Quartz
Rbk	Riebeckite
Rc Fsp	Re-crystallized feldspar
REE	Rare Earth Elements
RRG	Rift related granites
s	sodic
Sam	Samarskite
sec	secondary mineral
SEM	Scanning Electron Microscope
s-c	sodic-calcic
Syn-COLG	Syn-collisional granites
TAP	Thallium acid phthallate crystal
TAPH	Thallium acid phthallate-high intensity crystal
TD-ICP	Total Digestion Ion Coupled Plasma
Tna	Titania mineral
Tnt	Titanite
Trt	Thorite
VAG	Volcanic Arc granites
WDS	Wavelength Dispersive Spectroscopy
WPG	Within-plate granites
XRF	X-Ray Fluoresence
Zrn	Zircon

CHAPTER 1: INTRODUCTION

1.1. Purpose of the study and objectives

The Wentworth Pluton is a complex bimodal intrusion, the felsic part of which consists of two generations of granites and is the most alkaline magmatic body, in a series of late Devonian to early Carboniferous plutons, related to the Cobequid Shear Zone. The petrology and geochemistry of the late plutons in the Cobequid Highlands has been thoroughly studied over the last few decades and the regional tectonic setting is well understood. However, it is still unclear why the Wentworth Pluton presents such a distinct geochemical character. The purpose of this study is to investigate this complicated magmatic system and identify the cause of the principal variations in the geochemistry of the late Devonian Wentworth granites. Some questions this research aims to answer are the following:

1) Do syn- or post-gabbro granites and early granites in the Wentworth pluton have the same source and geochemistry as each other? If not what are the geochemical processes that created the syn- and post-gabbro granites? Examine mechanisms of

   a) Anatexis of pre-existing granite at middle to upper crustal levels

   b) Chemical diffusion of elements between mafic and felsic magmas

   c) Mechanical mixing

   d) Continuation of lower crust melting

2) Within the observed geochemical variability, what are the implications for mineralization?

   a) Are there REE accessory minerals in the granites? Do they relate to the igneous system?

   b) How Th is distributed in the pluton and how does this relate to mineralization?

1

1.2 Thesis organization

The main body of this thesis consists of chapters 4 and 5 In chapter 4, the accessory minerals present in the Wentworth granites that contain rare earth elements and rare metals are investigated This study reveals that there are significant amounts of REEs in this intrusion, reflected in a wide variety of magmatic and hydrothermal mineral phases Significant evidence is provided from this study for several stages of REE-mineral crystallization/precipitation during the geological evolution of the granites and also illustrates the REE-rich nature of the original granitic magma from the presence of primary magmatic REE phases

Chapter 5 investigates the petrogenetic history of the Wentworth Pluton granites through their whole-rock geochemistry Specific geochemical characteristics and isotopic data from these rocks provide evidence about the origin and evolution of the granites In this study a petrogenetic model is proposed for the granites that suggests a possible source for the granitic magma and explains a) the REE enrichment of the original granitic magma, b) the distinct alkaline character of the intrusion reflected in the presence of sodic amphiboles, c) the geological processes responsible for certain geochemical differences between the early and late granites, and d) the implications of this model to the tectonic environment

Both chapters were prepared as separate manuscripts for publication Therefore it is unavoidable that some repetition of key figures and text occurs in this thesis, particularly in the introductory parts of these chapters since each one was written as to stand-alone

CHAPTER 2: REGIONAL GEOLOGY

2.1. Regional Setting

The Cobequid Highlands are located on the northern part of the Appalachian orogenic belt, just north of the boundary between the Avalon and Meguma terranes (Calder, 1998, Pe-Piper and Piper, 2002) This boundary is marked by the northern part of the Cobequid-Chedabucto fault zone, in which strike-slip motion took place during Late Paleozoic Distributed shear on this zone in Late Devonian and Early Carboniferous has been termed the Cobequid Shear Zone (Pe-Piper et al , 2002)

Within the Cobequid Highlands the Cobequid Shear zone consists of a series of faults The Cobequid Fault marks the margin of the Cobequid Highlands horst (Pe-Piper and Piper, 2002) The Rockland Brook Fault was the major fault during Late Paleozoic and is located in the eastern part of the Highlands whereas the Kirkhill Fault is in the western part and is considered to be an offset continuation of the Rockland Brook Fault (Koukouvelas et al , 2006) The northwestern margin of the Cobequid Highlands coincides with the Spicers Cove Fault (Pe-Piper and Piper, 2002)

The Cobequid Highlands are underlain by Neoproterozoic rocks, Silurian to Lower Devonian sedimentary rocks and Late Paleozoic plutons and their extrusive equivalents (Pe-Piper and Piper, 2002) The emplacement of the Late Paleozoic plutons is related to the development of Cobequid Shear Zone The plutons are mainly granite, gabbro and diorite bodies In the western Cobequid Highlands the plutons appear to be related to the Kirkhill and Cobequid Faults These intrusions are the Cape Chignecto, Hanna Farm, West Moose River and North River plutons (Pe-Piper and Piper, 2002) In

the eastern Cobequid Highlands the Late Paleozoic plutonism is represented by the Pleasant Hills, Wyvern-Gilbert Hills and Wentworth plutons

The intrusion of the Late Paleozoic plutons in the Cobequid Highlands is related to the extension of the Magdalen Basin, which led to the underplating of gabbroic melts beneath the central and eastern part of the highlands, during Middle to Late Devonian and Early Carboniferous (Marillier and Reid, 1990) The large volume of mafic rocks indicates that the extension of the basin played an important role in the pluton emplacement The intrusion of the plutons was synchronous with the deposition of the Horton Group (Piper et al , 1993, Dunning et al , 2002)

The igneous activity in the Cobequid Highlands during Latest Devonian (Strunian) to Early Carboniferous (Early Tournaisian) was focused along the Rockland Brook Fault and the Kirkhill Fault (Dunning et al , 2002) The mafic magmatism of Late Tournaisian to Early Visean resulted to the intrusion of mafic dykes which cut Horton Group near the Cobequid Fault

The Neoproterozoic rocks of the Avalon terrane evolved along the active margin of Gondwana and during the Middle Paleozoic were involved in Appalachian orogen (Nance et al , 2002) The evolution of the Avalon terrane is characterized by the development of an arc (760-650 Ma), its transition to a platform, rifting from Gondwana in early Ordovician, and the accretion of the Avalon terrane to Laurentia during the development of the Appalachian orogen in late Ordovician-early Silurian The evolution of the Avalonian arc took place upon a juvenile basement comprising mantle-derived material, the isotopic signature of which was inherited by successive generations of

4

magmas which represent a mixture of juvenile basement and Avalonian crust (Nance et al, 2002)

2.2 Geological setting of the Wentworth pluton

East of the Pleasant Hills and the Wyvern plutons lies the Wentworth plutonic complex (Fig 2-1) Pe-Piper (1998) introduced the term Wentworth Pluton to include the Folly Lake gabbro/diorite pluton in the southwestern part and the Hart Lake-Byers lake granite pluton of Donohoe and Wallace (1982), located in the northeastern part This was done because it is not possible to map them as two distinct units Rather there are extensive areas where the two rock units show mingling and cross-cutting relationships (Pe-Piper et al, 1997)

The southwestern Wentworth plutonic complex consists of gabbro–diorite cut by medium-grained granite in globular pods, irregular sheets, net-veined zones, and linear dykes, some of which are pegmatitic The northeastern part of the pluton narrows eastwards and consists principally of equigranular alkali granite which (Fig 2-1), passing to a kilometer-wide zone of Fountain Lake rhyolites (Koukouvelas et al, 2002, Pe-Piper and Piper, 2002) The gabbroic and granitic parts of the Wentworth pluton are separated by a zone in which granite and gabbro occur in sub-equal abundances (Koukouvelas et al, 2002, Pe-Piper, 2007)

The presence of mafic enclaves in the granites, with mixing and mingling textures at the contact with the granite, indicates that there was a period when the two magmas were immiscible (Koukouvelas et al, 2002) Furthermore, in the transition zone it is the granite that most commonly intrudes the gabbro, indicating that this late granite post-dates the gabbroic intrusion It is argued, by the presence of hybrid rocks, that the later

5
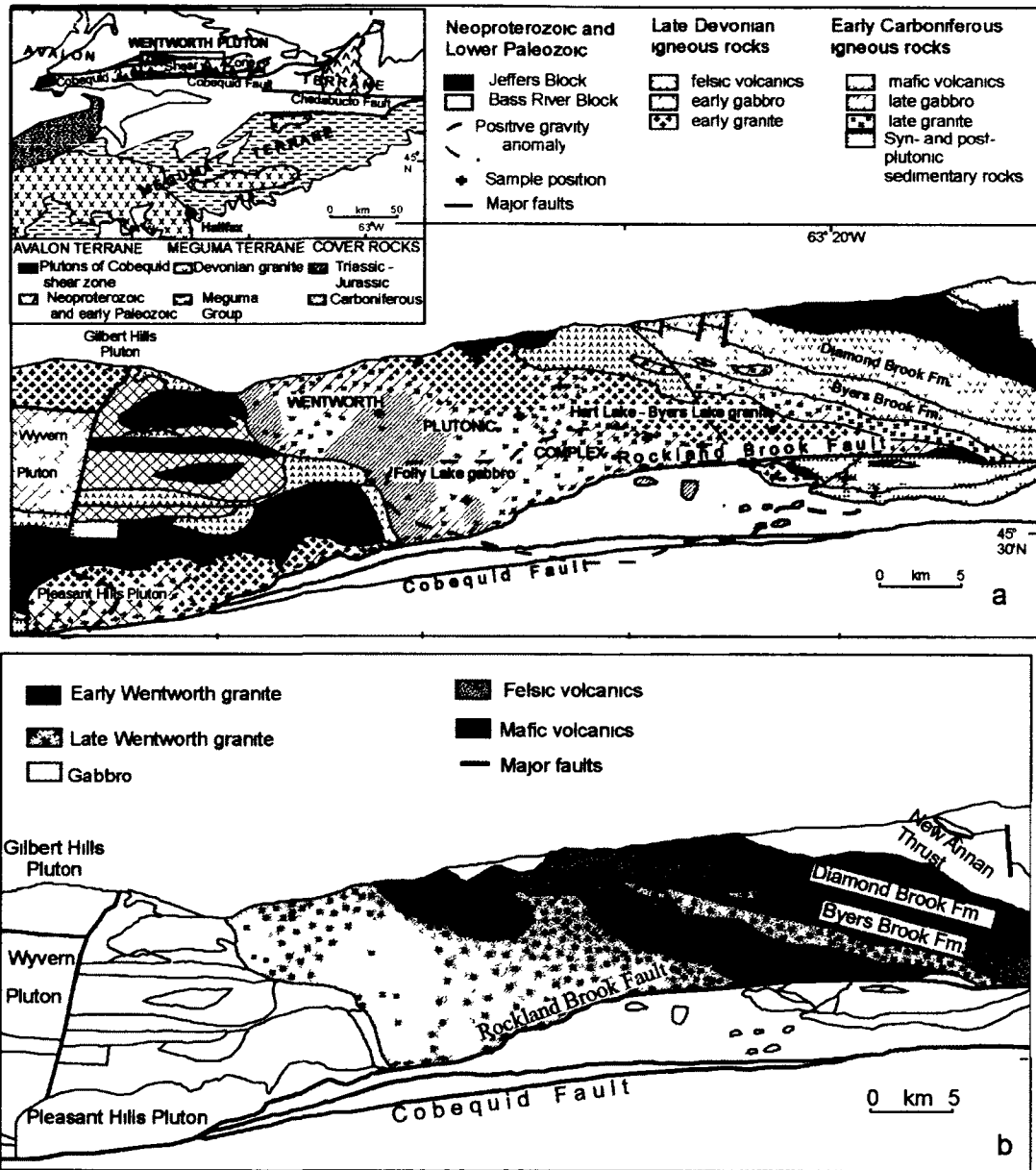
Figure 2-1 Detailed (a) and simplified (b) geological map of the late Paleozoic
Wentworth Pluton of the Cobequid Highlands Inset in map (a) shows the location of
Avalon and Meguma terranes

gabbroic magma remelted and assimilated parts of the early granite, resulting in the formation of the late granites with slightly different composition (Koukouvelas et al, 2002)

Field relationships show that the gabbro of the Wentworth pluton is younger than the main Cobequid shear zone plutons This is sustained by a 357±2Ma Ar-Ar (hornblende) age and two Ar-Ar biotite ages of 353±2 Ma and 355±2 Ma for this mafic intrusion (Pe-Piper et al, 2004) On the other hand, the granite yielded a 360-365 Ma U-Pb (zircon) age (Doig et al, 1996) and Ar-Ar (sodic- amphibole) age of 368±4 Ma (Pe-Piper et al, 2004) (Table 2-1) The original reported Ar-Ar ages of Pe-Piper et al (2004) have been corrected in this thesis for recent improvement in the intercalibration of U-Pb and Ar-Ar time scales (Kuiper et al, 2008) (Table 2-1)

2.3 Petrography and geochemistry of the Wentworth pluton

2.3.1. Gabbro

The Folly Lake gabbro of the Wentworth pluton is fine to coarse grained with subophitic texture and contains augite, plagioclase and amphibole as major minerals The augite grains are anhedral to subhedral and commonly rimmed with actinolite (Pe-Piper, 1998) Actinolite alteration of the pyroxene is variable The plagioclase crystals are euhedral to subhedral, appear zoned and moderately to strongly altered to clay minerals The amphibole is either hornblende or actinolite The hornblende, where present, occurs as anhedral to subhedral olive-green grains with biotite overgrowths and actinolite alteration around the edges Greenish-blue actinolite fine-grained aggregates, are also common in some types of gabbros These aggregates probably formed at the expense of hornblende, since hornblende relics can be seen in these aggregates Opaque minerals

7

consist of magnetite and pyrite while accessory minerals include apatite, titanite, biotite, zircon, quartz, chlorite and epidote (Pe-Piper, 1998)

Compositionally, the mafic rocks in the Wentworth plutonic complex possess composition which classifies them as ferro-gabbro (Koukouvelas et al, 2002) On an AFM diagram (after Irvine and Baragar, 1971), they plot in the Fe-rich and Mg-rich tholeiite field and the calc-alkaline field (Pe-Piper, 1998) The gabbros plot in the within plate basalt field of a TiO_2 vs Zr/P_2O_5 diagram (Floyd and Winchester, 1975), similar to the olivine-normative continental tholeiites of the West Moose River pluton (Pe-Piper, 1998, Pe-Piper et al, 1991)

2.3.2 Granite

The Hart Lake-Byers Lake granite of the Wentworth pluton consists mainly of medium grained alkali feldspar granite which contains 50-60% K-feldspar, biotite, amphibole, and quartz never less than 25% Some granites appear to be plagioclase-rich and relatively equigranular, while others contain at least 20% amphibole and are mostly medium to coarse grained (Pe-Piper, 1998)

The granite of the main phase of the Hart Lake-Byers Lake granite contains sodic amphibole, contains about 76% SiO_2, high F (> 500 ppm) , and moderate Li (>20 ppm) (Koukouvelas et al, 2002) A few granites, interpreted as synchronous with the gabbro have particularly high Zr contents (>500 ppm) Many of syn- and post-gabbro granites are alkalic, with >75 ppm Y Some granites that occur as pods within the gabbro are geochemically distinct, with a wide range of SiO_2 contents, relatively low Y, Zr, Li and F and the amphibole, where present, is hornblende Similar low-Y, low-Li granites occur within the Hart Lake–Byers Lake granite and have rather higher TiO_2 contents than the

8

alkali Hart Lake–Byers Lake granites of the main phase, with the same SiO_2 content (Koukouvelas et al, 2002)

2.4 Deformation associated with the emplacement of the Late Paleozoic plutons

The Late Paleozoic plutons of the Cobequid Highlands are bounded by major faults Structures within the plutons suggest that movement in the Cobequid Shear Zone played an important role in the pluton emplacement (Pe-Piper et al, 1998, Koukouvelas et al, 2002) The plutons adjacent to the Cobequid Shear Zone show vertical boundaries in map view, and in cross-section most plutons are generally southward dipping (Koukouvelas et al, 2006)

All Late Paleozoic plutons are asymmetric and developed within the north fault block of a component fault of the Cobequid Shear Zone Many of these plutons show evidence of ductile deformation, some of which is syn-magmatic (Pe-Piper et al, 1993) Within the plutons, steeply dipping foliation planes are found close to the plastic zone of the fault and moderately dipping foliation planes to the north (Koukouvelas et al, 2002) All plutons are defined by tectonic south-dipping contacts with the southern contact steeper that the northern (Koukouvelas et al, 1996) Structural data support intrusion by wedging, and many intrusive zones have been affected by sinistral strike-slip shear zones Internal lithological contacts are parallel to major faults

Syn-intrusion deformation, with foliated plutonic phases cut by less deformed phases, is largely restricted to two faults within the Cobequid Highlands, the Kirkhill fault in the west, and the Rockland Brook fault in the east (Koukouvelas et al, 2002) Ductile foliation in the fault zones is cut by brittle shears, principally along the Cobequid

9

Fault, which experienced major late Carboniferous dextral strike–slip motion (Murphy et al, 2011)

The Wentworth pluton is in direct contact with the Rockland Brook Fault at its southern margin Deformed granites and gabbros show evidence of deformation resulting from dextral shear (Miller et al, 1995) Rare sinistral kinematic indicators in the deformed portions of these plutons, reflect antithetic shearing, local folding, or complex ductile deformation within an overall dextral regime (Miller et al, 1995) Syn-magmatic deformation of the Wentworth pluton resulted in the development of small scale shear zones in the central and southern part of the pluton and most of which are dextral Syn-magmatic foliation is related to the finite flattening by the magma emplacement whereas the lineation relates to the finite stretching during this event (Koukouvelas et al, 2002) In contrast with the regional scale shear zones, the small scale ones are neither cross cut nor related to brittle faults (Koukouvelas et al, 2002) Wrench deformation along the contact between the early granites and the gabbros controlled a horizontal gabbroic magma flow reflected in areas of almost horizontal lineations north of the Folly Lake gabbro (Koukouvelas et al, 2002) The syn-magmatic foliation close to the southern boundary of the pluton dips southward almost parallel to the solid-state foliation of the Rockland Brook Fault Almost all major contacts of different units in the pluton were active faults The plutonic complex was compartmentalized into smaller blocks with faults parallel to the Rockland Brook Fault during the final stages of emplacement (Koukouvelas et al, 2002)

Table 2-1 Ages of rock units within the Wentworth Pluton

Rock Unit	Geochronology control	Original age	Corrected age*	Sample Position (UTM)		Reference
				Northing	Easting	
Wentworth granites						
	U-Pb (Zrn)	365		n a	n a	Doig et al , 1996
	U-Pb (Zrn)	361		n a	n a	Doig et al , 1996
	U-Pb (Zrn)	360		n a	n a	Doig et al , 1996
	U-Pb (Zrn)	364		n a	n a	Doig et al , 1996
	U-Pb (Zrn)	362		5048870	449984	Pe-Piper and Piper, 1998
	Ar-Ar (amph)	365	368	n a	n a	Pe-Piper et al , 2004
Wentworth gabbros						
	Ar-Ar (bt)	350	353	n a	n a	Pe-Piper et al , 2004
	Ar-Ar (hbl)	354	357	n a	n a	Pe-Piper et al , 2004
	Ar-Ar (bt)	352	355	n a	n a	Pe-Piper et al , 2004
	U-Pb (Zrn)	360		5044814	457020	Pe-Piper and Piper, 1998
	U-Pb (Zrn)	362		5044305	457394	Pe-Piper and Piper, 1998
Late dykes						
Late gabbro dyke	U-Pb (Zrn)	345		5043380	453375	Pe-Piper and Piper, 1998
Coeval volcanic rocks						
Upper Byers Brook rhyolites	U-Pb (Zrn)	358		5047821	474489	Dunning et al , 2002
Upper Diamond Brook Fm	U-Pb (Zrn)	354		5049804	470847	Pe-Piper and Piper, 1998
Mid-Diamond Brook Fm	U-Pb (Zrn)	354		5050458	470586	Dunning et al , 2002
Lower Diamond Brook Fm	U-Pb (Zrn)	350		5050749	470780	Pe-Piper and Piper, 1998

Notes Corrected ages (*) refer to all Ar-Ar ages as a result of new intercalibrations in Ar-Ar dating (Kuiper et al , 2008, Murphy et al , 2011)

CHAPTER 3: METHODOLOGY

The Cobequid Highlands have been studied and mapped for several years. In this study, the majority of the samples from the Wentworth Pluton are located in the 1 50000 scale geological maps of Pe-Piper and Piper (2005) and their geochemical data are reported in Pe-Piper (1998). The archived samples are located in Saint Mary's University and include, thin sections, polished thin sections, hand specimens, rock slabs and powders. Additional fieldwork was done for this thesis for certain areas of the Wentworth Pluton that were lacking sample representation.

The Wentworth Pluton includes mafic, intermediate and felsic rocks. Since the subject of this thesis is the petrological study of the granitoid rocks of the Wentworth pluton, only intermediate to felsic samples are included (SiO_2> 64%). These rocks, using archived field notebooks, were further classified into types based on their relative age according to field relations. A few granite outcrops in the northern part of the pluton have been dated at ~368 Ma (Doig et al , 1996, Pe-Piper et al , 2004). Similar uniform outcrops of granite cut by gabbro are considered to be part of the early granitic phase. Granites with lobate contacts with the gabbro and abundant mafic enclaves are taken as synchronous with the mafic intrusion. Bodies of granite that either cut the Wentworth gabbros or occur in it as globular pods or irregular sheets are considered to post-date the gabbroic intrusion. When field relations for a sample were sufficiently clear for its classification then the sample is characterized as a "definite" sample of one of the previous types. When the relative age of a sample was not clear from field relations in the same outcrop, but its age was assumed from the geology of nearby outcrops, then the sample is classified as a "probable" sample of a certain type.

12

3.1. Geochemical analyses

A total of 98 analytical samples were used for the purpose of this study The analytical samples were prepared for geochemical analyses in the Geology Department of Saint Mary's University The samples were first cut into slabs using a Contempo Lapidary 18-inch slab saw and they were trimmed using a Felker AR-40 trim saw to remove weathered surfaces The slabs were cut into chips of approximately 1 cm diameter, using a Wards hydraulic rock trimmer and then were washed with de-ionized water, using a 75-1970 Ultramet sonic cleaner to remove any loose contaminants The chips then were dried and pulverized, using a shatter box with an iron bowl at the Minerals Engineering Centre of Dalhousie University

All the major elements and certain trace elements (Ba, Rb, Sr, Y, Zr, Nb, Th, Pb, Ga, Zn, Cu, Ni, V, Cr and Co) of the analytical samples were determined by X-ray fluorescence analyses (XRF), whereas instrumental neutron activation analyses (INAA) were performed for the REEs and specific trace elements (Ba, Co, Cr, Cs, Hf, Sb, Sc, Ta, Th, and U) During this study 25 selected, previously analyzed, samples were sent for trace element analyses and 9 new samples were sent for complete whole-rock geochemical analyses The major and trace elements of the new analyses reported here were performed by Activation Laboratories according to their code 4Lithoresearch and Code 4B1 packages Code 4Lithoresearch combines lithium metaborate/tetraborate fusion ICP whole rock analysis for major elements (code 4B) with trace elements determination by ICP-MS (code 4B2) Code 4B1 includes total digestion ICP (TD-ICP)

for certain trace elements such as Ni, Cu, Sn, Ag, Cd and S for analysis with better precision than those of ICP-MS

Furthermore, 35 archived rock powders were sent for fluorine analyses These powders were fused with sodium carbonate and potassium nitrate flux in nickel crucibles The crucible and fused melt were leached with distilled water and filtered into 100 ml volumetric flasks The filtrate solution was buffered and the fluoride was measured by standard addition using a specific ion electrode

Most of the Sm-Nd data used in this thesis and the way they were analyzed are reported by Pe-Piper and Piper (1998), but eight additional Sm-Nd analyses were made of selected granites from the Wentworth Pluton on the basis of relative age, at Activation Laboratories For these samples, rock powders were dissolved in a mixture of HF, HNO_3 and $HClO_4$ Before decomposition, the sample was totally spiked with ^{149}Sm-^{146}Nd mixed solution REE were separated using conventional cation-exchange techniques Sm and Nd were separated by extraction chromatography on HDEHP covered Teflon powder Accuracy of the measurements of Sm, Nd contents is ±0 5% $^{143}Nd/^{144}Nd$ ratios are relative to the value of 0 511860 for the La Jolla standard Analyses were performed on Triton-MC mass-spectrometer

3.2. Optical microscopy

Thin sections and polished thin sections are available for the majority of the studied samples However new ones were cut in Saint Mary's University for all the samples that lacked either a thin or a polished thin section To produce small pieces for the thin sections, slabs of these rocks were cut by an Ingram 137-U thin section cut-off saw and then by an Ingram 400-U thin section grinder to achieve the desirable thickness

of 30 μm The thin sections were polished using a Logitech LP30 optical lapping and polishing machine

A total of 40 thin and 57 polished sections were first examined with a petrographic microscope using polarized and reflected light, in order to determine the mineralogy and the rock textures of the samples The microscope is a Nicon Eclipse E400 POL microscope, with a PixelINK PL-A686C camera Images were processed using PixelInk Capture OEM imaging software Coordinates of the grains located on the petrographic microscope were recorded as to allow relocation of the grains on the scanning electron microscope (SEM) and the electron microprobe (EMP)

3.3. Scanning Electron Microscope (SEM)

All polished thin sections were carbon-coated at the Regional Electron Microprobe Center at Dalhousie University The samples were analyzed by electron dispersion spectroscopy (EDS) using a LEO 1450 VP SME scanning electron microscope with a maximum resolution of 3 5 nm at 30 kV and a detection limit > 0 1% The SEM uses a conventional high vacuum with a cooling system of liquid nitrogen to − 180°C A tungsten filament supplies electrons to produce back-scattered electron images of the grains A copper standard was used for the calibration of the microscope

3.4. Electron microprobe

All WDS geochemical analyses of the studied minerals were done, using a JEOL-8200 electron microprobe with five wavelength spectrometers and a Noran 133 eV energy dispersion detector The operating conditions were at 15kV of accelerating voltage with a 20nA beam current, a beam diameter of 1 micron and duration of analysis approximately 11 minutes Analyzing REE and rare metals with the microprobe requires

15

avoiding peak interference The peak overlaps observed between the determined elements were those of Er-Nb, Ti-Hf, Zr-P, Hf-Ho, Er-Hf, Hf-Er and F-Ce As a first step to deal with this problem, the apparent intensities of these elements were measured in standards that do not contain the elements whose peaks are being overlapped   Using these intensities, peak-overlap correction factors were then calculated as to estimate the real concentrations of measured elements WDS perform quantitative analyses whereas the EDS perform qualitative analyses and along with the fact that the standards used in the probe were more similar to the analyzed grains than the copper standard of the SEM, make the probe analyses more accurate than those from the SEM

All geochemical data were processed using MINPET software for Windows, whereas calculations for geochemical modeling were done in Microsoft Excel Geographic plots were created with ArcGIS software and further editing of maps and diagrams was done using Corel software package for Windows

CHAPTER 4: THE RELATIONSHIP BETWEEN REE-Y-Nb-Th MINERALS AND THE EVOLUTION OF AN A-TYPE GRANITE, WENTWORTH PLUTON, NOVA SCOTIA

4.1 Abstract

The Wentworth Pluton in the Eastern Cobequid Highlands consists principally of metaluminous to peralkaline A-type granite (~362 Ma), a large part of which was remelted by a major gabbro intrusion (~357 Ma). Magmatic minerals like allanite-(Ce), chevkinite-(Ce), zircon, and hingganite-(Y) and post-magmatic mineral phases, such as REE-epidote, samarskite, aeschynite-(Y), fersmite, thorite, and hydroxylbastnasite-(Ce), were identified. The presence of fluorine, kept the rare metals in solution and changed the behavior of the REE, increasing the solubility of monazite and xenotime and thus the rare earths and rare metals remained in the magmatic system for prolonged periods. The fractionation of allanite-(Ce) and chevkinite-(Ce) led to a magma enriched in HREE, from which hingganite-(Y) crystallized during late magmatic stages. The remelting of the early granite led to fluorine and sulfur release in volatile phases, which circulated with hydrothermal fluids, thus mobilizing the REEs and rare metals. Reduction of fluorine activity during the late to post-solidus crystallization resulted in the precipitation of HREEs and rare metals in samarskite, thereby enriching the residual hydrothermal fluids in LREEs. Post-magmatic LREE-minerals such as hydroxylbastnasite-(Ce) either replaced earlier minerals or precipitated from these hydrothermal fluids. Carbonate fluids involved in a late regional hydrothermal circulation along the Cobequid-Chedabucto fault (320-315 Ma) resulted in titanium mobility and the formation of titania minerals and probably of aeschynite-(Y). This unusual mineral assemblage, in addition to the complex geological history of the pluton, provides a unique opportunity to correlate the formation

of these minerals to different stages of pluton evolution and thus provide an insight to the conditions under which each mineral was formed

4.2 Introduction

A-type granites usually occur in extensional settings and have a distinct alkaline geochemical signature (Loiselle and Wones, 1979) Enrichment in rare earth elements (REE) and rare metals, such as Y, Nb, Ta, Th and U, is common in these rocks REE and rare metal-rich minerals like allanite, monazite, chevkinite, xenotime, cerite, synchysite and gadolinite are commonly found in A-type granites worldwide (Forster, 2000, Wood and Ricketts, 2000, Jiang, 2006, Vlach and Gualda, 2007, Saveleva and Karmanov, 2008)

Accessory minerals in granitic rocks are essential carriers of rare metals and rare earth elements Their internal zoning, compositional variations and alterations provide a valuable source of information concerning the host magmatic and post magmatic evolution including fractionation, rock-fluid interaction and metamorphic overprint (Uher et al , 2009) The accessory minerals in granitic rocks show more chemical and textural variability than the major minerals Their crystallization is sensitive to various environmental parameters and therefore they are a useful indicator of the magmatic history of the rock in which they are hosted (Wang et al , 2001)

The Wentworth pluton is known to have REE mineralization (MacHattie, 2009) The granites and their volcanic equivalents in the northeast are generally enriched in fluorine and uranium (Gower, 1988) Associated mineralization includes fluorite-zircon-titanite-calcite-allanite veins, with highly anomalous REE concentrations, hosted by the granite in the north-eastern part of the pluton (Gower, 1988)

18

The variety of REE and rare metal-minerals in the Wentworth pluton is unusual. The occurrences of Nb-REE-Y oxides from A-type granites worldwide and the understanding of their formation are still limited. The complex geological history of the Wentworth pluton provides a rare opportunity to correlate mineral assemblages to magmatic evolution. The purpose of this study is to identify and characterize the REE and rare metal minerals present and relate their textural features to the different relative ages of the host rocks. Comparison of whole-rock and mineral geochemistry is then used to infer the conditions under which each mineral is found.

4.3 Geological setting

The Cobequid Highlands are located in the southern part of the Canadian Appalachians, just north of the boundary between the Avalon and Meguma terranes (Calder, 1998; Pe-Piper and Piper, 2002). This boundary is marked by the Cobequid-Chedabucto fault zone, along which strike-slip motion took place during the Late Paleozoic (Murphy et al., 2011). In the Late Devonian and Early Carboniferous, granite plutons with lesser gabbros intruded along a regional shear zone that encompassed the entire Cobequid Highlands (Pe-Piper, 2007). Coeval volcanism in the Cobequid Highlands is represented by felsic pyroclastic rocks (Byers Brook Formation) that are geochemically similar to the granites, and by basalt flows (Diamond Brook Formation) that are geochemically similar to gabbros in the Wentworth pluton (Dessureau et al., 2000).

The Wentworth pluton is located in the eastern part of the Cobequid Highlands (Fig.4-1). The northeastern part of the pluton consists of the Hart Lake-Byers Lake (HLBL) granite, which is separated from the Folly Lake gabbro in the southwest by a

19
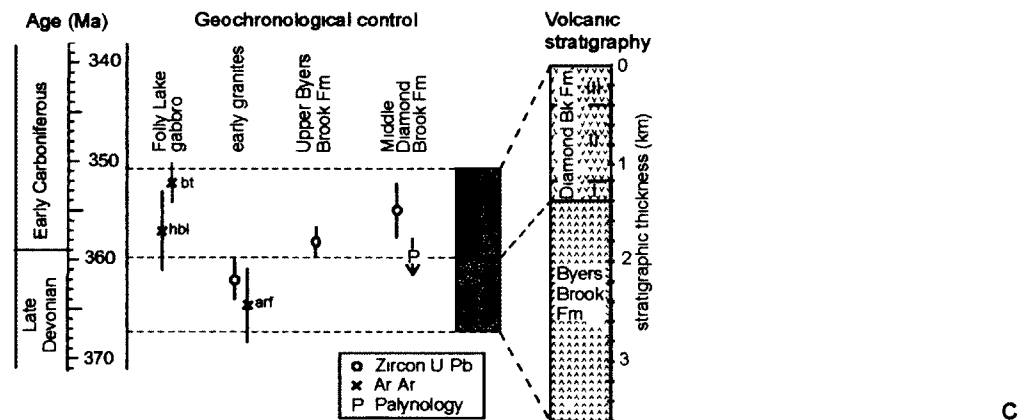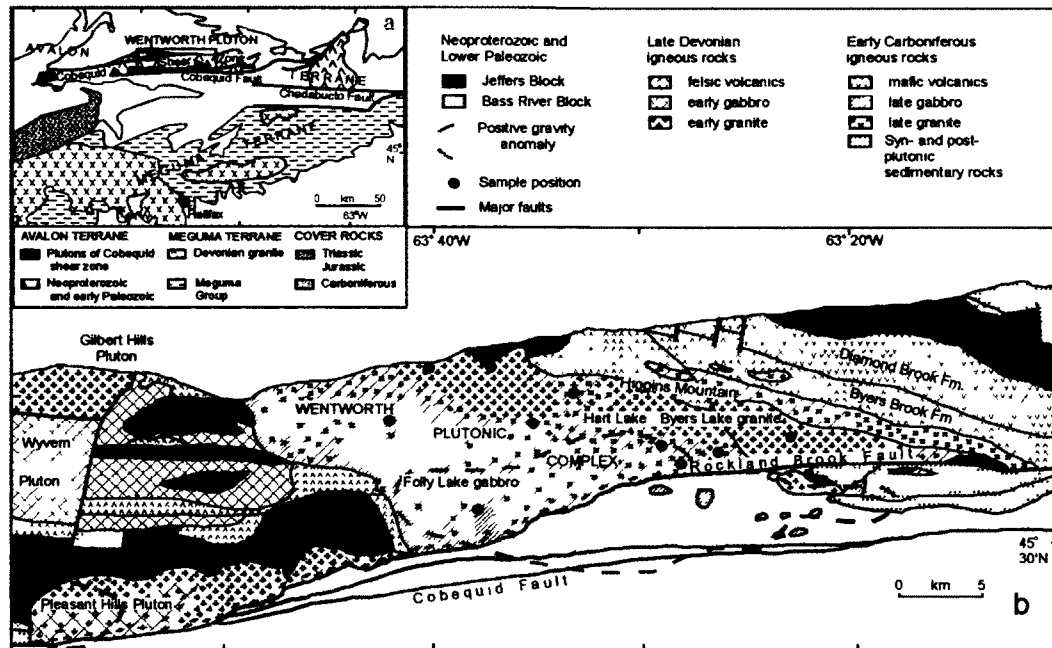
Figure 4-1 (a) Regional location of Wentworth Pluton (b) Geological map of the

Wentworth pluton area with the geographic distribution of the studied samples that

contain REE and rare metal accessory minerals, (c) geochronological data from the

studied formations combined with the stratigraphy of the associated volcanic rocks

Ages from Doig et al (1996) and Pe-Piper et al (2004), recalibrated as in Murphy et al

(2011).

20

zone in which younger granite and gabbro are predominant (Koukouvelas et al , 2002)
The Wentworth pluton includes all the granite and the gabbro phases

Field relationships show that the Folly Lake gabbro is younger than the HLBL
granite (Koukouvelas et al , 2002) The Folly Lake gabbro yielded a 357±4 Ma 40Ar/^{39}Ar
(hornblende) age (Pe-Piper et al , 2004, Murphy et al, 2011) (Fig 4-1b), whereas the
HLBL granite has yielded a 362±2 Ma U-Pb (zircon) age (Doig et al , 1996) (Fig 4-1b)

The age of the equivalent volcanic rocks is constrained by U-Pb zircon ages of
358±1 Ma from the top of the Byers Brook Formation and 355±3 Ma from the middle of
the Diamond Brook Formation (Fig 4-1b) Palynomorphs show that minor interbedded
sediment in the Byers Brook Formation is of late Famennian age and in the Diamond
Brook Formation is of mid Tournaisian age (Dunning et al 2002) (Fig 4-1b)

Part of the granite near the Folly Lake gabbro of the Wentworth pluton was
evidently remelted, resulting in bodies of "late" granite with slightly different
compositions from the HLBL granite Some of these bodies have textures indicating
magma mixing with gabbro (Pe-Piper, 2007) The Folly Lake gabbro consists of gabbro–
diorite cut by this "late" medium-grained granite in globular pods, irregular sheets, net–
veined complexes, and linear dykes, some of which are pegmatitic Mafic enclaves are
common in the granites and their presence indicates mixing with gabbro (Koukouvelas et
al , 2002)

The southern margin of the Wentworth pluton is in direct contact with the
Rockland Brook Fault (Fig 4-1), which was a major dextral shear zone at the time of
pluton emplacement (Miller et al , 1995, Koukouvelas et al , 2002) Syn-magmatic
deformation of the Wentworth pluton is widespread, and almost all major contacts of

different units in the pluton were active faults (Koukouvelas et al , 2002) The plutonic complex was compartmentalized into smaller blocks with faults parallel to the Rockland Brook Fault during the final stages of emplacement Later, between 315 and 320 Ma, there was a major phase of brittle faulting and mineralization associated with E-W faulting on the Chedabucto fault (Fig 4-1a)and its continuation along the Cobequid Fault (Murphy et al , 2011)

The Wentworth granites are fine to coarse grained monzogranites and syenogranites (Pe-Piper, 2007) Individual samples may be amphibole, amphibole-biotite or biotite bearing Amphiboles are sodic, sodic-calcic or calcic, any of which can coexist with biotite Most granites are equigranular, however some samples are porphyritic or granophyric (interpreted as high level granites) Most granite samples of the Wentworth pluton show brittle deformation and alteration is represented by secondary minerals like white mica, epidote, quartz, albite, chlorite, actinolite and riebeckite Hydrothermal quartz and epidote are also present in veinlets

The A-type granite of the Wentworth pluton is the most alkaline of a series of Late Paleozoic metaluminous to mildly peralkaline (Fig 4-2) plutons along the Cobequid shear zone (Pe-Piper, 2007) The aluminum saturation index ((A/NK) = molar $Al_2O_3/(Na_2O+K_2O)$), Maniar and Picolli, 1989) of the Wentworth Pluton granites ranges between 0 8 to 1 16, close to the boundary between metaluminous and peralkaline compositions (Table 4-1, Fig 4-2) The Fe-index (FeOt/ FeOt+MgO, Frost et al , 2001) of these rocks is between 0 75 and 0 99, which classifies them as ferroan (Table 4-1, Fig 4-3), typical for A-type granites

22
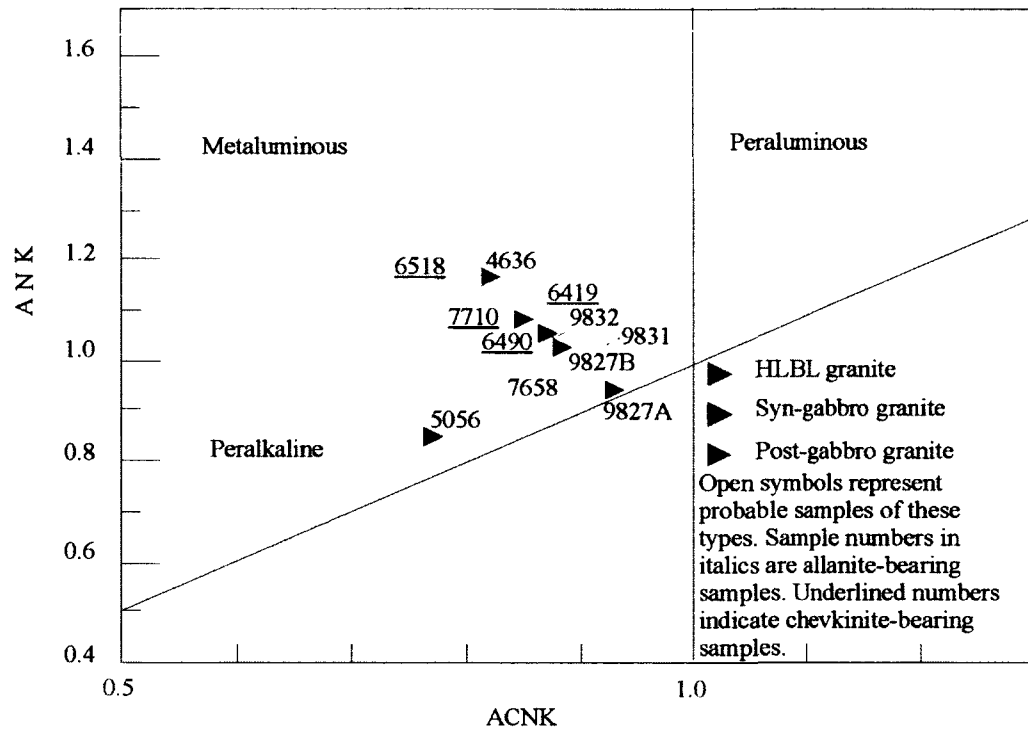
Figure 4-2: Alkalinity diagram ANK vs. ACNK of the analyzed samples from the Wentworth pluton (fields after Maniar and Piccoli, 1989).
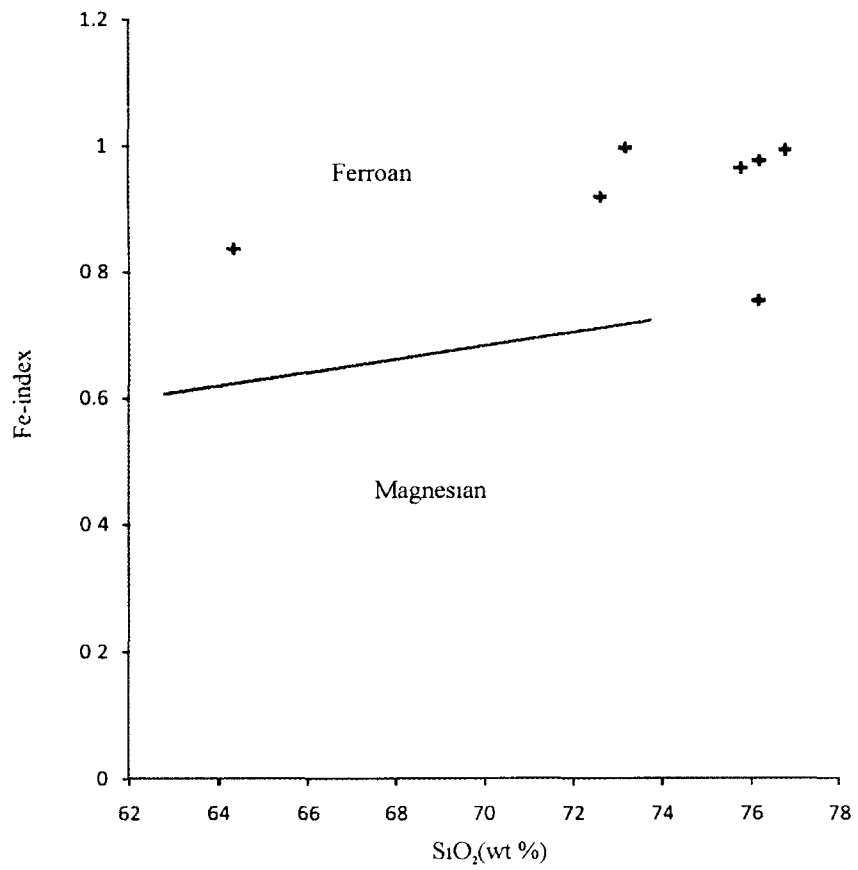
Figure 4-3: Fe-index (FeOt/(FeOt+MgO) vs SiO$_2$ (Frost et al , 2001)

The HLBL granite, the early phase of the Wentworth Pluton, has a composition of about 76% SiO_2, high F (>500 ppm), and moderate Li (>20 ppm) (Koukouvelas et al , 2002) This early granite shows subtle differences in bulk geochemistry from the syn- and post-gabbro granites for the same SiO_2 content, F tends to be higher in the early granite (Koukouvelas et al 2002, Pe-Piper 2007) Some granites that occur as pods within the gabbro are geochemically distinct, with a wide range of SiO_2 contents, relatively low F and the amphibole, where present, is hornblende The particularly low F may indicate that melting of the early granite by the gabbro, resulted in the release of F in volatile phases (Koukouvelas et al , 2002)

4.4 Analytical methods and samples

Samples were located on the 1 50000 maps of Pe-Piper and Piper (2005) The studied samples are classified into types according their location and field relations with the gabbro (Table 4-1) Uniform outcrops of granite cut by gabbro are considered to be of the early granitic phase (HLBL granite) Granites with lobate contacts with the gabbro and hybrid enclaves are taken as synchronous with the mafic intrusion Bodies of granite that either cut the Folly Lake gabbro or occur in it as globular pods or irregular sheets are considered to be of the late granitic phase When field relations were clear, sample classification is characterized as "definite" When the relative age of a sample was not clearly defined from field relations in the same outcrop, but was assumed from the geology of nearby outcrops, then the sample is classified as "probable"

A total of 40 thin and 57 polished sections were first examined with a petrographic microscope using polarized and reflected light, in order to determine the mineralogy and the rock textures of the samples Minerals that were not identified using

the petrographic microscope were analyzed in carbon-coated slides by electron dispersion

spectroscopy (EDS) using a LEO 1450 VP SME scanning electron microscope with a

maximum resolution of 3 5 nm at 30 kV and a detection limit > 0 1% The EDS analyses

from the SEM revealed groups of minerals that were further analyzed using a JEOL-8200

electron microprobe with five wavelength spectrometers and a Noran 133 eV energy

dispersion detector The operating conditions were at 15kV of accelerating voltage with a

20nA beam current and a beam diameter of 1 micron The standards used and detection

limits are listed in Table 4-2 Analyzing REE and rare metals with the microprobe

requires avoiding peak interference The overlaps we had to deal with were those of Er-

Nb, Ti-Hf, Zr-P, Hf-Ho, Er-Hf, Hf-Er and F-Ce As a first step to deal with this problem

the apparent intensities of these elements were measured in standards that do not contain

the elements whose peaks are being overlapped (Table 4-2) Using these intensities,

peak-overlap correction factors were calculated as to estimate the real concentrations of

measured elements (Table 4-2) From the 57 polished sections that were examined, only

12 samples contained REE-rare metal-rich minerals

4.5 Silicate minerals

4.5.1. Allanite-(Ce) and REE-epidote

Allanite-(Ce) is found principally in the HLBL granite but also in some late

granites (Table 4-1) In thin section, allanite-(Ce) appears dark yellow to brown and

occurs a) as large euhedral, isolated crystals (Fig 4- 4A and B), and b) as inclusions in

amphibole crystals (Fig 4-5) Most of the allanite-(Ce) grains are inhomogeneous and

some of them present optical (progressive) zoning, whereas others show more irregular

optical and compositional variation Microprobe analyses (Table 4-3) of euhedral,
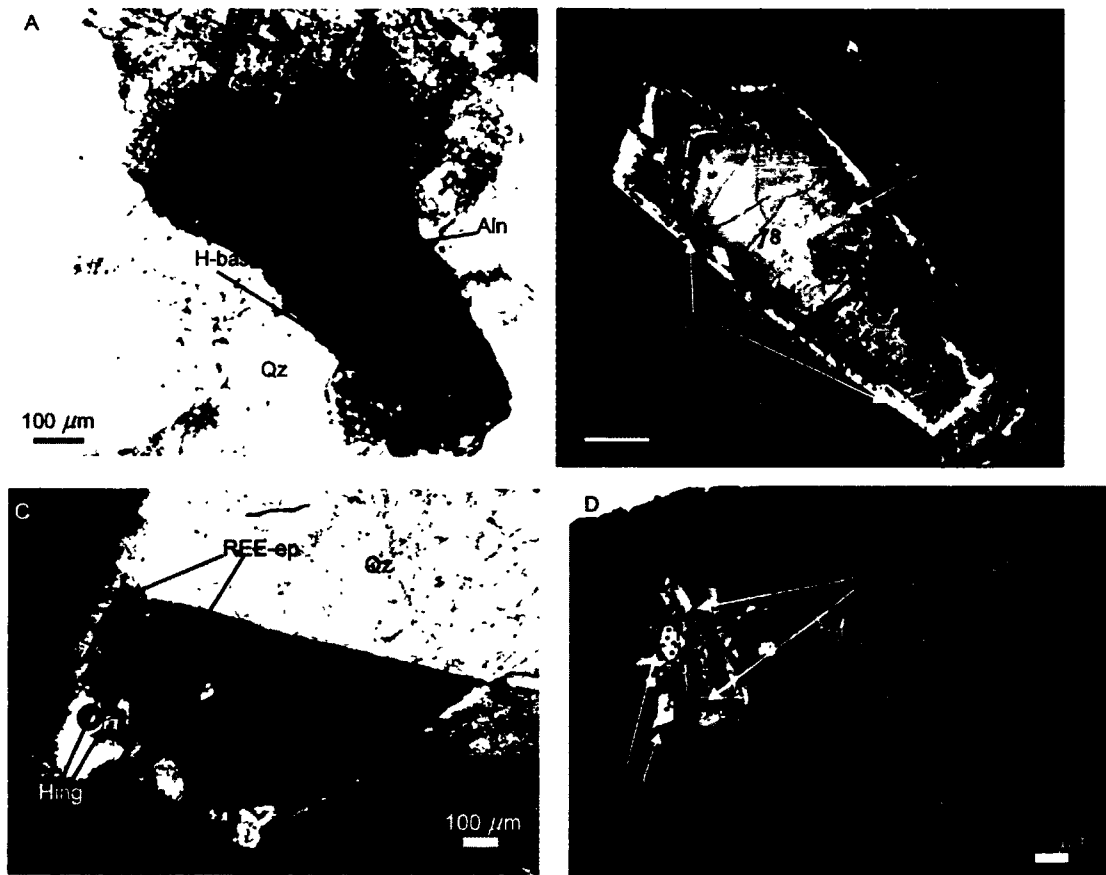
Figure 4-4: Microphotographs (A and C) and BSE images (B and D) of allanite (aln) and
REE-rich epidote (REE-ep). Images A and B show a euhedral magmatic allanite replaced
by hydroxylbastnäsite-(Ce) (H-bas)from sample 7658 (granite intruding the Byers Brook
Formation). REE-rich epidote in images C and D (sample 6419,probable HLBL granite)
engulfs a grain of hingganite (Hing). Hingannite optically looks like zircon but in the
BSE image is much brighter.

independent grains show a total of about 20 wt% LREE, 10 wt% FeOt, 10 wt% Al_2O_3 and 8 wt% CaO REE patterns for allanite-(Ce) show enrichment in LREE relative to HREEs, with a positive Eu anomaly and a negative Sm anomaly (Fig 4- 6A) and some variability in the relative amounts of different LREEs

Anhedral overgrowths and interstitial grains that look optically similar to allanite-(Ce) were also analyzed These show lower amounts of LREE (15 wt%) and higher amounts of CaO (15 wt%), FeOt (18 wt%) and Al_2O_3 (15-20 wt%) (Table 4-3, Fig 4-6a) compared with analyses of euhedral allanite-(Ce) They classify as REE-rich epidotes based on the nomenclature of Armbruster et al (2006) (Table 4-3)

4.5.2. Chevkinite-(Ce)

Chevkinite-(Ce) occurs in four granite samples that appear to be synchronous with or post-date the gabbroic intrusion (Table 4-1) In thin section, most chevkinite-(Ce) forms dark red, close to opaque, euhedral crystals associated with zircon, Fe-Ti oxides, feldspar and quartz (Figs 4-7 and 4- 8) A magmatic ferro-edenite grain forms an interlocking texture with chevkinite-(Ce) (Fig 4-7E and F) and some similar grains contain inclusions of chevkinite-(Ce) (Fig 4-8C and D)

Chevkinite-(Ce) is enriched in LREE, particularly Ce_2O_3 (20 wt%), and contains moderate amounts of ThO_2 (up to 5 wt %) and Nb_2O_5 (up to 4 6 wt%) (Table 4-4) The main characteristics of REE patterns for chevkinite-(Ce) are similar to those described for allanite but the REE concentrations are higher LREE are enriched relative to HREEs with a positive Eu anomaly and a negative Sm anomaly (Fig 4- 6B) Chevkinite-(Ce) patterns vary less than those of allanite-(Ce), only La and Er seem to present small variations (Fig 4-6B) In places chevkinite-(Ce) crystals are surrounded by a yellowish,
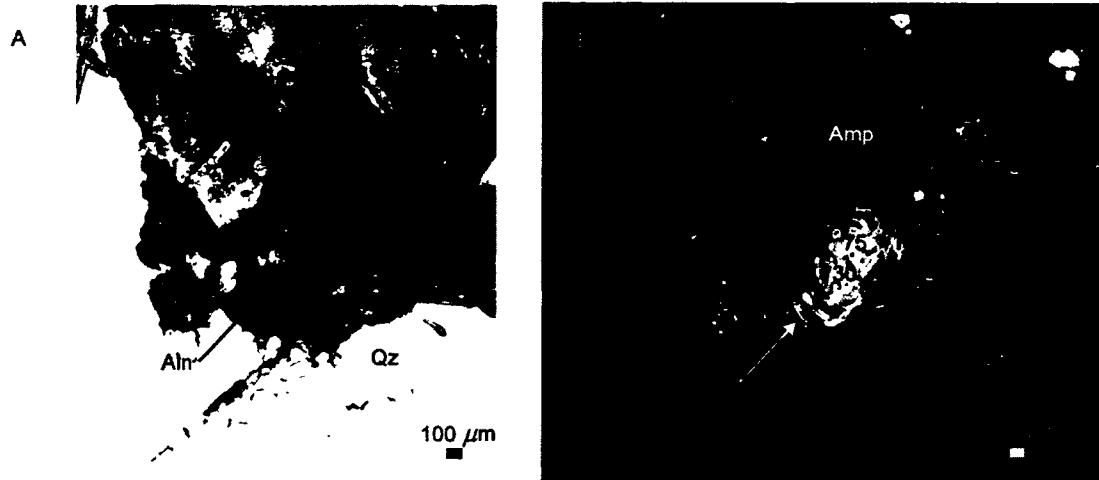
Figure 4-5: Microphotograph (A) and BSE image (B) of a magmatic allanite which appears as an inclusion in an amphibole crystal (Amp) surrounded by quartz (Qz) and feldspar (Fsp) (sample 7658, granite intruding the Byers Brook Formation).
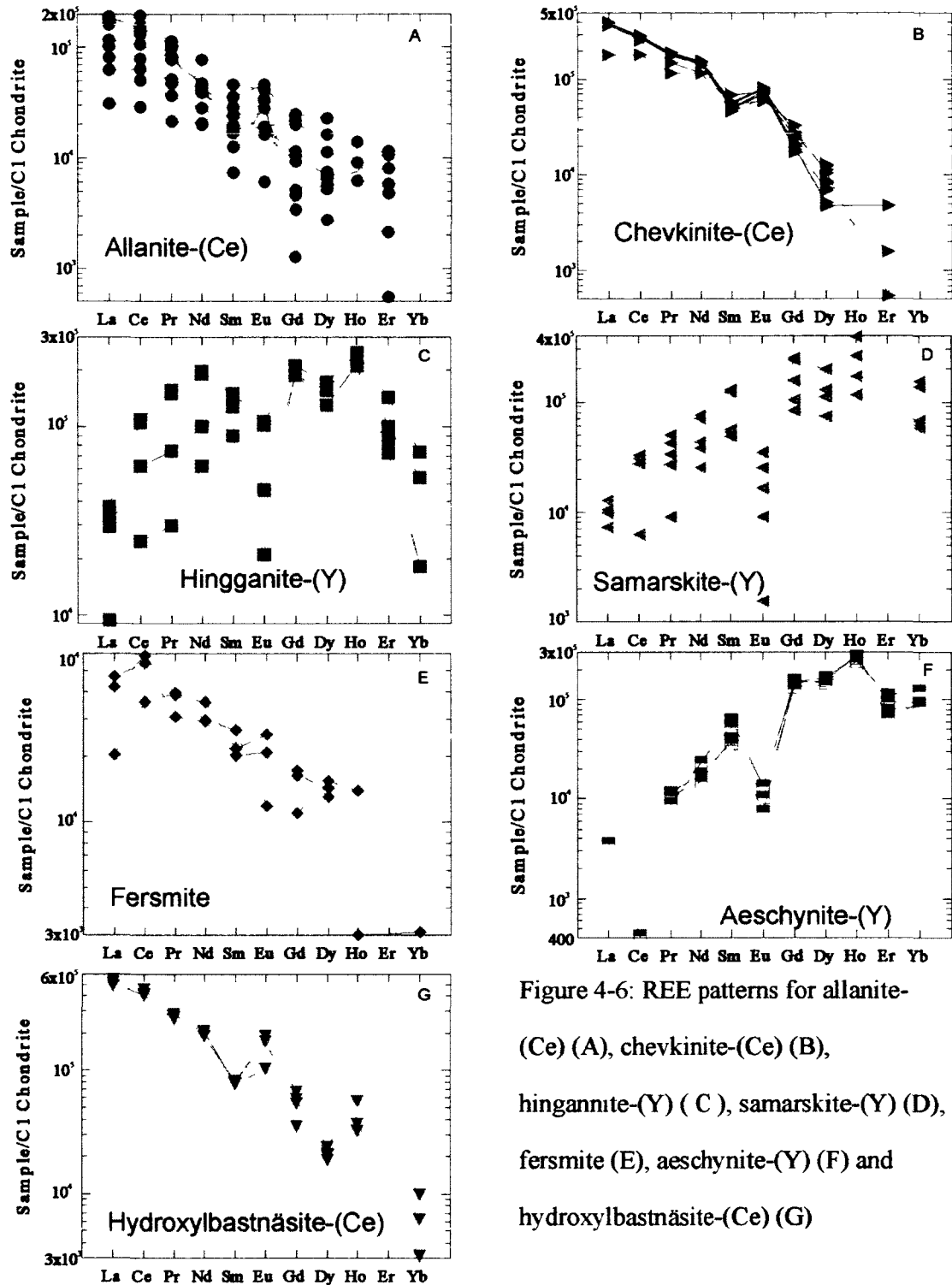
Figure 4-6: REE patterns for allanite-
(Ce) (A), chevkinite-(Ce) (B),
hingannite-(Y) (C), samarskite-(Y) (D),
fersmite (E), aeschynite-(Y) (F) and
hydroxylbastnäsite-(Ce) (G)
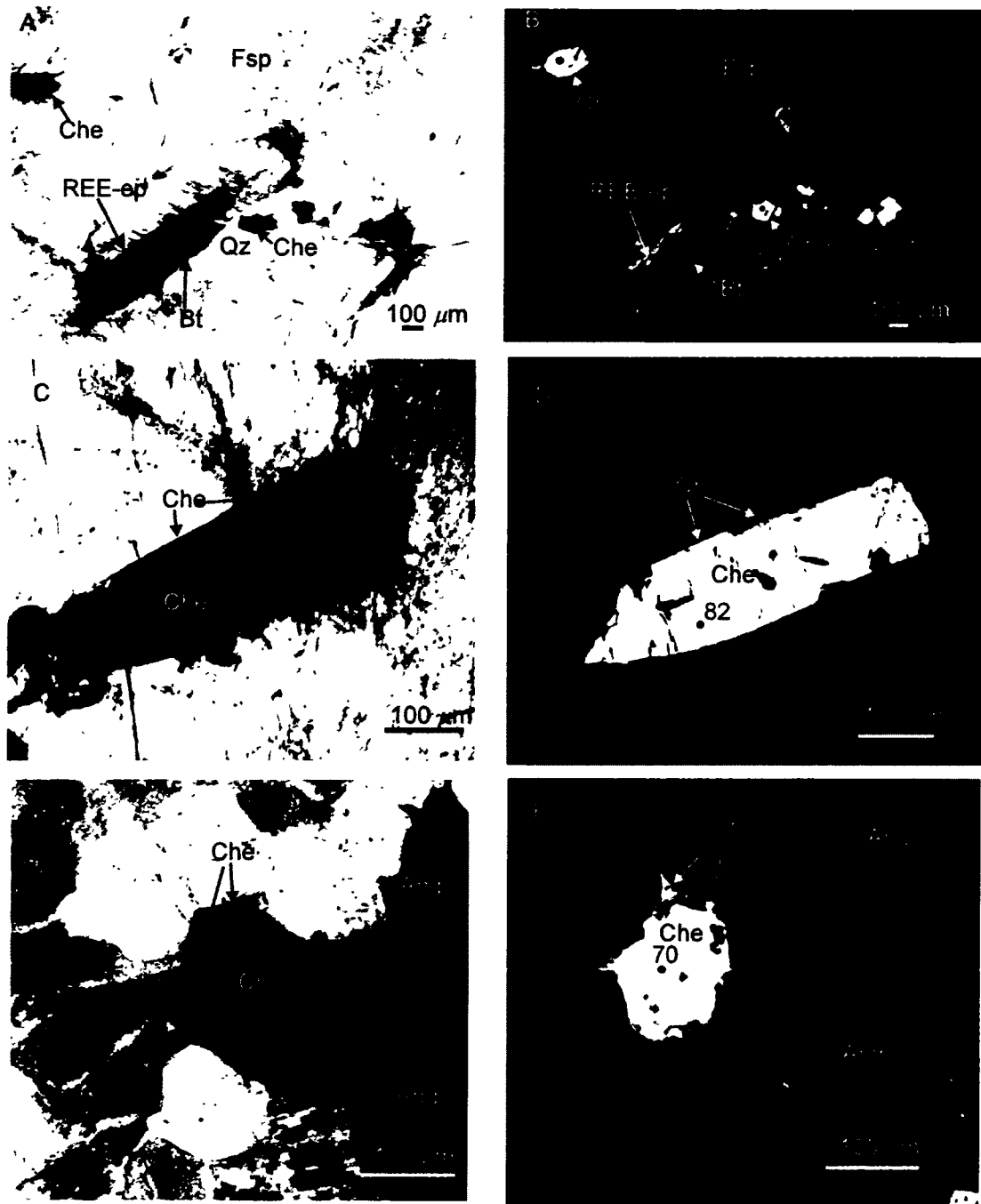
Figure 4-7: Microphotographs (A, C and E) and BSE (Backscattered electron) image (B, D and F) of chevkinite crystals (Che). Images A to D are from sample 6518 (probable post-gabbro granite), whereas images E and F are from sample 7710 (late fine grained granitic dyke).
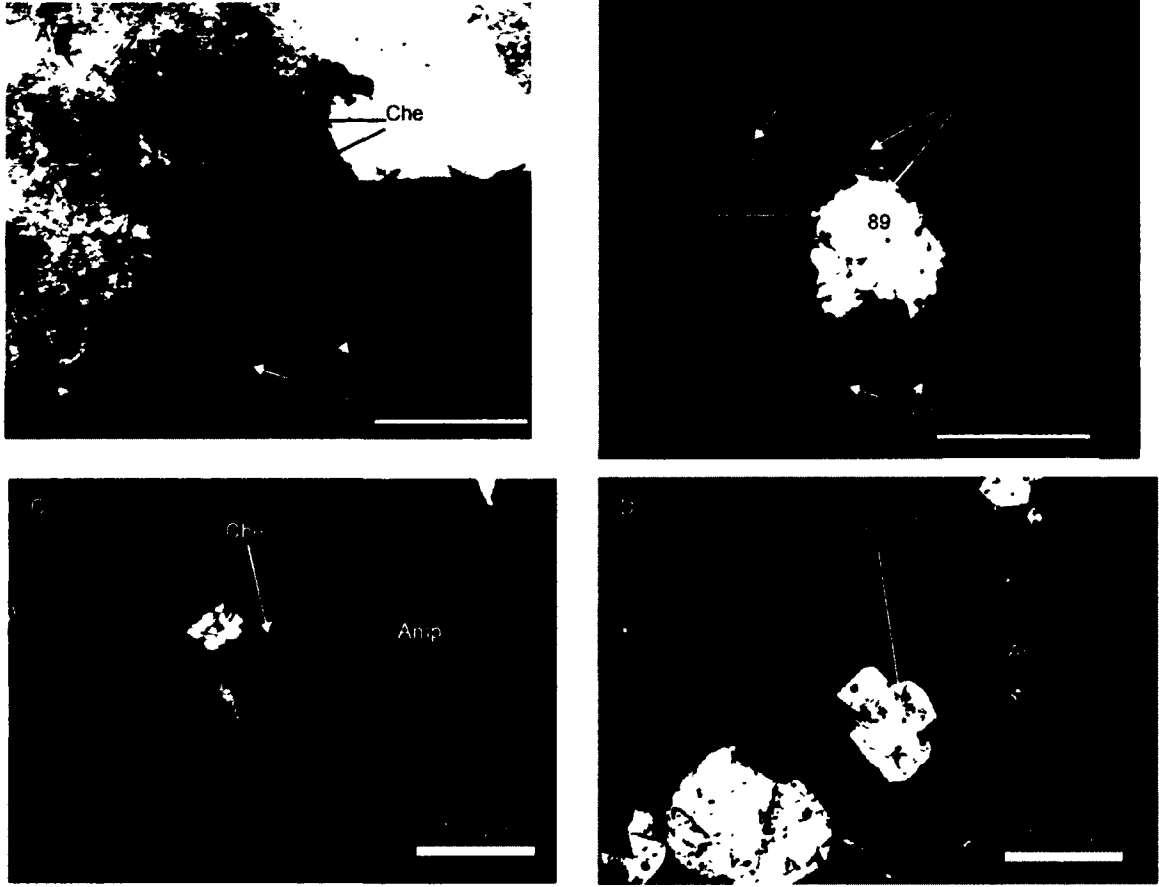
Figure 4-8: Microphotographs (A and C) and BSE images (B and D) of chevkinite (sample 7710, late fine-grained granitic dyke). Images A and B show chevkinite occurring as an independent grain whereas images C and D present chevkinite as an inclusion in amphibole.

continuous phase (Fig 4-8) and the core appears corroded (Fig 4-8E and F) Compared

to the core, the surrounding phase has less Ce_2O_3 (18 2 wt%) and more Ti, Al and Fe

Chemical analyses (Table 4-4, analysis 122) indicate that this yellow mineral phase is

also chevkinite-(Ce) but is depleted in LREE and enriched in Ti and Fe

4.5.3. Altered (?)Chevkinite-(Ce)

A crystal of an Fe-rich mineral was found in a syn-gabbro granite (sample 6490)

The crystal is strongly fractured and appears inhomogeneous Fractures within this grain

do not continue or cross cut adjacent grains suggesting that they are not of tectonic origin

but they indicate a change of volume during mineral replacement X-ray compositional

mapping (Fig 4- 9) shows that although this mineral is a REE mineral with optical

properties of chevkinite, there are significant compositional differences between it and

chevkinite The Fe concentration is three times higher (30 wt %) than that of chevkinite

and the REE amounts are lower Cerium shows a random distribution of high

concentration spots throughout the grain (Fig 4-9d) that could be remnants of what was

once a Ce-rich phase that is now completely altered Areas of high Ce correspond to areas

of low Fe (Fig 4-9b) Probe analyses show large chemical variations even over distances

of a few microns, with very low totals, making the identification of individual phases

impossible Titanium is higher in the core, which has the widest fractures (Fig 4-9a) and

corresponds to areas of low Ca (Fig 4-9e) This grain is also tentatively identified as

altered chevkinite-(Ce) on the basis of optical properties and the absence of other large

euhedral Ce-rich accessory minerals
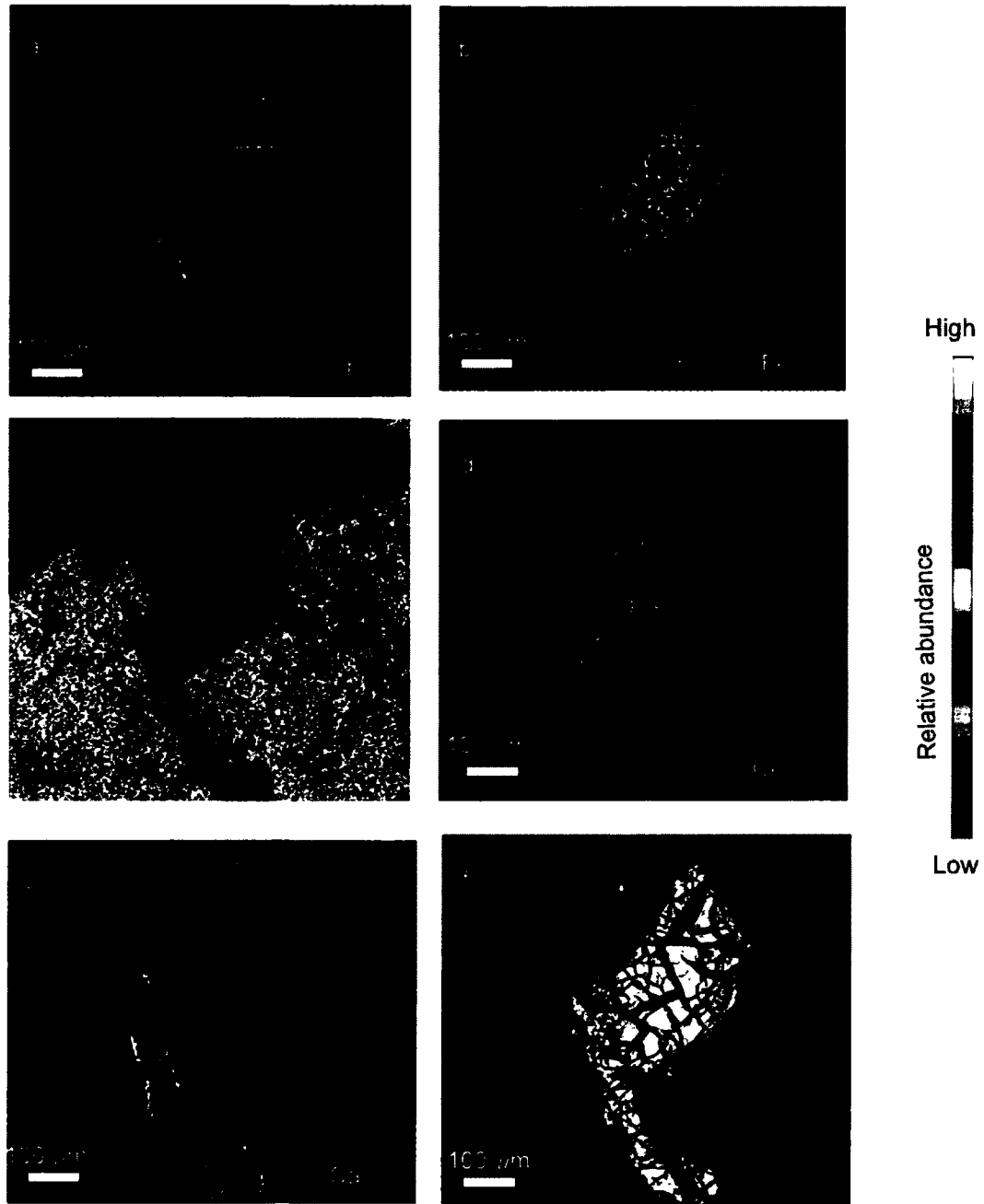
Figure 4-9: X-ray compositional maps (A-E) and BSE image (F) of an altered crystal of

an unidentified mineral (sample 6490, syn-gabbro granite, definite). The crystal shows

clear zoning for Ti and Ca (images A and E respectively). whereas Fe shows more

patchy concentration rather than zoning.

4.5.4. Zircon

Zircon is a common accessory mineral in the studied granites Most zircon

crystals are euhedral Some are optically and compositionally zoned, with Hf showing

large variation (Table 4-5) Zircons in HLBL granite sample (9832) have dusty

appearance, appear fractured and contain inclusions rich in Th (Fig 4-10) Other zircons

(sample 6518) are bounded by fractures and have an optically clear core surrounded by a

dusty, discontinuous, fractured, porous zircon depleted in Zr and enriched in Th (Fig 4-

11) This overgrowth is relatively rich in Y (up to 3 6 wt%), Hf (up to 2 6 wt%) and Th

(Table 4-5) All analyzed zircons contain small amounts of REE, particularly the

medium and heavy REEs

4.5.5. Hingganite-(Y)

Hingganite-(Y) is found in only one sample of post-gabbro granite (6419, Table

4-1) In thin section it has similar optical properties to zircon but in the BSE images

appears brighter Both analyzed grains of hingganite-(Y) are adjacent to a much larger

grain of secondary allanite, which occurs as a clot adjacent to another undetermined

alteration mineral (Fig 4-4C and D) The hingganite-(Y) is enriched in middle REE and

particularly Gd and Dy, relative to the remaining REEs (Fig 4-6C) REE patterns show a

negative Eu anomaly and a slight depletion of LREEs relative to the HREEs (Fig 4-6C)

It contains Y up to 31 wt% (Table 4-6) Hingganite-(Y) grains are zoned showing a

rimward slight depletion of Y and enrichment in Ce (Table 4-6, analyses 145 and 146)

Low totals ($\leq$ 87%) are attributed to undetermined Be
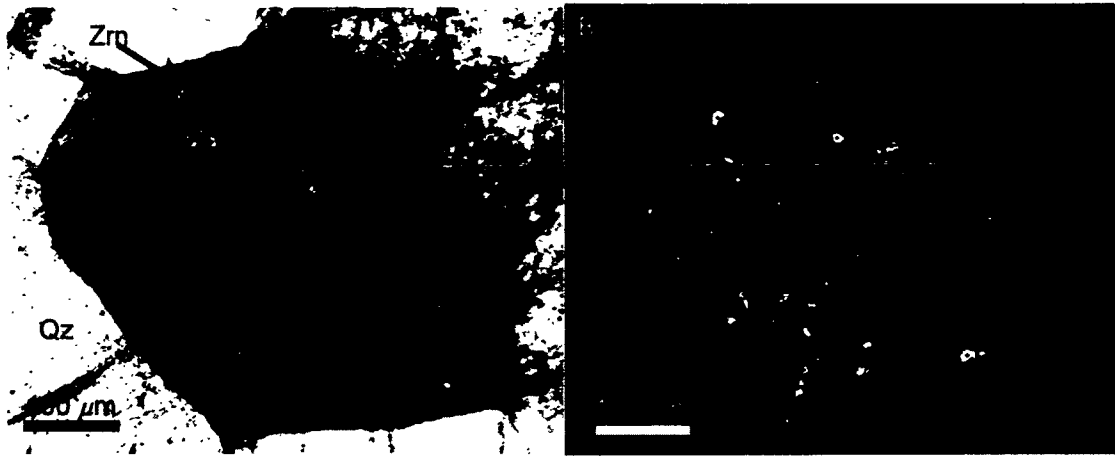
Figure 4-10: Microphotos (A) and BSE images (B) of magmatic zircon (Zrn) from the HLBL granite (9832) containing Th-rich inclusions (bright areas in BSE image). Numbers indicate analyses (Table 4-7).
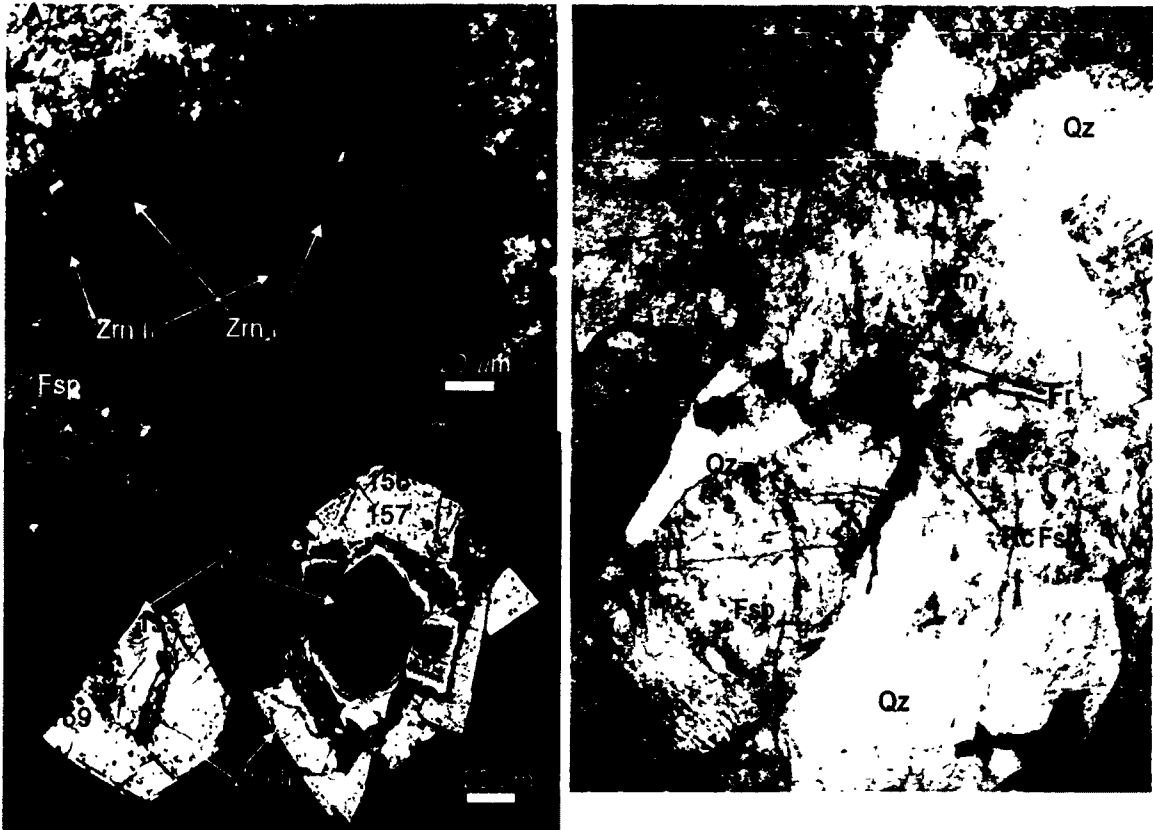
Figure 4-11: Microphotographs (A and B) and BSE image (C) of two zircon inclusions

in feldspar (sample 6518 probable post-gabbro granite). (Rc Fsp= recrystallized contact

between the two feldspar crystals, Fr= fractures). Numbers indicate analyses (Table 4-5).

4.5.6. Thorite

Thorite was found in one sample of syn-gabbro granite (6490) as a small independent grain (10 μm) showing interlocking texture with zircon (Fig 4-12F), but occurs more commonly as inclusions in the zircon (Fig 4-10) It is enriched in FeOt (9 4 wt%), Nb_2O_5 (7 7 wt%) and shows moderate enrichment in Y_2O_3 (2 1 wt%) Small amounts of REE are present (<1 wt%) (Table 4-7)

4.6. Oxide minerals

4.6.1. Samarskite-(Y)

Samarskite-(Y) is a radioactive, Y-rich, Nb-oxide, found in four of the studied samples of various ages (Table 4-1) Samarskite-(Y) occurs both as isolated euhedral rhombic crystals (sample 9827A) (Fig 4-12A and B) and as patches in crystals together with another Nb-oxide, fersmite (Fig 4-12C and D) In thin section, it occurs as euhedral crystals that are yellow to pale green (Fig 4-12A) One samarskite-(Y) crystal (sample 9827A) contains an inclusion of euhedral zircon (Fig 4-12A and B) The mineral is classified as samarskite-(Y) based on the strong dominance of Y over REEs (Table 4-8) It contains up to 25 wt% Y_2O_3 and up to 53 wt% Nb_2O_5, and almost equal amounts of Gd and Dy (3-5 wt% as oxides) The HREEs are represented mostly by Yb (Table 4-8) LREE are also present, Nd being the dominant element (up to 4 wt% Nd_2O_3) (Table 4-8) The REE patterns of samarskite show a negative Eu anomaly and HREE enrichment relative to the LREEs (Fig 4-6D)

4.6.2. Fersmite

Fersmite grains were found in four samples, principally from the HLBL granite (Table 4-1) Fersmite occurs as small (<10 μm) isolated grains (sample 4636) (Fig 4-

38
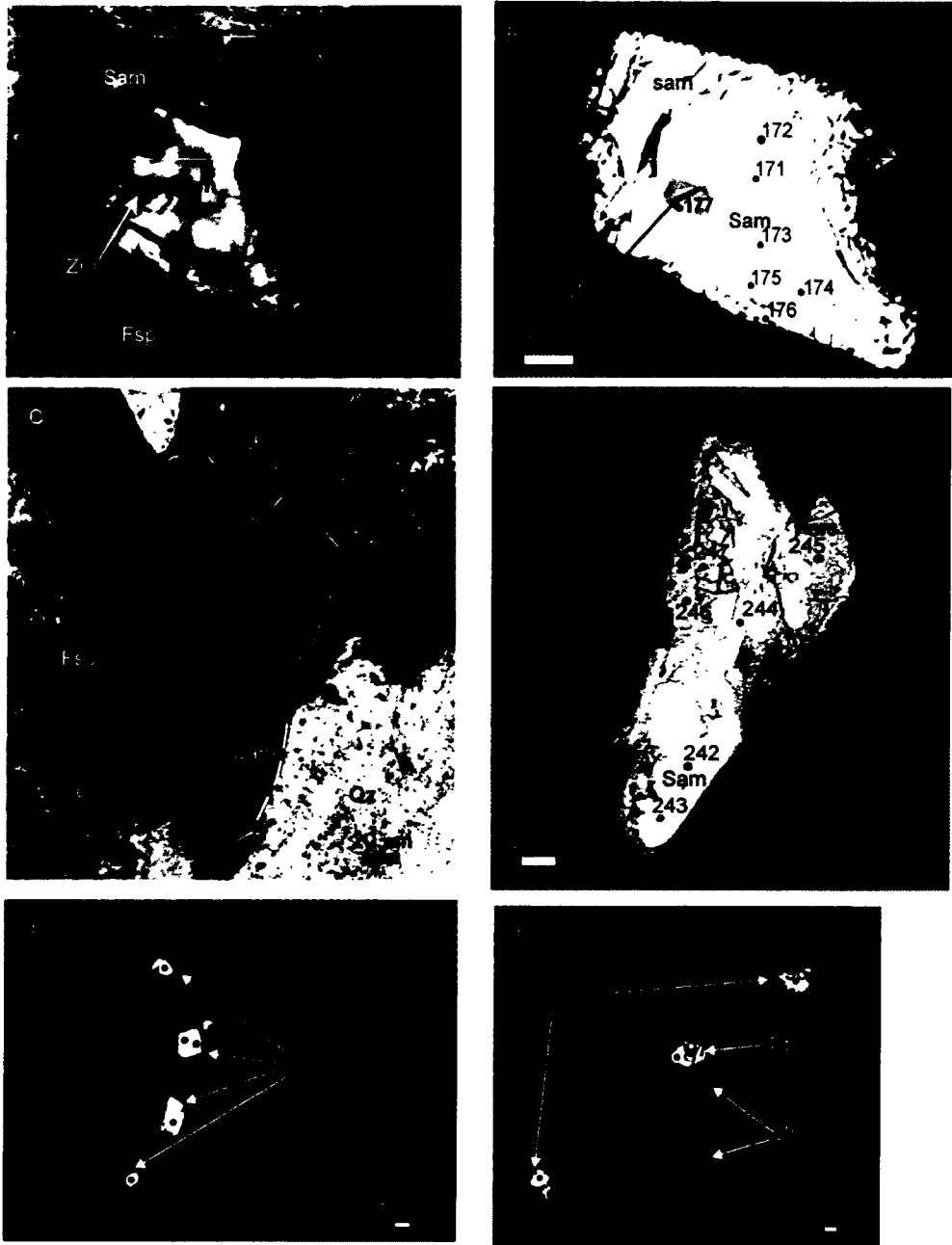
Figure 4-12: Microphotographs (A and C) and BSE images (B, D, E and F) of samarskite (Sam) and fersmite (Fers) grains. Images A and B are samarskites from sample 9827A (late, fine-grained granitic dyke). Images C and D are samarskite and fersmite from sample 9831 (probable HLBL granite). Image E is fersmite from sample 4636 (HLBL granite) and F is a BSE image of samarkite grains together with thorite (Trt) from sample 6490 (syn-gabbro granite). Numbers indicate analyses (Table 4-8).

12E), inclusions in fluorite which grew between fractured feldspar crystals (sample 7658) (Fig 4-13), and patches associated with samarskite (samples 9831 and 9832) (Fig 4-12C and D) Grains with fersmite and samarskite patches are dark brown and dusty Microprobe analyses (Table 4-8) show that samarskite and fersmite contain the same amounts of niobium, but fersmite, is depleted in Y(5 5 wt% Y_2O_3), and enriched in U and Th (6 3 and 13 wt% as oxides, respectively) Furthermore, fersmite is enriched in LREE and particularly Ce (close to 4 wt% Ce_2O_3) (Table 4-8) whereas samarskite has high concentrations of middle and heavy REEs (Fig 4-6E) LREE enrichment is also indicated by REE patterns of this mineral (Fig 4-6E), with most analyses showing a positive Ce anomaly

4.6.3. Aeschynite/Polycrase-(Y)

Another Y-rich mineral was identified in one sample of the HLBL granite (sample 9832) In thin section, it is dark brown and appears dusty (Fig 4-14) It occurs associated with clots of titanite grains, a titania mineral, and secondary REE-rich epidote, or associated with fractures In places aeschynite-(Y) appears engulfing titanite grains (Fig 14) Microprobe analyses (Table 4-9) show that TiO_2, Y_2O_3 and Nb_2O_5 (42 wt%, 23 wt% and 12 wt% respectively) are the major components It is a moderately enriched in middle REE, particularly Gd and Dy (3 8 wt% and 4 8 wt% as oxides respectively) and contains smaller amounts of LREE and HREE (Table 4-9, Fig 4-6F) The chemistry of this mineral resembles aeschynite-(Y) or its chemical equivalent polycrase-(Y) Th is more abundant than U (Fig 4-15), which is a characteristic of the aeschynite group minerals (Ewing, 1975) Furthermore the analyzed grains are enriched in HREEs relative to the LREEs (Table 4-9), which is another characteristic for the aeschynite group (Škoda

40
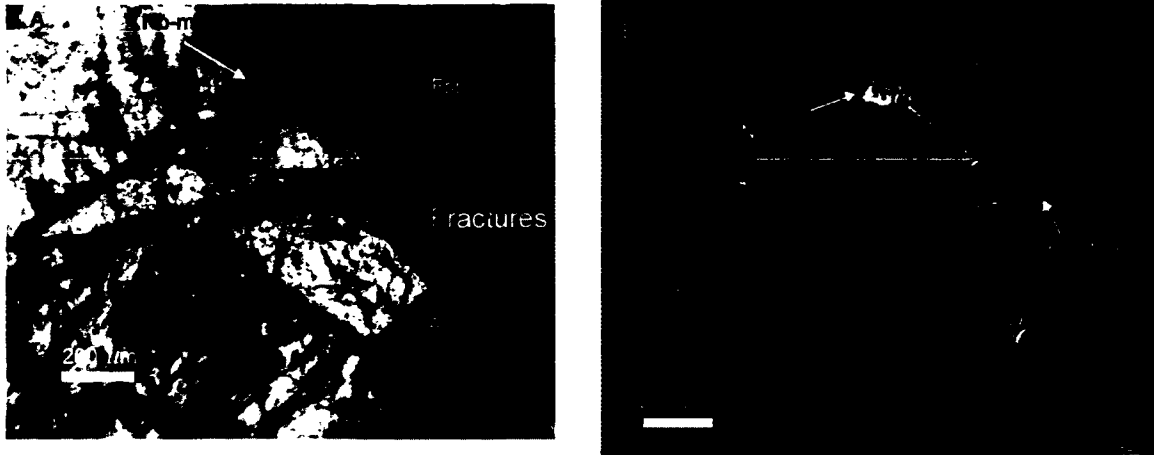
Figure 4-13: Microphotograph (A) and BSE image (B) of a Nb-oxide (Nb-min) (an: 128,129) occurring as an inclusion in fluorite (Fl) (sample 7658, granite intruding the Byers Brook Formation).
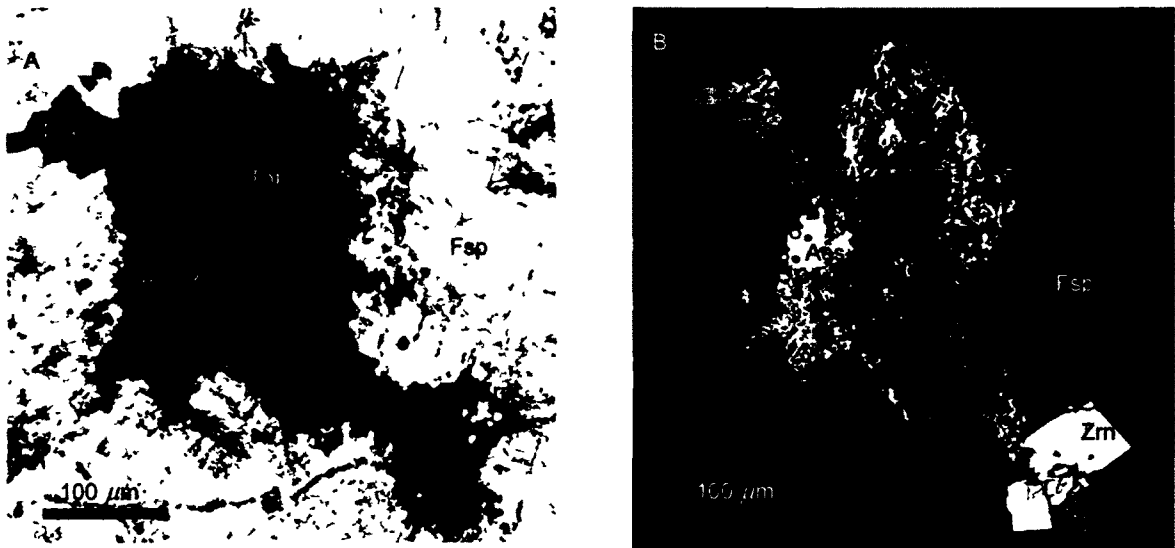
Figure 4-14: Microphoto (A) and BSE image (B) of aeschynite-(Y) (Aes-Y) in a clot of

titanite (Tnt) crystals associated with titania mineral (Tna) (analysis 237, Table 4-9)

(sample 9832, probable HLBL granite).
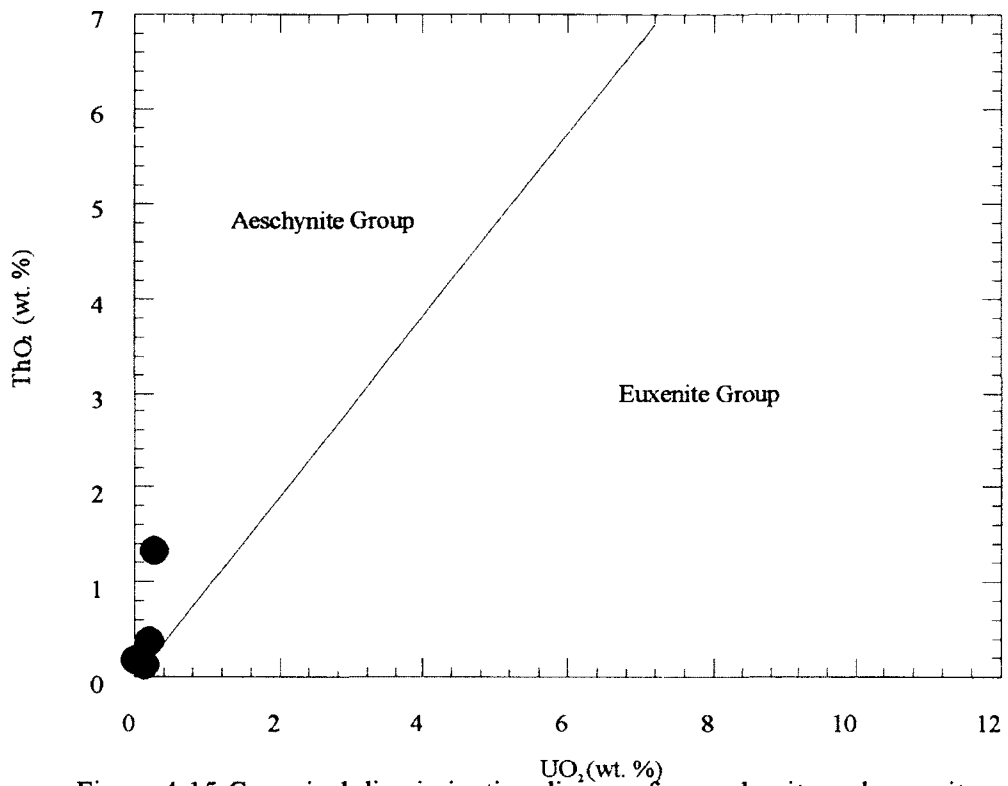
Figure 4-15:Canonical discrimination diagram for aeschynite and euxenite group

minerals (fields after Ewing (1976). Analyses of aeschynite-(Y) from the Wentworth

Pluton plot close to the boundary between these two fields.

and Novák, 2007) However due to the metamict nature of these minerals and their minor chemical differences, microprobe analyses alone cannot precisely determine the identity of this mineral As the main elemental characteristics resemble those described for aeschynite-(Y) (i e , HREE enrichment and Th>U), in the present study we will refer to it as aeschynite-(Y)

4.6.4. Titania mineral

A single grain of titanium oxide was found in one sample from the HLBL granite (9832) It is dark brown, almost opaque, bounded by fractures and is associated with a clot of titanite grains hosting aeschynite-(Y) (Fig 4-14) It contains 2 8 wt% Nb_2O_5 (Table 4-9), traces of Fe, Ca and Ta, but there is an almost complete absence of REE (0 2 wt%) (Table 4-9) Due to the lack of XRD data, we cannot determine which polymorph of TiO_2 (rutile, anatase or brookite) has been formed in our sample, and therefore we will refer to it as a titania mineral

4.7. Sulphide minerals

4.7.1. Pyrite.

Pyrite was found in one sample probably from the early HLBL granite (9820, not listed in Table 4-1) It occurs either as small inclusions in euhedral hematite, or as anhedral grains rimmed by hematite (Fig 4-16) The pyrite contains up to 49 wt% Fe and 52 wt% S with small amounts of Co (up to 1 5 wt%), traces of Se and Au are also present In addition, pyrite is abundant in the Folly Lake gabbro
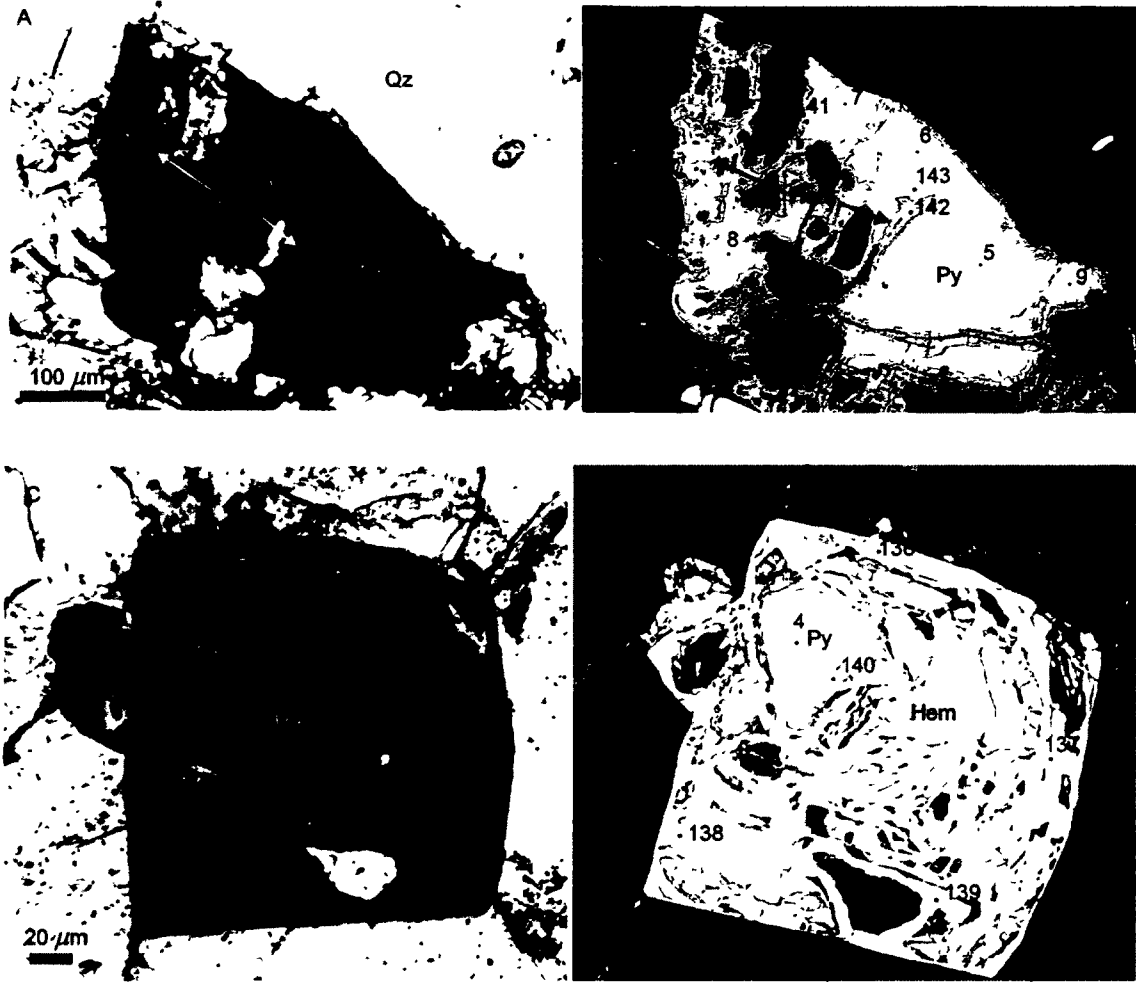
Figure 4-16: Microphotos (A and C) and BSE images (B and D) of pyrite (Py) found in the Wentworth granites surrounded by hematite (Hem).

4.8 Carbonate minerals

4.8.1. Hydroxylbastnäsite-(Ce)

Hydroxylbastnasite-(Ce) is a F-bearing carbonate mineral which was found in one

sample of granite intruding the Byers Brook Formation (sample 7658)

Hydroxylbastnasite-(Ce) is formed around the rims of euhedral crystal of allanite-(Ce)

(Fig 4-17D) In thin section, hydroxylbastnasite-(Ce) has a yellowish color and appears

dusty (Fig 4-4A and B) In BSE images hydroxylbastnasite-(Ce) is brighter than the

surrounded allanite, since it has close to 60 wt% LREEs Microprobe analyses (Table 4-

10) have low totals due to the presence of hydroxyl and carbon that were not determined

by the microprobe The analyzed hydroxylbastnasite-(Ce) contains up to 32 wt% Ce_2O_3,

15 wt% La_2O_3, 11 wt% Nd_2O_3, and smaller amounts of the remaining REEs (Table 4-10)

REE patterns show LREE enrichment relative to the HREEs, with positive Eu and Ho

anomalies and negative Sm and Dy anomalies (Fig 4- 6G)

4.9. Discussion

Peralkaline granitic rocks are commonly associated with economical to

subeconomical deposits of rare earth elements and trace metals with high field strength

(Schmitt et al , 2002) The high oxidation number and their large ionic radii make the

REEs incompatible with common minerals in igneous rocks and as a result they remain in

solution until the last stages of magmatic evolution, concentrated in residual melts that

form pegmatites and alkali granites The difference in ionic radii between the LREE and

the HREE makes the former even more incompatible than the latter, explaining the

enrichment in LREE in highly fractionated granitic rocks High field strength elements,

due to their high charge, ionic radii and low initial concentration, do not participate easily
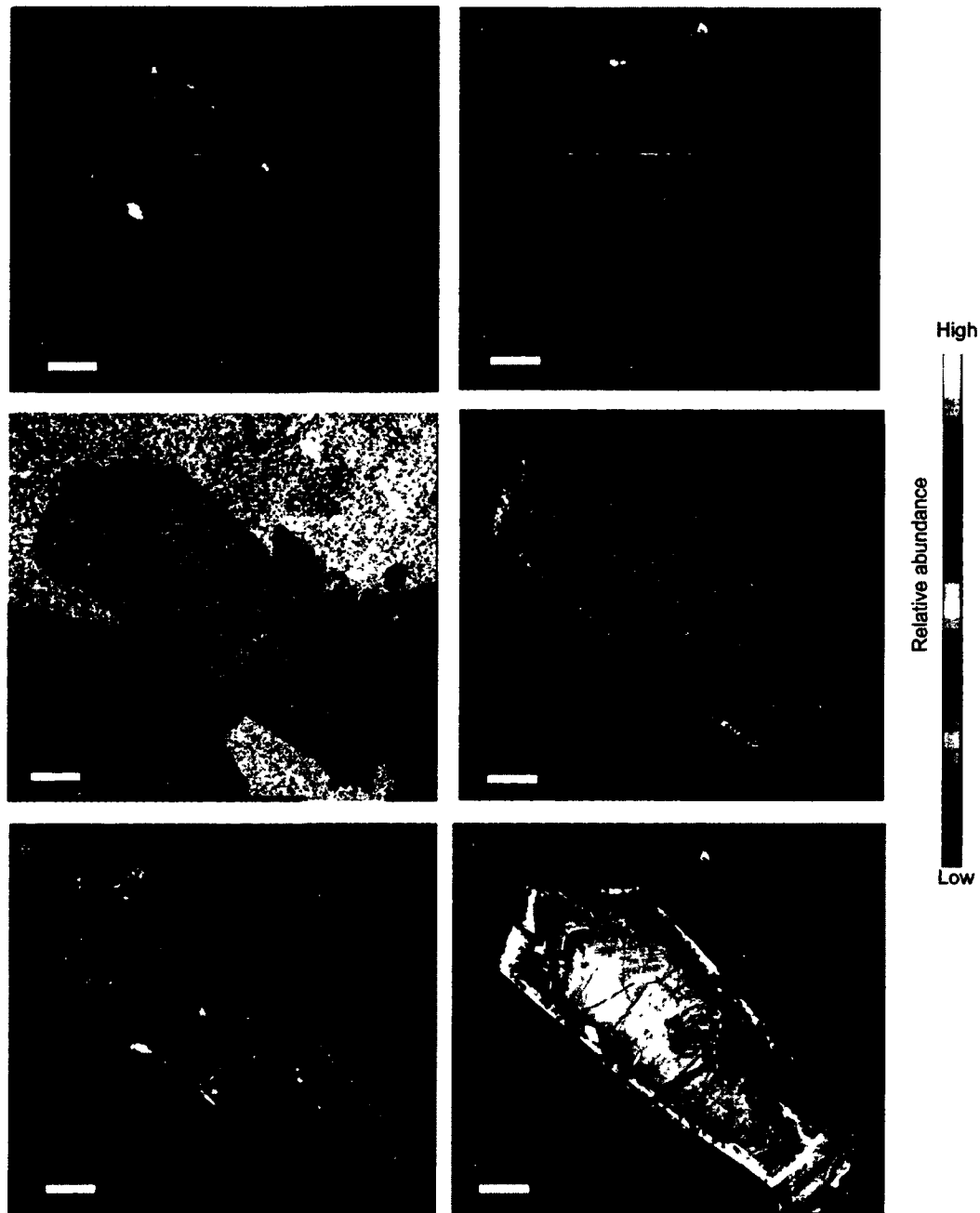
Figure 4-17: X-ray compositional maps (A-E) and BSE image (F) of magmatic allanite
with hydroxylbastnäesite-(Ce) rim and replacement zones (white in Fig. 4-15F) (sample
7658, granite intruding the Byers Brook Formation). The crystal appears inhomogeneous
and shows clear zoning for Ce and Ca (images D and E respectively). The highest
relative abundance of Ce is along the rim of the crystal where hydroxylbastnäsite-(Ce)
has been formed.

in substitutions in common minerals Elements like Zr, Ti and REE show a more

compatible behavior in common granitic melts, but in alkaline melts they tend to

concentrate in late magmatic stages due to the presence of fluorine (Keppler, 1993)

Fractionation can segregate and concentrate them in residual melts where they form their

own minerals such as zircon, monazite, allanite and titanite, if the concentrations are high

enough

4.9.1. Stability conditions and origin of the minerals present

Euhedral **allanite** crystallizes between 760-770 °C under oxygen fugacities close

to NNO and at 7 kbar pressure (Vasquez and Reid, 2004) and the composition of the

analyzed grains (Table 4-3) is characteristic of magmatic crystallization (Meintzer and

Mitchell, 1988) Secondary overgrowths and anhedral crystals (Fig 4c and d) with less

LREE are REE-rich epidotes During post-magmatic alteration mobility of LREE can

result to the formation of REE-rich epidote after allanite's breakdown (Rolland et al ,

2003) Therefore given these geochemical and textural data, we consider the REE-rich

epidotes of post-magmatic origin

The REE titanosilicate **chevkinite-(Ce)** is the dimorph of perrierite-(Ce) The

composition of the grains reported here plot in the chevkinite field of the discrimination

diagram (Fig 4-18) proposed by MacDonald et al (2002) Chevkinite-(Ce) is always

magmatic (Vlach and Gualda, 2007) It is stable in water rich melts at high temperatures

(600-1000 °C at 1-4 kbar), under oxygen fugacities lower than FQM to higher than NNO

(MacDonald et al , 2002) The magmatic origin of chevkinite-(Ce) in the Wentworth

granite can be demonstrated by its presence as inclusions in ferro-edenite (Fig 4-8C and

D), which itself has been interpreted as a magmatic amphibole by Pe-Piper (2007), and
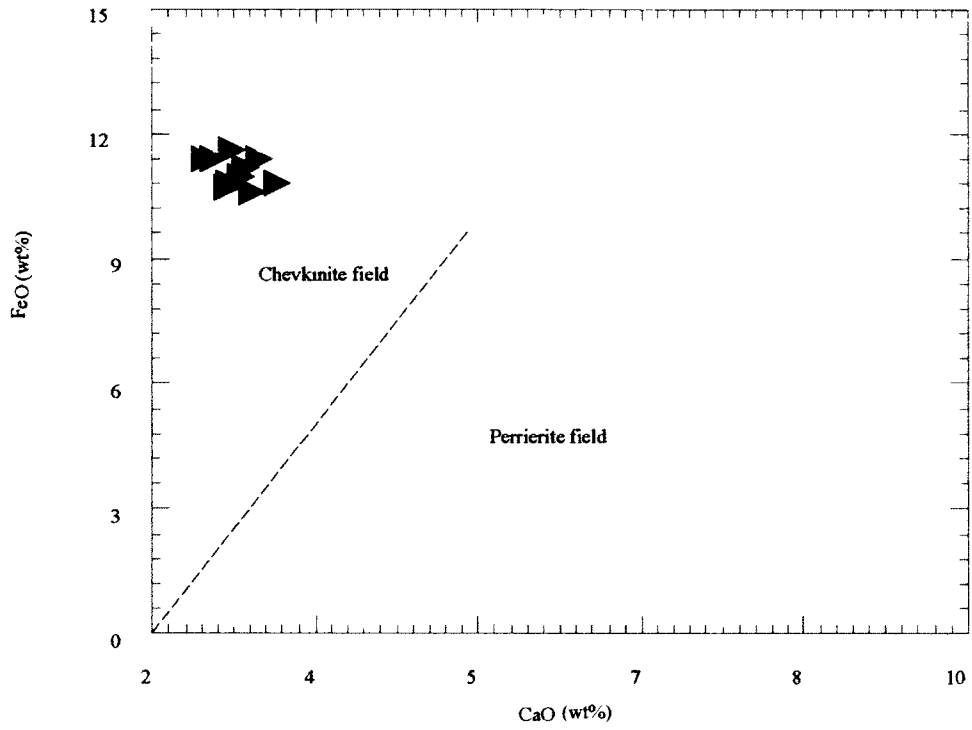
Figure 4-18: Plot of chevkinite grains from the Wentworth granites on a FeO vs CaO

discrimination diagram (after Macdonald and Belkin, 2002).

by the interlocking texture between these two minerals (Fig 4-7E and F) Scaillet and

Macdonald (2001) reported that the stability field of chevkinite-(Ce) increases at high

temperatures and oxidizing conditions In peralkaline granites, it probably crystallizes

under conditions close to water saturation (Vlach and Gualda, 2007) Chevkinite-(Ce)

crystallizes at higher temperatures than allanite-(Ce) and was not found in any of the

early HLBL granites (Table 4-1), indicating that the thermal effect of the later gabbro

intrusion was crucial for the crystallization of this mineral in the anatectic later granites

Jiang et al (2006) suggested that chevkinite-(Ce) can be replaced by allanite-(Ce)

and ilmenite during hydrothermal alteration The Fe-Ti- rich (Table 4-4), yellow

alteration halo observed around many of the chevkinite-(Ce) grains (Fig 4-7 and 4-8) in

the Wentworth granite samples is interpreted as an early stage of chevkinite-(Ce)

breakdown The altered chevkinite-(Ce) also in sample 6490 (Fig 4-9) provides evidence

of enrichment in Ti and depletion in Ca during hydrothermal alteration This Ti

enrichment is associated with the widest fractures (10μm), interpreted as a result of

volume loss during alteration Loss of Ce presumably occurred earlier, as it affected the

entire grain and not just the Ti-rich core (Fig 4-9)

Small euhedral crystals of **hingganite-(Y)** occur adjacent to a larger anhedral

crystal of secondary REE-rich epidote (Fig 4-4C and D) This mode of occurrence

suggests that the hingganite-(Y) predates the epidote and therefore is late magmatic

Yttrium serves as a proxy for the middle and heavy REEs, since they have similar

chemical properties based on their almost identical ionic radii (Krauskopf and Dennis,

2003) Magmatic enrichment in such elements could be expected after the fractionation

of allanite-(Ce) and chevkinite-(Ce) which serve as LREE sinks

Samarskite-(Y) occurs as euhedral small crystals (Fig 4-12A and B), one of them

containing an inclusion of euhedral zircon, and is therefore interpreted as late magmatic

It has similar chemical composition as fergusonite Ercit (2005) introduced

discrimination diagrams for Nb-Y-REE oxides based on statistical models from chemical

alteration trends Canonical variables that can be used in the discrimination diagrams are

calculated for chemical analyses None of the analyses from the Wentworth Pluton plot

within the fergusonite field (Fig 4-19) Therefore, the Nb-Y-REE-mineral in the

Wentworth Pluton granitic samples is considered samarskite-(Y), not fergusonite

Fersmite differs from samarskite-(Y) in the absence of Y and the predominance

of LREE (Table 4-8) Each mineral is found as independent grains, but where both

minerals coexist, the Y-HREE-rich samarskite-(Y) has altered partially to the LREE-rich

fersmite This is indicated by specific textural evidence such as a) most samarskite-(Y)

patches are enclosed by fersmite (Fig 4-12C and D), and b) fersmite appears in more

corroded and fractured parts of the grain where hydrothermal alteration could have been

more intense (Fig 4-12C and D)

The close association of three titanium minerals in one of the studied samples

from the Wentworth granites provides a unique opportunity for the study of Ti behavior

These minerals are **aeschynite-(Y), polycrystalline titanite and a titania mineral**

(TiO₂) and are located together as a composite grain (Fig 4-14). This mode of

occurrence suggests that titanium was mobilized at least locally, so as to form different

mineral phases Titanium can be mobilized and transferred by complexing with carbonate

ions in hydrothermal systems (Parnell, 2004) Furthermore the chemical stability of Ti-

minerals can be affected by high temperatures and SO_4^2 rich fluids (Rabbia et al , 2009

51
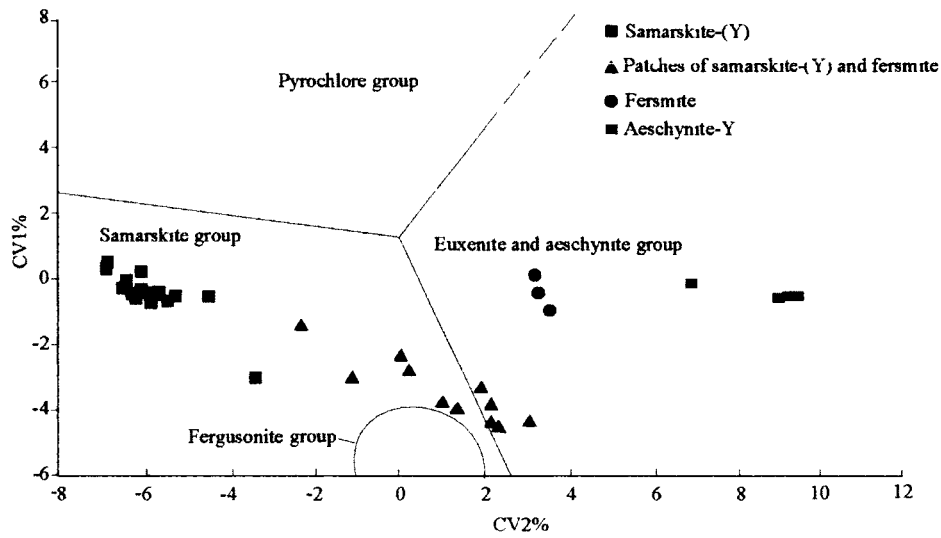
Figure 4-19: Plot of canonical variables CV1 % vs. CV2 % for Nb oxides from the Wentworth granite, in a three-group model introduced by Ercit (2005). CV1= 0.106 Ca - 0.077 Fe + 0.220 Y + 0.280 LREE + 0.137 HREE + 0.100 U +0.304 Ti +0.097 Nb + 0.109 Ta- 12.81. CV2= -0.113 Ca - 0.371 Fe - 0.395 Y - 0.280 LREE - 0.265 HREE- 0.182 U- 0.085 Ti- 0.166 Nb- 0.146Ta + 17.29

and references therein) From textural evidence alone, it is difficult to determine the paragenetic sequence between titanite and the titania mineral (Fig 4-14), however considering that they are hosted in alkaline, Ca-poor igneous rocks some assumptions can be made Clark and Williams-Jones (2004) state that rutile can replace titanite only in rocks with Ca-rich bulk compositions and high carbon values, which cannot apply in the Wentworth A-type granites due to their low Ca On the other hand, Tilley and Eggleton (2005) describe the complete breakdown of titanite to anatase due to hydrothermal alteration Leaching of titanite from mineralizing fluids can result in the formation of titania minerals as described in Abraham and Spooner (1995) in shear zone- related igneous rocks Therefore we interpret that the titania mineral in this sample is a product of titanite alteration

The relationship between titanite and aeschynite-(Y) is more complex The formation of this Y-Ti-Nb oxide is still poorly understood and there is only one report of coexistence of titanite and Y-REE-Ti oxides, specifically yttrobetafite (Liferovich and Mitchell, 2005) In the Wentworth samples, aeschynite-(Y) occurs only together with and in places engulfing polycrystalline titanite (Fig 4-14) This might imply that aeschynite-(Y) post-dates titanite Breakdown of titanite to a titania mineral would release Ca and Si Addition of REEs and Y from hydrothermal fluids to the residual Ti could form an Y-REE-Ti oxide such as aeschynite-(Y), which has a few % more TiO_2 than the surrounding titanite

Textural evidence from the grain of altered (?)chevkinite (Fig 4-9) suggests REE mobility prior to that of Ti as discussed earlier This may also apply to the relationship between the titania mineral and aeschynite-(Y) It is thus suggested that the formation of

aeschynite-(Y), which involves REE mobility, was after titanite and prior to titania mineral, requiring greater Ti-mobility

The alteration of allanite-(Ce) to the F-bearing carbonate **hydroxylbastnäsite-(Ce)** (Fig 4- 4A and B) and the presence of fluorite (Fig 4-13) suggest the presence of F-rich fluids The hydroxylbastnasite-(Ce) found around the rims of primary allanite-(Ce) (Fig 4-4) contains about 60 wt% REE in total (Table 4-10), which is almost twice the concentration of REE in the original allanite Furthermore the presence of secondary REE-rich epidote (Table 4-3) indicates removal of LREE during alteration (Rolland et al . 2003) Such LREE mobility can be influenced by HCO_3^- and SO_4^{2-} in fluids (Rolland et al , 2003, Parnell, 2004) Even though the presence of this carbonate mineral indicates a contribution of CO_2 in the hydrothermal fluids, the importance of CO_2 to REE mobility in the Wentworth pluton is questionable The analyzed grain has low La/Nd ratios (1 3 to 1 4, Table 4-10) and such ratios are related to fluids with amounts of CO_2 below detection limits (Rolland et al , 2003) It is therefore more likely that SO_4^{2-}-rich fluids were responsible for LREE transportation in the hydrothermal system at that stage

The oxidation of **pyrite** to hematite (Fig 4-16) could account for the release of SO_4 in the hydrothermal fluids The presence of hematitic rims around pyrite indicates the breakdown of the latter in temperatures above 450 °C, resulting in the release of sulfur as a volatile phase (Bhargava et al , 2009) The presence of pyrite in the Folly Lake Gabbro and also in the Byers Brook Formation, the volcanic equivalents of the Wentworth granites (Piper et al , 1999) indicates that there was sulfur present in the parent magma during emplacement of the early granites that could mobilize the LREEs when released in the hydrothermal system

Zirconium is generally considered an immobile element and is highly stable in

nonmagmatic environments, however it can be mobile under low temperature

hydrothermal conditions and high pressure metamorphism (Tomaschek et al , 2003,

Rubatto et al , 2008) High F concentrations can also promote Zr mobility (Rubin et al ,

1989) An indication of Zr mobility in the Wentworth granites is the distinct optical and

compositional zoning of the zircons in sample 6518 (Fig 4-11) The rims of these zircons

have less Zr than the core (Table 4-5) and appear porous and fractured These

overgrowths may record Zr mobility in the presence of F-rich fluid Furthermore the

enrichment in Th in the fractured rims of these zircons (Fig 4-11) is interpreted as a

result of hydrothermal alteration and, together with the inclusions of thorite, observed in

fractured magmatic zircons with dusty appearance (Fig 4-10), imply the presence of Th

in hydrothermal fluids

4.9.2. Relationship of minerals to host-rock chemistry

Chevkinite-(Ce) is widely interpreted to occur in rock associations produced

from evolved peralkaline magmas (Troll et al , 2003, Vlach and Gualda, 2007) In

contrast, allanite-(Ce) is the typical REE-rich mineral in many metaluminous and

peraluminous granites (Vlach and Gualda, 2007) The aluminum saturation index

$((A/NK) = molar\ Al_2O_3/(Na_2O + K_2O))$ Maniar and Piccoli, 1989) of all samples from the

Wentworth pluton that contain chevkinite-(Ce) ranges between 1 00 and 1 10, very

similar to that of the allanite-(Ce) bearing samples that ranges between 1 00 and 1 16

(Table 4-1) All these samples that contain either chevkinite-(Ce) or allanite-(Ce), plot in

the lower part of the metaluminous field, close to peralkaline field of Maniar and Piccoli

(1989), with no significant variation This indicates that it was temperature and not the

alkalinity of the parent magma that determined which of these two minerals was formed Magmatic allanite-(Ce) and chevkinite-(Ce) are not known to coexist (Vlach and Gualda, 2007), and this general rule applies to the Wentworth granite

4.9.3. Fluorine abundance

Fluorine abundance appears to be an important factor in the formation of REE and rare metal minerals Uher et al (2009) related the presence of REE-Nb-rich minerals like hingganite, and samarskite to the presence of late-stage, F-rich fluids The separation between HREEs and LREEs depends on their affinity to form complexes with F (Aurisicchio et al , 2001) Fluorine complexes with HREE are more stable compared to those with LREE, which can be mobilized by SO_4^{2-}-rich fluids (Rolland et al , 2003) According to Aurisicchio et al (2001), as the activity of Y and HREEs decreases then the LREEs precipitate from the fluids to form LREE- enriched, late minerals (Fig 4-20)

The presence of F-rich fluids is also suggested by the geochemical features of amphiboles from the Wentworth pluton (Pe-Piper, 2007) Magmatic amphiboles from the early HLBL granites differ from those of the late granites only in having higher fluorine content Breakdown of magmatic amphiboles can lead to the release of fluorine as volatile phase (Schonenberger et al , 2006) The lack of fluorine in the magmatic amphiboles from the late granites suggests that the anatectic process resulted in loss of F in hydrothermal circulation, so that it was less concentrated in the magmas that produced the syn- and post-gabbro granites (Fig 4-20) These late F-rich fluids are presumably related to the mobilization of rare metals and HREEs and the formation of fluorite

The high amounts of fluorine in the early magmatic amphiboles (Pe-Piper, 2007) also indicate that fluorine was in high concentrations in the parent magma Fluorine has
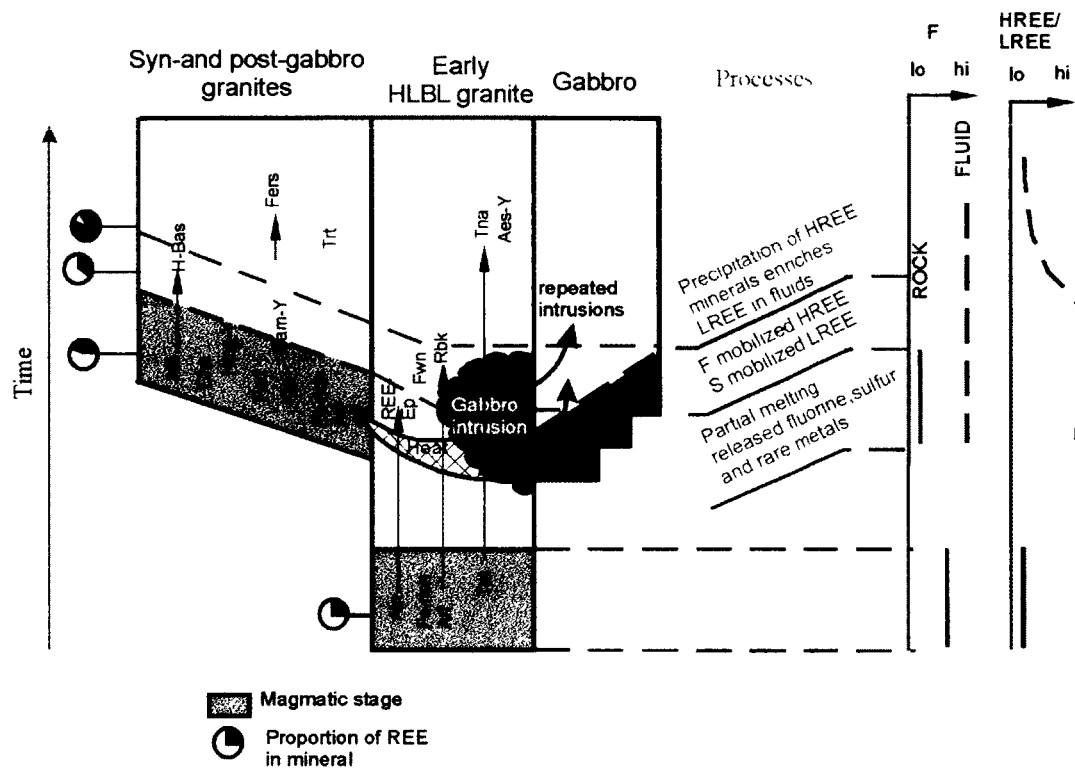
Figure 4-20: Summary of the magmatic processes during the evolution of the
Wentworth Pluton related to the formation of the studied minerals. The left part of this
figure describes the evolution of REE-minerals and amphiboles present in the granites,
from magmatic to hydrothermal stages. Details on geochemical processes and the
evolution of hydrothermal fluids are explained in the right part of the figure. Fed=ferro-
edenite, Fwn=ferrowinchite, Ktp=Katophorite, Arf=arfvedsonite, Tnt=titanite,
Trt=thorite, Ep =epidote, Aln=allanite (abreviations after Whitney and Evans, 2010).
Sam-Y=samarskite-(Y), Hing-Y=hingganite-(Y), Che=chevkinite, Fers=fersmite,
H-bas=hydroxylbastnäsite (abreviations after Orris and Grauch, 2002).
Tna= titania mineral.

the ability to keep zirconium in solution for longer periods and changes the behavior of REEs in the granitic systems increasing the solubility of monazite and xenotime (Keppler, 1993) Zircon is the major sink for rare metals like Th and therefore they were kept in solution, reaching the late stages of magmatic evolution and enriching residual melts

4.9.4. Relationship to pluton evolution

The magmatic and hydrothermal processes that formed the minerals presented here started with the crystallization of the early HLBL granite of the Wentworth pluton This was followed a few million years later by partial melting, which led to the complete anatexis of some of the early granite by the Folly Lake gabbro intrusion (Fig 4-21) During the crystallization of the anatectic syn- and post-gabbro granites, the availability of heat from the gabbroic magma resulted in the crystallization of chevkinite-(Ce) rather than allanite-(Ce) Anatexis resulted in the syn- and post-gabbro granitic magma being depleted in F, Nb, and Th (Koukouvelas et al , 2002, Pe-Piper, 2007) The depletion in these elements after the anatexis suggests that during the partial melting phase some volatiles were released to form a hydrothermal system that was able to transfer some incompatible elements (Fig 4-21) Such volatiles were fluorine, released from the breakdown of amphibole, and sulfur from the decomposition of pyrite Such volatile release may have resulted from reheating of the crystallized early granite, not enough as to cause anatexis but sufficient to mobilize volatiles

The observation of the HREE-rich minerals such as samarskite-(Y) altered to LREE-rich minerals (Fig 4-12C and D) suggests preferential F-complexing of HREE promoting crystallization of HREE minerals, leaving the hydrothermal fluids enriched in
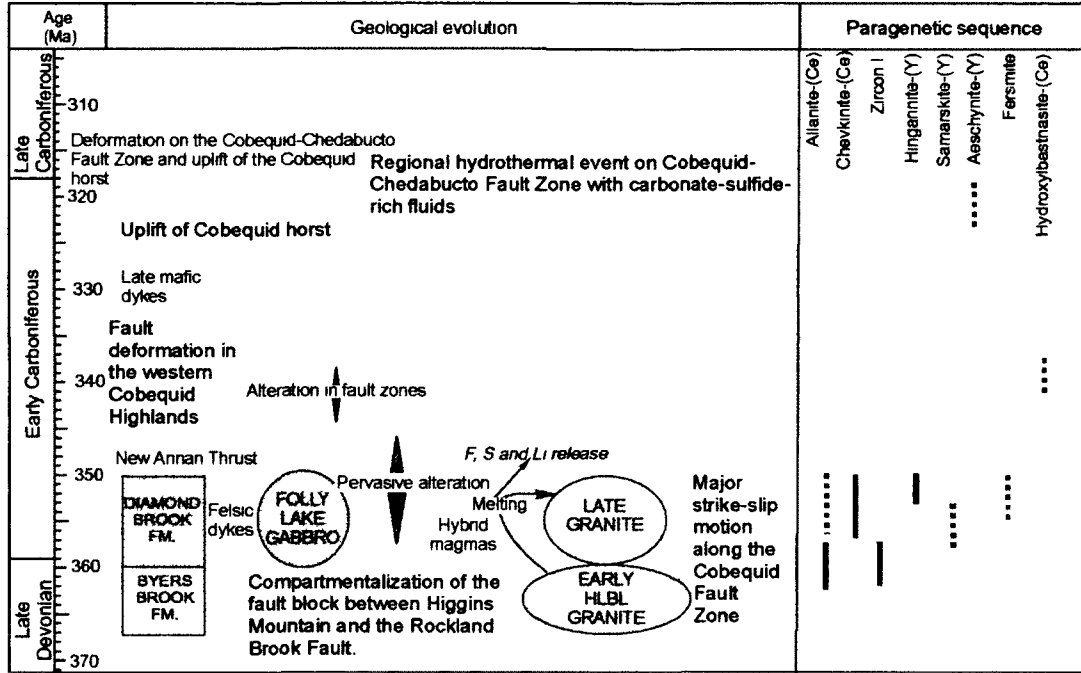
Figure 4-21: Summary of the geological evolution of the Wentworth pluton combined with the paragenetic sequence of the rare earth and rare metal accessory minerals found in the Wentworth granite. Geological evolution synthesized from Pe-Piper and Piper (2002); Koukouvelas et al. (2002); Pe-Piper et al. (2004) and Murphy et al. (2011). Solid lines in the paragenetic sequence represent definite times of formation whereas dashed lines represent probable ones.

less compatible LREE complexed with sulfur (Fig 4-20) It was likely these S-rich hydrothermal fluids that removed LREE from altered (?)chevkinite (Fig 4-9) Resetting of mica ages along the Rockland Brook Fault persisted for about 15 million years after the last major gabbro intrusion (Pe-Piper et al , 2004) suggesting that the observed sequence of mineral alteration could have occurred over a period of tens of millions of years (Fig 4-21)

The evidence of hydrothermal alteration within the pluton cannot be precisely correlated with the phases of hydrothermal circulation Nevertheless, some tentative interpretations can be made Only the 320–315 Ma hydrothermal event appears associated with significant carbonates (e g siderite and ankerite at Londonderry, immediately south of the Folly Lake gabbro Wright, 1975) Thus aeschynite-(Y) and titanite alteration to titania mineral might date from this event when the amount of CO_2 in the fluids was sufficient enough as to promote Ti mobility Evidence from the carbonate hydroxylbastnasite-(Ce) is ambiguous The presence of carbonate suggests high HCO_3^-, but the La/Nd ratios suggest low HCO_3^- (Fig 4-21) This suggests that the formation of hydroxylbastnasite-(Ce) is not necessarily related to the late hydrothermal event with carbonate fluids, but could be related to an earlier hydrothermal system related to the granite emplacement

The main characteristics of many REE-rare metal systems are alkaline magmatism and metasomatism, presence of sodic amphibole and close or direct association with carbonate and metasedimentary rocks (Schmitt et al , 2002, Jiang, 2006, Ridolfi et al , 2006, Saveleva and Karmanov, 2008) Only a few reported REE and rare metal systems involve the effects of more than one intrusive phase In the Bergslagen

60

mining region in Sweden, the mineralization is restricted to marbles and felsic

metavolcanic rocks that have been intruded by at least two generations of plutonic rocks

and hydrothermally altered (Holtstam and Andersson, 2007) Similarities with the

Wentworth pluton are the occurrence of sulfide mineralization and the association of F-

rich minerals with the REEs The Amis Complex in Namibia is another example of a

mineralized, late phase that intruded older anorogenic granites (Schmitt et al , 2002) As

the mineralization is hosted only in that late phase, the importance of anatexis to the

mineralization is not clear The Wentworth pluton on the other hand hosts REE and rare

metal minerals in the granites of both the older and younger phases To the author's

knowledge, no analogues have been found in the literature of anatexis producing

principally silicate minerals and later oxide-dominated hydrothermal minerals

4.10. Conclusions

Based on their respective stability fields and crystallization conditions, the

presence of the REE and rare metal accessory minerals in the Wentworth granite indicate

that they were formed in several stages during the geological evolution of the pluton

The presence of fluorine in the parent magma kept Zr in solution for prolonged

periods and along with it, rare metals like Y, Th and Nb Furthermore, fluorine changed

the behavior of REEs so that monazite-xenotime saturation was never achieved and

allanite-(Ce) was formed in the early Wentworth granite Heat supplied by the

Wentworth gabbro led to the formation of chevkinite-(Ce) in the syn and post-gabbro

granites Fractionation of allanite-(Ce) and chevkinite-(Ce) led to magma enrichment in

middle and heavy rare earths so that hingganite-(Y) was formed during the late magmatic

stages Remelting of the early granite caused F, and S release from the breakdown of

amphibole and pyrite These components circulated through hydrothermal fluids that may

have persisted for at least 15 Ma, based on mica resetting along the Rockland Brook Fault

(Pe-Piper et al, 2004) Yttrium and middle and heavy REE were mobilized by F-

complexing and were the first rare metals to precipitate from these fluids, forming

samarskite-(Y) in late to post-magmatic stages This caused relative LREE enrichment in

the fluid that was influenced by the presence of sulfur LREEs then precipitated, forming

post-magmatic REE-rich epidote, fersmite and most probably hydroxylbastnasite-(Ce)

Carbonate and sulphide-rich fluids were involved in a regional phase of hydrothermal

circulation along the Cobequid-Chedabucto fault at 320-315 Ma These fluids may have

been responsible for a late stage of Ti and REE mobilization aeschynite-(Y) and titanite

alteration to titania mineral could be related to this late event Correlation between

mineral formation and the evolving stages in the Wentworth Pluton provide the record of

a unique mineralizing system which was affected by anatectic processes and changed

from mainly magmatic to hydrothermal

4.11. Acknowledgements

was performed at the facilities of the Regional Analytical Centre at Saint Mary's

University This project was supported by NSERC grants to Dr Georgia Pe-Piper

4.12. CHAPTER 4: APPENDIX

All tables with data cited in chapter 4 can be found in this section following similar format to the general style of peer-reviewed journals, as required for manuscript submission

Table 4-1 Petrology and geochemistry of the studied samples from the Wentworth pluton

Sample	Type (Based on relative age)	Mineral association	ANK	Fe-index	Minerals analyzed
4636	HLBL granite, definite	Qz,Pl,Kfs, Amp (s,s-c),Zrn, qz (sec), clay minerals (sec), REE-ep, Ilm, Mgt	1 16	0 75	Allanite-(Ce), ilmenite, titanian magnetite, titaniferous magnetite, fersmite
9831	HLBL granite, probable	Qz,Pl,Kfs, Bt, Amp (s,s-c),Zrn, Opq, Ap, Aln, Sam-Y, Fers, Qz(sec), mica (sec), clay minerals (sec)	1 04	0 98	Allanite, samarskite, fersmite
9832	HLBL granite, probable	Qz,Pl,Kfs, Bt, Amp (s,s-c),Zrn, Opq, Ap, Aln, Aes-Y, Sam-Y, Fers, Tna, Qz(sec), mica (sec), clay minerals (sec)	1 06	0 95	Allanite-(Ce), zircon, aeschynite-(Y), samarskite-(Y), fersmite, niobian rutile
7658	Granite intruding the Byers Brook Fm	Qz,Pl,Kfs, Bt, Amp (s,s-c),Zrn, Opq, Ap, Qz(sec), Aln, Aes, Bsn, mica (sec), clay minerals (sec)	0 98	0 91	Allanite-(Ce), fersmite, hydroxylbastnasite-(Ce)
5056	Syn-gabbro granite definite	Qz,Pl,Kfs, Bt, Amp (c),Zrn, Ilm, Mgt, Ap, Qz(sec), Mica (sec), clay minerals (sec)	0 84	0 83	Ilmenite, titaniferous magnetite, magnetite
6490	Syn-gabbro granite definite	Qz,Pl,Kfs, Amp (s,s-c),Zrn, Che, mgt, Qz (sec), clay minerals (sec)	1 04	0 97	Chevkinite-(Ce), thorite, titaniferous magnetite, magnetite, samarskite-(Y)
6419	Large post-gabbro bodies of granite, probable	Qz,Pl,Kfs, Amp (s),Zrn,Che, REE-ep, Hng, Opq, mica (sec)	1 11	0 99	Chevkinite-(Ce), allanite-(Ce), zircon, hingganite-(Y)
6518	Large post-gabbro bodies of granite, probable	Qz,Pl,Kfs, Amp (s,s-c),Zrn, Chv, Ilm, Mgt, Bt (sec), Chl (sec)	1 14	0 99	Chevkinite-(Ce), zircon, ilmenite, magnetite
7710	Late fine grained granite dyke	Qz,Pl,Kfs, Amp (s,s-c), Chv, Zrn, Ilm, Mgt, Ep (sec)	1 08	0 96	Chevkinite-(Ce), ilmenite, titanian magnetite, titaniferous magnetite
9827 a	Late fine grained granite dyke	Qz,Pl,Kfs, Bt, Amp (s,s-c),Zrn, Opq, Ap, Qz(sec), Aln, Sam-Y, mica (sec), clay minerals (sec)	0 94	0 9	Allanite-(Ce), samarskite-(Y)
9827b	Late fine grained granite dyke	Qz,Pl,Kfs, Bt, Amp (s,s-c),Zrn, Mag, Ap, Qz(sec), mica (sec), clay minerals (sec), Hem	1 02	0 92	Magnetite, hematite

Notes
1) ANK= alkalinity index $(Al_2O_3/(Na_2O+K_2O)$, after Maniar and Piccoli, 1989), 2) Fe-index= FeOt/ (FeOt+MgO, after Frost et al , 2001), 3) Mineral abbreviations (after Whitney and Evans, 2010) Qz= quartz, Pl= plagioclase, Kfs= K-feldspar, Bt=biotite, Amp=amphibole, Zrn=zircon, Opq= opaque minerals, Ap=apatite, Chl=chlorite, Ep=epidote, (sec)= secondary mineral, (s)=sodic, (s-c)= sodic-calcic, (c)=calcic

Table 4-2 Conditions and standards used for microprobe analyses

Element	Line	Peak Position	Standard	Crystal	Detection limit (wt%)	Correction Factors (peak overlap correction)
P	Kα	197 327	Monazite	PETJ	0 003	
Nb	Lα	183 487	Columbite	PETJ	0 066	
Ta	Lα	106 200	Tantalite	LIFH	0 000	
Si	Kα	77 531	Sanidine	TAP	0 003	
Ti	Kα	88 207	Kaersutite	PETJ	0 028	Ti-Hf 0 05429
Th	Mα	132 606	ThO₂_MAX	PETJ	0 000	
U	Mβ	119 104	UO₂	PETJ	0 000	
Zr	Lα	194 590	Zirconia	PETJ	0 000	Zr-P 0 00110
Hf	Lα	109 527	Zirconia	LIFH	0 000	Hf-Ho 0 05675 and Hf-Er 0 53361
Y	Lα	70 180	YAG	TAP	0 000	
Al	Lα	90 712	Sanidine	TAP	0 014	
La	Lα	185 485	LaPO₄_MAX	LIF	0 002	
Ce	Lα	178 226	CePO₄_MAX	LIF	0 000	
Pr	Lβ	157 292	REE3 (Drake and Weill, 1972)	LIFH	0 002	
Nd	Lβ	150 924	REE2 (Drake and Weill, 1972)	LIFH	0 000	
Sm	Lβ	139 251	REE2 (Drake and Weill, 1972)	LIFH	0 001	
Eu	Lα	147 767	REE1 (Drake and Weill, 1972)	LIFH	0 005	
Gd	Lβ	128 794	REE1 (Drake and Weill, 1972)	LIFH	0 000	
Dy	Lα	132 811	REE4 (Drake and Weill, 1972)	LIF	0 000	
Ho	Lα	128 629	REE4 (Drake and Weill, 1972)	LIFH	0 000	
Er	Lα	124 120	REE4 (Drake and Weill, 1972)	LIF	0 000	Er-Nb 0 08450 and Er Hf 0 00263
Yb	Lα	116 276	REE2 (Drake and Weill, 1972)	LIF	0 001	
Fe	Kα	199 338	Magnetite53	LIF	0 002	
Mn	Kα	146 214	Pyrolusite	LIF	0 010	
Ca	Kα	107 711	F-apatite	PETJ	0 000	
F	Kα	199 338	F-apatite	TAPH	0 010	F-Ce 0 05096

Representative microprobe analyses of silicate minerals
Table 4-3 Allanite-(Ce) and REE-rich epidote

Sample	4636	6419	6419	7658	9827A	9827A	9831	9832
Mineral	ep	ep	ep	ep	aln	aln	aln	aln
Analysis	99	87	88	73	239	240	215	230
P_2O_5	0 02	b d	b d	0 02	0 04	0 08	b d	b d
Nb_2O_5	0 07	0 06	b d	b d	0 04	0 01	b d	0 09
Ta_2O_5	0 15	b d	b d	b d	b d	b d	0 04	0 00
SiO_2	34 94	34 97	35 87	33 88	31 13	31 05	33 15	32 73
TiO_2	0 57	b d	b d	0 10	0 05	0 34	0 11	0 23
ZrO_2	b d	b d	b d	b d	b d	b d	b d	b d
ThO_2	0 09	0 03	0 11	b d	0 13	0 11	0 06	b d
UO_2	0 10	0 01	0 01	0 09	b d	b d	0 06	b d
Al_2O_3	14 45	14 49	19 42	16 14	14 71	14 45	16 79	18 29
Y_2O_3	0 28	0 29	1 40	0 11	0 50	0 73	0 04	0 24
La_2O_3	1 76	2 88	2 24	3 25	5 16	4 44	4 68	5 26
Ce_2O_3	4 61	5 72	3 63	7 66	11 10	11 27	14 10	9 83
Pr_2O_3	0 57	0 53	0 41	0 88	1 18	1 26	1 09	0 95
Nd_2O_3	2 34	2 15	1 56	2 61	4 09	4 23	2 56	2 57
Sm_2O_3	0 51	0 43	0 33	0 35	0 64	0 82	0 13	0 22
Eu_2O_3	0 11	0 13	0 13	0 22	0 31	0 28	0 23	0 19
Gd_2O_3	0 22	0 25	0 52	0 12	0 48	0 59	0 03	0 11
Dy_2O_3	0 21	0 08	0 33	0 20	0 47	0 66	0 22	0 17
Ho_2O_3	b d	b d	0 06	b d	b d	0 09	b d	b d
Er_2O_3	b d	0 04	0 01	0 15	0 09	0 20	b d	b d
Yb_2O_3	b d	b d	b d	b d	b d	b d	b d	b d
FeOt	19 60	18 16	14 39	16 48	15 93	14 81	14 31	12 20
MnO	0 11	0 07	0 12	0 34	0 77	1 19	0 42	0 42
CaO	16 47	15 77	16 77	14 33	10 15	10 26	10 81	12 67
F	b d	b d	b d	b d	b d	b d	b d	b d
Total	97 19	96 04	97 30	96 94	96 96	96 95	98 82	96 17
Norm	Σ=8	Si=3	Si=3	Si=3	Σ=8	Σ=8	Si=3	Si=3
Si	3 029	3 000	3 000	3 000	3 029	3 036	3 000	3 000
Al	0 000	0 000	0 000	0 000	0 000	0 000	0 000	0 000
ΣZ	3.029	3.000	3.000	3.000	3.029	3.036	3 000	3.000
Ti	0 038	0 000	0 000	0 007	0 004	0 025	0 007	0 016
Al	1 505	1 538	1 970	1 727	1 687	1 665	1 854	2 010
Fe	1 448	1 368	1 036	1 252	1 297	1 211	1 122	0 951
Mn	0 009	0 005	0 008	0 026	0 063	0 099	0 034	0 033
Σ M	3.000	2.911	3 014	3 012	3.050	3.000	3 017	3.011
Ca	1 559	1 522	1 546	1 394	1 058	1 075	1 085	1 265
La	0 057	0 096	0 071	0 109	0 185	0 160	0 162	0 181
Ce	0 149	0 189	0 114	0 255	0 396	0 403	0 484	0 336
Pr	0 018	0 017	0 013	0 029	0 042	0 045	0 037	0 032
Nd	0 074	0 069	0 048	0 085	0 142	0 148	0 086	0 085
Sm	0 015	0 013	0 010	0 011	0 021	0 028	0 004	0 007
Eu	0 003	0 004	0 004	0 007	0 010	0 009	0 007	0 006
Gd	0 007	0 007	0 015	0 004	0 015	0 019	0 001	0 003
Dy	0 006	0 002	0 009	0 006	0 015	0 021	0 007	0 005
Ho	0 000	0 000	0 002	0 000	0 000	0 003	0 000	0 000
Er	0 000	0 001	0 000	0 004	0 003	0 006	0 000	0 000
Yb	0 000	0 000	0 000	0 000	0 000	0 000	0 000	0 000
Th	0 002	0 001	0 002	0 000	0 003	0 002	0 001	0 000
U	0 002	0 000	0 000	0 002	0 000	0 000	0 001	0 000
Nb	0 003	0 002	0 000	0 000	0 002	0 001	0 000	0 004
Ta	0 004	0 000	0 000	0 000	0 000	0 000	0 001	0 000
Zr	0 000	0 000	0 000	0 000	0 000	0 000	0 000	0 000
Y	0 013	0 014	0 064	0 005	0 026	0 038	0 002	0 012
ΣREE	0 330	0 400	0 290	0 510	0 830	0 840	0 790	0 660
Σ A	1 912	1 938	1 899	1 910	1.917	1.958	1 877	1.937

Notes
b d⁻ below detection limit Elements calculated in the basis of 8 cations When calculations yielded Si> 3 05 then it is normalized to Si-=3 (Armbruster et al , 2006)

Representative microprobe analyses of silicate minerals

Table 4-4 Chevkinite-(Ce)

Sample	6518	6518	6518	6518	6518	7710	7710	7710
Analysis	71	72	74	80	82	70	89	122
P_2O_5	0 04	0 02	0 05	0 04	0 05	0 u5	0 05	0 37
Nb_2O_5	0 75	0 80	0 78	0 79	0 55	2 16	0 97	3 10
Ta_2O_5	b d	b d	b d	b d	b d	b d	b d	b d
SiO_2	20 06	19 97	20 43	20 37	20 32	19 82	20 38	18 26
TiO_2	19 15	18 72	18 30	18 66	18 62	16 88	18 09	19 89
ZrO_2	0 70	0 40	0 66	0 46	0 55	0 33	0 38	0 46
HfO_2	b d	0 114	b d	b d	b d	b d	b d	0 09
ThO_2	0 41	0 16	0 45	0 34	0 30	0 88	0 38	1 72
UO_2	b d	0 06	b d	b d	b d	0 10	0 11	0 04
Al_2O_3	0 12	0 13	0 13	0 11	0 10	0 11	0 12	0 21
Y_2O_3	0 56	0 58	0 59	0 63	0 67	0 76	0 76	1 02
La_2O_3	10 69	10 90	10 67	10 69	10 81	10 90	10 32	10 20
Ce_2O_3	21 03	21 06	20 32	20 90	20 53	20 77	21 12	18 23
Pr_2O_3	1 95	1 74	1 87	1 85	1 92	1 85	2 10	1 67
Nd_2O_3	8 83	8 98	8 96	8 54	8 64	7 76	9 22	6 28
Sm_2O_3	1 20	1 00	0 92	0 94	0 88	0 90	1 24	0 82
Eu_2O_3	0 60	0 55	0 61	0 52	0 57	0 63	0 67	0 43
Gd_2O_3	0 57	0 54	0 72	0 73	0 46	0 57	0 70	0 61
Dy_2O_3	0 17	0 30	0 26	0 30	0 31	0 33	0 30	0 33
Ho_2O_3	b d	b d	b d	b d	b d	b d	b d	b d
Er_2O_3	0 12	b d	0 04	0 06	0 06	b d	0 07	b d
Yb_2O_3	b d	b d	b d	b d	b d	b d	b d	b d
FeOt	11 07	11 61	10 88	10 79	10 86	11 62	11 58	11 98
MgO	b d	0 04	0 05	0 02	0 01	0 08	0 07	b d
MnO	0 01	b d	0 00	0 01	b d	0 02	b d	0 02
CaO	2 78	2 61	2 61	2 69	2 64	2 56	2 43	3 16
F	b d	b d	b d	b d	b d	b d	b d	b d
Total	100 784	100 267	99 272	99 42	98 845	99 061	101 047	98 89
Y	0 060	0 064	0 065	0 069	0 073	0 084	0 083	0 111
Th	0 019	0 007	0 021	0 016	0 014	0 042	0 017	0 080
La	0 802	0 823	0 809	0 808	0 822	0 838	0 776	0 769
Ce	1 566	1 580	1 529	1 569	1 549	1 585	1 577	1 364
Pr	0 144	0 130	0 140	0 138	0 144	0 140	0 156	0 124
Nd	0 641	0 657	0 658	0 625	0 636	0 577	0 671	0 458
Sm	0 084	0 071	0 065	0 066	0 062	0 064	0 087	0 058
Eu	0 041	0 038	0 042	0 036	0 040	0 045	0 047	0 030
Gd	0 039	0 037	0 049	0 050	0 031	0 039	0 047	0 042
Dy	0 011	0 020	0 017	0 020	0 020	0 022	0 020	0 022
Ho	0 000	0 000	0 000	0 000	0 000	0 000	0 000	0 000
Er	0 007	0 000	0 002	0 004	0 004	0 000	0 004	0 000
Yb	0 000	0 000	0 000	0 000	0 000	0 000	0 000	0 000
Ca	0 605	0 573	0 575	0 590	0 583	0 571	0 531	0 692
Sum A	4.019	3.999	3 972	3.991	3.979	4 007	4.016	3.748
Fe	1 000	1 000	1 000	1 000	1 000	1 000	1 000	1 000
Mn	0 000	0 000	0 000	0 000	0 000	0 000	0 000	0 000
Mg	0 000	0 000	0 000	0 000	0 000	0 000	0 000	0 000
Sum B	1.000	1.000	1.000	1.000	1.000	1.000	1.000	1.000
Fe	0 881	0 998	0 870	0 850	0 872	1 024	0 975	1 047
Mn	0 001	0 000	0 000	0 001	0 000	0 004	0 000	0 004
Mg	0 000	0 012	0 014	0 006	0 003	0 026	0 021	0 000
Ti	0 928	0 884	0 828	0 878	0 885	0 645	0 775	1 057
Al	0 029	0 030	0 031	0 025	0 025	0 027	0 028	0 050
Zr	0 070	0 040	0 066	0 046	0 055	0 034	0 038	0 045
Nb	0 069	0 074	0 073	0 074	0 052	0 204	0 090	0 286
Ta	0 000	0 000	0 000	0 000	0 000	0 000	0 000	0 000
Sum C	1.978	2.038	1.881	1.880	1.892	1 963	1 926	2.490
Ti (D)	2 000	2 000	2 000	2 000	2 000	2 000	2 000	2 000
Si	4 077	4 090	4 199	4 177	4 186	4 130	4 157	3 731
Σcations	13.073	13.128	13 052	13 049	13.057	13 100	13 099	12 969

Notes

b d= below detection limit Analysis 122 represents a yellowish alteration halo around chevkinite Formula calculated in the basis of 22 oxygens

68

Representative microprobe analyses of silicate minerals
Table 4-5. Zircon

Sample	6419	6419	6518	6518	6518	9832
Analysis	120*	121	154	155	157	197*
P_2O_5	b d	0 28	b d	0 21	0 51	0 39
Nb_2O_5	b d	b d	b d	b d	b d	0 12
Ta_2O_5	b d	0 06	b d	b d	0 10	b d
SiO_2	30 31	30 58	32 61	31 69	30 16	30 99
TiO_2	0 02	b d	b d	b d	b d	b d
ZrO_2	67 34	63 88	63 74	59 40	54 79	60 47
HfO_2	0 81	1 24	0 85	0 92	2 52	1 66
ThO_2	0 00	0 13	b d	0 44	4 01	1 22
UO_2	0 11	0 10	0 03	0 35	0 22	0 36
Al_2O_3	b d	b d	b d	0 02	0 01	b d
Y_2O_3	0 23	1 28	0 18	2 68	2 96	2 42
La_2O_3	b d	b d	b d	b d	b d	b d
Ce_2O_3	0 07	0 06	0 03	0 03	0 08	0 01
Pr_2O_3	0 01	b d	0 02	b d	b d	b d
Nd_2O_3	0 00	0 00	0 01	0 03	0 15	0 02
Sm_2O_3	b d	b d	0 10	0 11	0 12	b d
Eu_2O_3	0 00	0 04	0 03	0 04	0 05	0 02
Gd_2O_3	0 22	0 10	b d	0 08	0 17	0 35
Dy_2O_3	0 10	0 09	0 14	0 31	0 25	0 43
Ho_2O_3	b d	0 08	b d	0 03	0 10	0 13
Er_2O_3	0 03	0 36	0 10	0 43	0 44	0 66
Yb_2O_3	0 04	0 32	0 13	0 37	0 48	0 96
FeOt	0 04	0 06	0 06	0 17	0 60	0 19
MnO	b d	0 03	b d	0 01	0 06	b d
CaO	0 02	0 04	b d	0 05	0 08	0 10
Total	99 35	98 72	98 04	97 36	97 85	100 51
P	0.000	0.007	0.000	0.006	0.014	0.010
Nb	0.000	0.000	0.000	0.000	0.000	0.002
Ta	0.000	0.001	0.000	0.000	0.001	0.000
Si	0.952	0.967	1.016	1 009	0 988	0.976
Ti	0.000	0.000	0.000	0.000	0.000	0.000
Zr	1.032	0.985	0.969	0.922	0 875	0.929
Hf	0.007	0.011	0.008	0.008	0.024	0.015
Th	0.000	0.001	0.000	0.003	0 030	0.009
U	0.001	0.001	0.000	0.003	0.002	0.003
Al	0.000	0.000	0.000	0.001	0.000	0.000
Y	0.004	0.022	0.003	0.045	0.052	0.041
La	0.000	0.000	0.000	0.000	0.000	0.000
Ce	0.001	0.001	0.000	0.000	0.001	0.000
Pr	0.000	0.000	0.000	0.000	0 000	0.000
Nd	0.000	0.000	0.000	0.000	0.002	0.000
Sm	0.000	0.000	0.001	0.001	0.001	0.000
Eu	0 000	0.000	0.000	0.000	0.001	0.000
Gd	0.002	0.001	0.000	0.001	0.002	0.004
Dy	0.001	0.001	0.001	0.003	0.003	0.004
Ho	0.000	0.001	0.000	0.000	0.001	0 001
Er	0.000	0.004	0.001	0.004	0.005	0.007
Yb	0.000	0.003	0.001	0.004	0.005	0.009
Fe	0.001	0.002	0.002	0.005	0.017	0.005
Mn	0.001	0.001	0.000	0.000	0.002	0 000
Ca	0 000	0.001	0 000	0.002	0.003	0.003
Total	2.003	2.002	1.999	2.013	2.013	2.010

Notes
1) *=analysis with good totals. 2)b d= below detection limit Formula calculated in the basis of 4 oxygen atoms

69

Representative microprobe analyses of silicate minerals

Table 4-6 Hingganite-(Y)

Sample	6419	6419	6419	6419
Analysis	86	143	145	146
P_2O_5	0 00	0 00	0 00	0 00
Nb_2O_5	b d	b d	b d	b d
Ta_2O_5	0 00	0 00	0 01	0 00
SiO_2	26 38	25 98	24 61	25 03
TiO_2	0 00	0 00	0 04	0 03
ThO_2	0 00	0 04	0 12	0 12
UO_2	0 04	0 00	0 09	0 11
Al_2O_3	b d	b d	b d	b d
Y_2O_3	26 43	31 30	18 22	18 29
La_2O_3	0 82	0 26	0 95	1 05
Ce_2O_3	4 40	1 77	7 56	7 84
Pr_2O_3	0 83	0 33	1 68	1 73
Nd_2O_3	5 50	3 37	10 36	10 77
Sm_2O_3	2 27	1 59	2 62	2 66
Eu_2O_3	0 31	0 14	0 68	0 72
Gd_2O_3	4 46	5 01	4 50	4 56
Dy_2O_3	4 56	5 04	3 83	3 83
Ho_2O_3	1 59	1 61	1 37	1 38
Er_2O_3	1 90	2 72	1 38	1 62
Yb_2O_3	1 04	1 42	0 35	0 35
FeOt	4 95	3 85	6 01	6 06
CaO	1 17	0 91	0 81	0 81
Total	86 66	85 35	85 17	86 98
P	0 000	0 000	0 000	0 000
Si	2 000	2 000	2 000	2 000
Sum T	**2.000**	**2.000**	**2.000**	**2.000**
Ti	0 000	0 000	0 005	0 004
Th	0 000	0 001	0 005	0 004
U	0 001	0 000	0 003	0 004
Y	1 081	1 263	0 813	0 801
La	0 023	0 007	0 029	0 032
Ce	0 124	0 049	0 232	0 236
Pr	0 023	0 009	0 051	0 052
Nd	0 151	0 091	0 310	0 316
Sm	0 060	0 042	0 076	0 075
Eu	0 008	0 004	0 019	0 020
Gd	0 114	0 126	0 125	0 124
Dy	0 113	0 123	0 103	0 101
Ho	0 039	0 039	0 037	0 036
Er	0 046	0 065	0 036	0 042
Yb	0 024	0 033	0 009	0 009
Ca	0 193	0 148	0 146	0 143
Sum A	**2.000**	**2.000**	**2.000**	**2.000**
Fe	0 314	0 248	0 408	0 405

Notes

1)b d= below detection limit, 2) n d = not determined Formula calculated on the basis of 10 oxygens, Si+P = 2 atoms, Ca+Y+REE=2 atoms, Be=2 atoms according to the theoretical formula of hingganite However Be was not determined

70

Representative microprobe analyses of silicate minerals.
Table 4-7: Thorite

Sample	6490	9832	9832
Analysis	97	199	210
P_2O_5	4 47	0 22	0 71
Nb_2O_5	7 72	6 78	0 15
Ta_2O_5	b d	b d	b d
SiO_2	12 83	18 57	17 20
TiO_2	3 26	0 32	0 02
ZrO_2	n d	11 31	1 39
HfO_2	n d	0 47	0 29
ThO_2	49 43	40 53	58 67
UO_2	0 76	1 41	3 53
Al_2O_3	1 02	0 33	0 15
Y_2O_3	2 12	2 93	1 64
La_2O_3	0 12	0 07	0 13
Ce_2O_3	0 37	0 27	0 20
Pr_2O_3	0 09	0 01	b d
Nd_2O_3	0 45	0 18	b d
Sm_2O_3	0 19	b d	b d
Eu_2O_3	0 01	b d	0 01
Gd_2O_3	0 33	0 17	0 46
Dy_2O_3	0 49	0 39	0 52
Ho_2O_3	0 10	0 17	0 18
Er_2O_3	b d	0 00	0 31
Yb_2O_3	0 14	0 46	0 21
FeOt	9 42	1 38	1 67
MnO	b d	0 12	0 05
CaO	0 30	1 36	1 86
F	b d	0 34	0 56
Total	93 64	87 62	89 67
P	0 180	0.009	0.033
Nb	0 166	0.149	0.004
Ta	0 000	0.000	0.000
Si	0 610	0.899	0.957
Ti	0 117	0.011	0.001
Al	0 057	0.019	0.010
Zr	0 000	0.267	0.038
Hf	0 000	0.006	0.005
Th	0 535	0.447	0.743
U	0 008	0.015	0.044
Y	0 054	0.076	0.049
La	0 002	0.001	0.003
Ce	0 006	0.005	0.004
Pr	0 001	0.000	0.000
Nd	0 008	0.003	0.000
Sm	0 003	0 000	0.000
Eu	0 000	0.000	0.000
Gd	0 005	0.003	0.009
Dy	0 008	0.006	0.009
Ho	0 002	0.003	0.003
Er	0 000	0.000	0.005
Yb	0 002	0.007	0.004
Fe	0 374	0.056	0.078
Mn	0 000	0.005	0.002
Ca	0 000	0 071	0.111
Sum	**2.138**	**2.057**	**2.110**

Notes
1)b d= below detection limit, 2) n d ¬ not determined Formula calculated on the basis of 4 oxygens

Representative microprobe analyses of oxides
Table 4-8 Samarskite-(Y) and fersmite

Mineral	Sam	Sam	Sam	Sam	Sam	Fers	Fers	Fers
Sample	6490	9827A	9831	9831	9832	4636	9832	9832
Analysis	98*	174	242	243	231*	103*	213	214*
P_2O_5	b d	b d	b d	b d	0 01	b d	0 01	b d
Nb_2O_5	48 32	42 25	47 35	47 44	53 06	45 20	53 23	55 56
Ta_2O_5	0 45	2 73	0 29	0 10	0 61	8 22	3 87	3 76
SiO_2	0 51	0 37	b d	0 02	2 25	8 76	0 17	0 14
TiO_2	1 13	1 43	0 31	0 41	1 61	9 51	6 55	6 44
ZrO_2	b d	b d	b d	0 01	b d	b d	0 41	0 76
HfO_2	b d	b d	0 09	b d	0 07	b d	0 17	b d
ThO_2	5 13	5 77	1 62	1 85	0 18	1 83	0 34	0 38
UO_2	2 36	3 04	0 69	0 92	0 59	5 75	3 34	3 34
Al_2O_3	b d	b d	b d	b d	0 56	b d	b d	b d
Y_2O_3	22 27	23 69	21 36	21 16	22 27	1 75	0 32	0 27
La_2O_3	0 20	b d	0 27	0 29	0 35	0 57	1 17	1 30
Ce_2O_3	1 97	0 45	1 98	2 18	2 35	2 56	4 22	3 84
Pr_2O_3	0 30	0 10	0 47	0 55	0 37	0 44	0 43	0 34
Nd_2O_3	2 06	1 36	3 86	4 08	2 35	1 61	1 95	1 59
Sm_2O_3	0 86	0 99	2 16	2 28	0 95	0 47	0 39	0 36
Eu_2O_3	0 06	0 01	0 11	0 17	0 23	0 08	0 17	0 14
Gd_2O_3	2 43	3 66	5 91	5 60	1 98	0 41	0 39	0 26
Dy_2O_3	3 23	3 74	5 75	5 73	2 14	0 38	0 42	0 45
Ho_2O_3	1 10	1 67	2 56	2 56	0 75	0 02	b d	0 09
Er_2O_3	b d	b d	b d	b d	b d	b d	b d	b d
Yb_2O_3	2 67	2 92	1 19	1 13	1 30	0 06	b d	b d
FeOt	0 43	0 67	0 02	0 09	1 78	0 15	2 53	0 60
MnO	b d	b d	b d	b d	0 11	b d	0 48	0 47
CaO	1 30	1 51	0 27	0 27	0 92	10 26	14 37	17 68
F	0 09	0 18	b d	0 23	0 13	0 21	0 81	0 90
Total	96 84	96 48	96 25	96 98	96 86	98 15	95 40	98 31

Samarskite cations (basis of 4 oxygens):

	Sam 6490 98*	Sam 9827A 174	Sam 9831 242	Sam 9831 243	Sam 9832 231*
P	0 000	0 000	0 000	0 000	0 000
Nb	0 993	0 900	1 009	1 006	1 004
Ta	0 006	0 035	0 004	0 001	0 007
Si	0 023	0 018	0 000	0 001	0 094
Ti	0 039	0 051	0 011	0 014	0 051
Sum B	**1.060**	**1.003**	**1.024**	**1.023**	**1.156**
Zr	0 000	0 000	0 000	0 000	0 000
Hf	0 000	0 000	0 001	0 000	0 001
Th	0 053	0 062	0 017	0 020	0 002
U	0 024	0 032	0 007	0 010	0 005
Al	0 000	0 000	0 000	0 000	0 028
Y	0 539	0 594	0 536	0 528	0 496
La	0 003	0 000	0 005	0 005	0 005
Ce	0 033	0 008	0 034	0 037	0 036
Pr	0 005	0 002	0 008	0 009	0 006
Nd	0 033	0 023	0 065	0 068	0 035
Sm	0 013	0 016	0 035	0 037	0 014
Eu	0 001	0 000	0 002	0 003	0 003
Gd	0 037	0 057	0 092	0 087	0 028
Dy	0 047	0 057	0 087	0 087	0 029
Ho	0 016	0 025	0 038	0 038	0 010
Er	0 000	0 000	0 000	0 000	0 000
Yb	0 037	0 042	0 017	0 016	0 017
Fe	0 017	0 026	0 001	0 004	0 062
Mn	0 000	0 000	0 000	0 000	0 004
Ca	0 063	0 076	0 013	0 014	0 041
Sum A	**0.921**	**1.020**	**0.960**	**0.963**	**0.821**

Fersmite cations (basis of 6 oxygens):

	Fers 4636 103*	Fers 9832 213	Fers 9832 214*
Nb	1 384	1 476	1 519
Ta	0 151	0 065	0 062
Ti	0 484	0 302	0 293
Al	0 000	0 000	0 000
Fe	0 008	0 130	0 030
Sum B	**2.028**	**1.972**	**1.905**
Th	0 028	0 005	0 005
U	0 087	0 046	0 045
Y	0 063	0 126	0 009
La	0 013	0 026	0 029
Ce	0 063	0 095	0 085
Ca	0 744	0 944	1 146
Sum A	**0.999**	**1.242**	**1.319**

Notes
1)*=analysis with good totals, 2)b d= below detection limit, 3) n d = not determined, 4) Sam=samarskite, 5)Fers= fersmite Elements calculated in the basis of 4 oxygens for samarskite and 6 oxygen atoms for fermite

Representative microprobe analyses of oxides
Table 4-9 Aeschynite-(Y) and Titania mineral

Mineral	Aes-Y	Aes-Y	Aes-Y	Aes-Y	Tna
Sample	9832	9832	9832	9832	9832
Analysis	232	236	217	218	237
P_2O_5	0.05	0.01	0.03	0.05	0.01
Nb_2O_5	9.62	6.70	5.06	4.21	2.82
Ta_2O_5	b.d	b.d	0.04	0.21	0.08
SiO_2	4.45	1.73	1.60	1.45	0.12
TiO_2	39.03	42.90	45.36	45.67	91.60
ZrO_2	b.d	b.d	b.d	b.d	0.02
HfO_2	b.d	b.d	b.d	b.d	0.21
ThO_2	1.33	0.39	0.13	0.17	0.02
UO_2	0.27	0.19	0.13	b.d	0.02
Al_2O_3	0.34	0.07	0.11	0.08	b.d
Y_2O_3	20.10	24.45	25.74	25.17	b.d
La_2O_3	0.02	b.d	b.d	b.d	b.d
Ce_2O_3	b.d	b.d	b.d	b.d	b.d
Pr_2O_3	0.16	0.05	b.d	b.d	b.d
Nd_2O_3	1.42	0.95	0.68	0.83	b.d
Sm_2O_3	0.95	1.00	0.39	0.61	b.d
Eu_2O_3	0.17	0.01	0.01	0.01	0.06
Gd_2O_3	4.74	4.43	3.23	3.91	0.04
Dy_2O_3	4.23	4.45	3.69	4.24	0.03
Ho_2O_3	1.78	1.88	1.36	1.60	0.05
Er_2O_3	1.67	1.78	2.85	2.53	b.d
Yb_2O_3	1.53	1.55	2.66	2.57	0.02
FeOt	1.85	1.46	1.43	1.45	1.24
MnO	0.15	0.02	0.05	0.02	0.01
CaO	1.12	0.56	0.42	0.31	0.28
F	0.21	0.06	0.11	0.05	0.01
Total	95.10	94.62	95.03	95.13	96.65
Al	0.021	0.005	0.007	0.005	0.000
Y	0.553	0.681	0.704	0.691	0.000
La	0.000	0.000	0.000	0.000	0.000
Ce	0.000	0.000	0.000	0.000	0.000
Pr	0.003	0.001	0.000	0.000	0.000
Nd	0.026	0.018	0.012	0.015	0.000
Sm	0.017	0.018	0.007	0.011	0.000
Eu	0.003	0.000	0.000	0.000	0.000
Gd	0.081	0.077	0.055	0.067	0.000
Dy	0.070	0.075	0.061	0.070	0.000
Ho	0.029	0.031	0.022	0.026	0.000
Er	0.027	0.029	0.046	0.041	0.000
Yb	0.024	0.025	0.042	0.040	0.000
Fe	0.081	0.065	0.062	0.063	0.014
Mn	0.006	0.001	0.002	0.001	0.000
Ca	0.062	0.031	0.023	0.017	0.004
Sum A	1.005	1.056	1.043	1.048	
P	0.002	0.000	0.001	0.002	0.000
Nb	0.225	0.158	0.118	0.098	0.018
Ta	0.000	0.000	0.000	0.003	0.000
Si	0.230	0.091	0.082	0.075	0.002
Ti	1.519	1.688	1.752	1.771	0.964
Zr	0.000	0.000	0.000	0.000	0.000
Hf	0.000	0.000	0.000	0.000	0.001
Th	0.016	0.005	0.002	0.002	0.000
U	0.003	0.002	0.002	0.002	0.000
Sum B	1.995	1.944	1.957	1.952	
Total	3.000	3.000	3.000	3.000	1.005

Notes
1) No-analysis number, 2) b.d = below detection limit, 3) n.d = not determined, 4) Min-mineral analyzed, 5) Aes-Y - aeschynite-(Y), 6) Tna-titania mineral Calculations for aeschynite were done in the basis of 2 B-cations and for rutile in the basis of 2

73

Representative microprobe analyses of carbonate minerals

Table 4-10 Hydroxylbastnasite-(Ce)

Sample	7658	7658
Analysis	148	149
P_2O_5	0 00	0 00
Nb_2O_5	0 03	0 03
Ta_2O_5	0 56	0 56
SiO_2	1 74	1 43
TiO_2	1 47	1 27
ZrO_2	0 00	0 00
HfO_2	0 81	0 88
ThO_2	3 34	4 43
UO_2	0 43	0 51
Al_2O_3	0 63	0 50
Y_2O_3	0 00	0 00
La_2O_3	14 30	13 47
Ce_2O_3	29 00	29 99
Pr_2O_3	2 91	2 89
Nd_2O_3	10 25	10 23
Sm_2O_3	1 40	1 45
Eu_2O_3	1 16	1 16
Gd_2O_3	1 27	1 37
Dy_2O_3	0 61	0 59
Ho_2O_3	0 21	0 24
Yb_2O_3	0 06	0 12
FeOt	1 62	1 47
MnO	0 05	0 07
CaO	4 48	4 62
F	0 08	0 11
CO_2-Calc	23 49	23 29
SUM	99 90	100 68
O = F	-0 03	-0 05
Total	99 87	100 63
Th	0 026	0 034
Y	0 000	0 000
La	0 181	0 168
Ce	0 365	0 372
Pr	0 036	0 036
Nd	0 126	0 124
Sm	0 017	0 017
Eu	0 014	0 013
Gd	0 014	0 015
Dy	0 007	0 006
Ho	0 002	0 003
Yb	0 001	0 001
Fe	0 047	0 042
Ca	0 165	0 168
Total	1 000	1 000

Notes

1) No=analysis number 2)b d⁻ below detection limit 3) n d = not determined Calculations were done in the basis of one cation carbon concentrations were calculated based on charge balance (Ridolfi et al 2006)

74

CHAPTER 5: THE GEOLOGICAL HISTORY OF THE A-TYPE GRANITES OF THE WENTWORTH PLUTONIC COMPLEX: EVIDENCE FROM GEOCHEMICAL DATA.

5.1. Abstract

A-type granites comprise a distinct category of granitoids, the origin of which may be the result of anhydrous melting of lower granulitic crust, partial melting of granodiorites and tonalites, or extreme differentiation of a mafic magma This study examines the geochemistry of the REE-enriched A-type granites of the Wentworth Pluton to test known petrogenetic models and provide further evidence on the genesis of this type of granitoids The granite of the Wentworth Pluton in the Cobequid Highlands, Nova Scotia, is a latest Devonian intrusion (~362 Ma) into predominantly juvenile Neoproterozoic, subduction-related, basement The granites were remelted by a major gabbro intrusion (~357 Ma) producing late granites with slightly different geochemistry Gabbro resulted from inferred asthenospheric upwelling, related to the extension of the Late Paleozoic Magdalen Basin

The geochemical characteristics of these granites have been investigated by whole-rock geochemical and Sm-Nd isotope analyses Specific geochemical features of the Wentworth granites include higher F abundance in the early granites rather than the late ones, small degrees of fractionation, bimodal distribution of Mg and Cr and relatively primitive isotopic signatures ($\varepsilon_{Nd(360)}$ 1 1 to 3 6) Similar $\varepsilon_{Nd(360)}$ values are found in Neoproterozoic gabbros and quartz diorites, but more felsic Neoproterozoic rocks are more negative

Anatexis of the pre-existing granites is interpreted to have resulted in the release

of fluorine from the early granites, resulting in the formation of F-depleted granitic rocks

Co-variation of Mg and Cr indicates that the high-Mg granites resulted from mixing of

the original low-Mg granitic magma with pristine gabbro Modeling of batch partial

melting of a feldspar-dominated rock with a REE composition similar to that of the

Neoproterozoic quartz diorites, shows that the resulting melt would have REE

concentrations similar to those of the Wentworth granites Therefore we conclude that the

Wentworth granites have been formed by melting of plagioclase-rich felsic lithologies in

the lower crust such as trondhjemites formed during Neoproterozoic subduction-related

gabbro underplating Partial melting of these rocks would produce alkaline granitic

magmas with limited fractionation and primitive isotopic characteristics, such as the A-

type granites of the Wentworth Pluton This study shows that partial melting of lower

crustal underplated intermediate rocks, from an old episode of subduction, can give

distinctive A-type granites with a narrow range of ε_{Nd} that reflects the ε_{Nd} in the earlier

subduction system

5.2. Introduction

The term "A-type granite" was initially introduced by Loiselle and Wones (1979) and

refers to granites that were generated along continental rift zones with mildly alkaline

geochemistry and crystallized under low water fugacities The fact that this type of

granite is richer in Fe, K, rare metals and REEs compared to other type of granitoids

(Whalen et al , 1987) implies a distinctive petrogenesis

When the term was introduced, the first petrogenetic model suggested that A-type

granites derive from fractionation of mantle-derived alkali basalt with or without crustal

contribution When a crustal source was involved it was hypothesized to be granulitic

lower crust Based on geochemical criteria, the term A-type granite was applied in a

wider range of granitoid rocks that would include not only anorogenic but post-orogenic

granites as well (Maniar and Piccoli, 1989) However the main concept for the

petrogenesis of these rocks remained the same, that A-type granites result from partial

melting of anhydrous granulitic residue in the lower crust at high temperatures and that

they are a subgroup of I-type granites (Whalen et al, 1987)

Creaser et al (1991), however, demonstrated that partial melting of granulitic

crust cannot produce A-type magmas, because such a melt would be depleted in Si, Fe

and K and enriched in Ca and Al compared to the protolith, such geochemical features

are not found in A-type granites Partial melting of tonalitic to granodioritic crust instead

can produce A-type magmas (Creaser et al, 1991, Frost and Frost, 2010) Experimental

results suggest that the dehydration melting of calc-alkaline granitoids in the shallow

crust gives rise to A-type granitic melts (Douce, 1997) The high temperatures required

for such melting imply the involvement of hot mafic magma close to the Earth's surface,

which can also have a chemical contribution (Douce, 1997) Metaluminous A-type

granites can also form by differentiation of a tholeitic basalt magma, whereas peralkaline

granites may form by differentiation of transitional basalt (Frost and Frost, 2010)

The Wentworth Pluton is a late Devonian- early Carboniferous A-type granite

pluton in the Cobequid Highlands of northern Nova Scotia, eastern Canada The oldest

rocks of the pluton are ~362 Ma granites, which were intruded at ~357 Ma by a 30 x 8

km gabbro body, resulting in anatexis of the early granite forming a later granite with

slightly different geochemistry (Koukouvelas et al, 2002, Koukouvelas et al, 2006,

Murphy et al , 2011) The supracrustal equivalent of the pluton is a 4 km thick pile of felsic pyroclastic rocks and tholeiitic basalt flows (Pe-Piper and Piper, 2002) Both early and late granites have significant amounts of REEs and rare metals represented in a wide variety of accessory minerals (Papoutsa and Pe-Piper, submitted) The pluton intrudes Neoproterozoic Avalon terrane rocks of the northern Appalachians It formed along the bounding shear zone of the transtentional pull-apart Carboniferous-Permian Magdalen Basin (Hibbard and Waldron, 2009)

The tectonic setting of the Wentworth pluton is well understood from previous work (Koukouvelas et al , 2002, Koukouvelas et al ,2006) The anatexis of early granite allows some geochemical processes to be constrained The Avalon terrane country rocks consist of Neoproterozoic juvenile crust formed in a subduction setting, with well known geochemical characteristics (Murphy and Nance, 2002) Any petrogenetic model must account for the strong REE enrichment of the Wentworth pluton The particular geological setting provides constraints on the evolution of this A-type pluton The specific objectives of this study are 1) to determine what geochemical features of A-type granites are found in the Wentworth pluton and how they differ between the early and late granites, 2) to determine the source of the granitic magma from radiogenic isotope studies, 3) to determine the petrogenetic role of the large gabbro intrusion and its inferred lower crustal equivalents and 4) establish a general petrogenetic model that links the evolution of this A-type granite pluton to its tectonic setting

5.3. Geological setting

5 3 1 Cobequid Highlands

The Cobequid Highlands are located in the Avalon terrane just north of the
Cobequid Fault, which separates this terrane from the Meguma terrane (Fig 5-1) The
Cobequid Highlands are underlain by Neoproterozoic rocks, minor Silurian to Lower
Devonian sedimentary rocks and Late Paleozoic plutons and their extrusive equivalents
(Pe-Piper and Piper, 2002)

Within the Cobequid Highlands the Cobequid Shear Zone consists of a series of
late Paleozoic faults that were active during latest Devonian to earliest Carboniferous
The Late Paleozoic plutons were emplaced in the actively deforming Cobequid Shear
Zone and consist mainly of granite, gabbro and diorite bodies The Rockland Brook
Fault, which was the major fault of the Cobequid Shear Zone, is located in the eastern
part of the Highlands separating the Neoproterozoic Jeffers Block to the north from the
Bass River Block to the south The Cobequid Fault marks the margin of the Cobequid
Highlands horst that was uplifted at 315 Ma along the Cobequid-Chedabucto Fault Zone
(Pe-Piper and Piper, 2002)

In the Late Devonian, the Rheic Ocean was subducted beneath Nova Scotia
producing the voluminous South Mountain Batholith and satellite plutons (Clarke et al ,
1997) Towards the end of the Devonian, incipient closure of the Rheic Ocean at
promontories led to orogen-parallel dextral strike slip faulting (Hibbard and Waldron,
2009), resulting in distributed extension in the Magdalen Basin at a step-over zone
Crustal thinning continued through at least the early Carboniferous, accompanied by
underplating of a thick gabbroic layer beneath the Gulf of St Lawrence (Marillier and
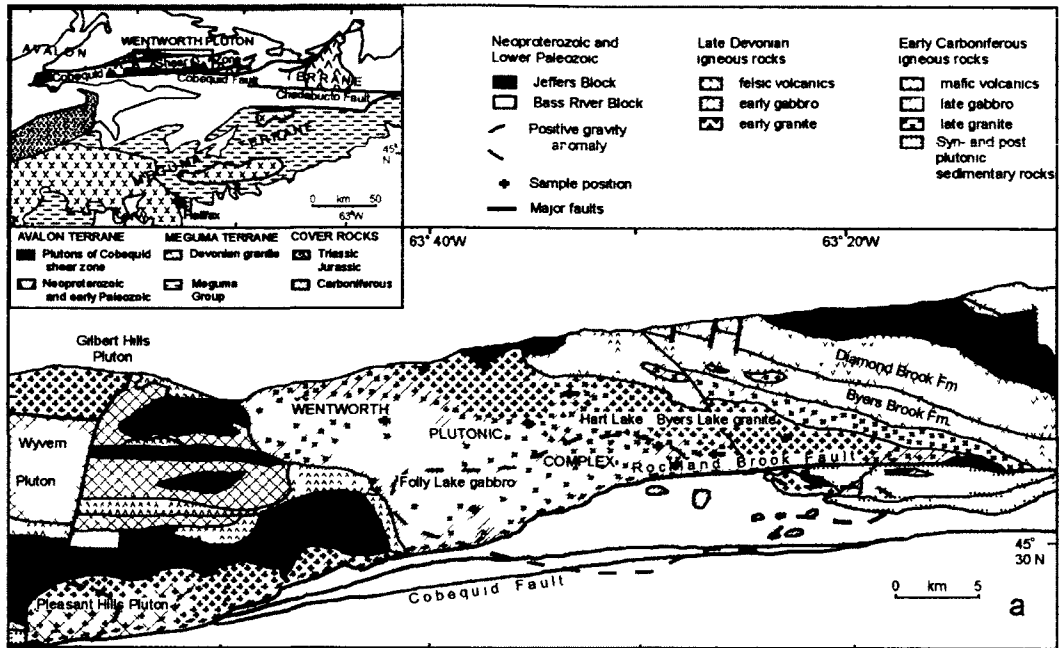
Figure 5-1 Geological map of the late Paleozoic Wentworth Pluton of the Cobequid

Highlands Inset shows the location of the Avalon and Meguma terranes

Verhoef, 1989, Marillier and Reid, 1990) This magma reached the surface through the basin-margin faults to give flood basalts >1 km thick in the Fisset Brook Formation of western Cape Breton Island and the Fountain Lake Group of the Cobequid Highlands (Pe-Piper and Piper, 1998)

All late Paleozoic granites in the Cobequid Highlands have A-type affinities, whereas the gabbros are olivine tholeiites (Pe-Piper and Piper, 2002) Synchronous with the plutons are the volcanic rocks of the Fountain Lake Group The felsic members of this group are the rhyolites of the Byers Brook Formation, whereas the mafic rocks are represented by the Diamond Brook Formation The rhyolites also have A-type affinities and the basalts are Fe-rich continental flood basalts (Dessureau et al , 2000) Geochemical similarities between the rhyolites and the granites, and the basalts and the gabbros suggest that the Fountain Lake Group is the extrusive equivalent of the Late Paleozoic plutons

5 3 2 Avalonian country rock

The Avalon terrane of the northern Appalachians in mainland Nova Scotia is characterized by Neoproterozoic (650-570 Ma) arc-related sequences that formed on the margin of Gondwana (Murphy and Nance, 2002), uncomformably overlain by thin lower Paleozoic supracrustal rocks The terrane comprises a series of collisional blocks including I-type plutons, coeval volcanic rocks, minor oceanic crust and clastic sedimentary successions (Pe-Piper and Murphy, 1989, Murphy, 2002) No crustal basement is known, but crustally-derived felsic rocks suggest derivation from sources with Nd depleted mantle model ages (T_{DM}) between 0 96 and 1 2 Ga (Murphy and Nance, 2002) In the Cobequid Highlands, the Jeffers Block comprises volcanic and

volcaniclastic rocks with small high-level plutons, whereas the Bass River Block consists

mostly of plutonic rocks

The mafic facies of the Jeffers Block show characteristics of alkaline rocks such

as relatively high Ti, Nb and have moderate amounts of REE (Pe-Piper and Piper, 1989)

The late Neoproterozoic mafic rocks have been divided into three types, based on their

geochemistry The first type includes Ti-rich porphyritic basalts with high Ni and Cr and

low La/Ce ratios These basalts show a LREE enrichment which is characteristic of

basalts related to subduction The second type includes Ti-depleted basaltic andesites that

are poor in Ni, and Cr (Pe-Piper and Piper, 1989) All the felsic rocks are enriched in K,

Ba, Th and Nb, whereas they appear to be depleted in Sm and Y These rocks show

substantial fractionation of LREEs The third type consists of calk-alkaline rocks that

resemble within plate lavas and mafic rocks that are depleted in Nb (Pe-Piper and Piper,

1989)

5 3 3 The Wentworth Pluton

The Wentworth Pluton consists of a granitic part in its northeastern part and a gabbroic

part in the southwestern part (Fig 5-1) (Pe-Piper and Piper, 2002) The latter is younger

(357±4 Ma, Pe-Piper et al , 2004, Murphy et al , 2011) than the other mafic intrusions in

the Cobequid Highlands and post-dates the main emplacement of the Wentworth Pluton

granites (362±2 Ma, Doig et al , 1996). This later gabbro intrusion and heat provided by

the underplated mafic melts, resulted in the partial melting to anatexis of the older

Wentworth granite, forming syn- and post-gabbro granites with slightly different

geochemistry (Koukouvelas et al , 2002) Mafic enclaves are common in the granites and

some of them show the characteristics of mixing and mingling between a mafic and felsic magma.

The A-type granites of the Wentworth pluton are the most alkaline rocks among all Late Paleozoic granites of the Cobequid Highlands (Pe-Piper, 2007) The early granite of the Wentworth pluton consists mainly of K-feldspar-rich medium grained granite which contains sodic amphibole, 76% SiO_2, high F, and moderate Li (Koukouvelas et al , 2002) A few granites, interpreted as synchronous with the gabbro, have particularly high Zr contents Many of the syn- and post-gabbro granites contain >75 ppm Y Some have high Li, but all samples reported by Koukouvelas et al (2002) have <400 ppm F Some late granites that occur as pods within the gabbro are geochemically distinct, with a wide range of SiO_2 contents, relatively low Y, Zr, Li and F and the amphibole, where present, is hornblende Similar low-Y, low-Li granites occur within the main Wentworth granite and have rather higher TiO_2 contents than the alkali granites of the early phase, with the same SiO_2 content (Koukouvelas et al , 2002)

5.4. Methods

More than a hundred granodioritic and granitic samples (64 to 79 wt% silica) have been analyzed from the Wentworth pluton The samples were classified into relative ages based on field relationships with the gabbro Uniform outcrops of granite cut by gabbro are considered to be of the early granitic phase, as are dated granites >358 Ma Granites with lobate contacts with the gabbro and hybrid enclaves are taken as synchronous with the mafic intrusion Bodies of granite that either cut the Wentworth gabbro or occur in it as globular pods or irregular sheets are considered to post-date the gabbroic intrusion When field relations for a sample were sufficiently clear for its classification then the

sample is characterized as a "definite" sample of one of these types When the relative

age of a sample was not clear from field relations in the same outcrop, but was assumed

from the geology of nearby outcrops, then the sample is classified as a "probable" sample

of a certain type

The major and trace elements were analyzed in two ways 1)at the Regional

Geochemical Centre, Saint Mary's University, by XRF and Instrumental Neutron

Activation Analysis and 2) at the Activation Laboratories using their code 4Lithoresearch

and Code 4B1 packages These packages combine lithium metaborate/tetraborate fusion

ICP whole rock analysis with trace elements by ICP-MS All the whole-rock geochemical

data are given as supplementary data (Table S1) They were processed using MINPET

2 2 software for Windows and the plotted samples are recalculated to 100% on volatile-

free basis Samples with outlying values in geochemical plots are not included in the

diagrams of elemental classification

Most of the Sm-Nd data used in this study were those reported by Pe-Piper and Piper

(1998), but eight additional analyses were made of selected granites from the Wentworth

Pluton (Table S2) These new analyses were made by Activation Laboratories Rock

powders for Sm-Nd studies were dissolved in a mixture of HF, HNO_3 and $HClO_4$ Before

decomposition, the sample was totally spiked with ^{149}Sm-^{146}Nd mixed solution REE were

separated using conventional cation-exchange techniques Sm and Nd were separated by

extraction chromatography on HDEHP covered Teflon powder Accuracy of the

measurements of Sm and Nd contents is ±0 5% $^{143}Nd/^{144}Nd$ ratios are relative to the value

of 0 511860 for the La Jolla standard Analyses were performed on Triton-MC mass-

spectrometer

5.5. Geochemical trends of the Wentworth granites

In general, the geochemistry of the Wentworth granites does not show significant variations with relative age (Figs 5-2 to 5-4) According to elemental classification diagrams of Whalen et al (1987) for granitoid rocks, the Wentworth granites are A-type granites (Fig 5-2) Geochemically the granites are metaluminous to peralkaline (Fig 5-3A), and plot as within plate granites in the tectonic discrimination diagram of Pearce et al (1984) (Fig 5-3B) However there is no clear discrimination between A1 (rift-related) and A2 (post collisional) groups in Eby's (1992) diagram for A-type granites (Fig 5-3C) The Wentworth granites plot as post orogenic in the diagram of Maniar and Piccoli (1989) (Fig 5-3D) In the classification scheme of Frost et al (2001), the Wentworth Pluton granites range from magnesian to ferroan (Fig 5-4A), even though A-type granites are typically ferroan (Frost and Frost, 2010) However, the alkalinity index of these rocks ranges from alkalic-calcic to alkalic, which is within the range for A-type granites (Fig 5-4C)

A striking feature in the major elements of the Wentworth Pluton granites is the bimodal distribution of MgO (Fig 5-5a) The granites, regardless of relative age, plot within two distinct groups in terms of MgO abundance (Fig 5-5b) High-MgO granites tend to be enriched in TiO_2, Cr and Fe_2O_3 (Figs 5-5c, e and f respectively) compared to the low-MgO group The concentration of fluorine, however, does not correlate with either group (Fig 5-5d)

In terms of relative age, fluorine, for the same SiO_2, generally appears in higher concentrations in the early Wentworth granites (Fig 5-6a and c) Fluorine also shows a positive correlation with TiO_2 especially for syn- and post-gabbro granites and late dykes
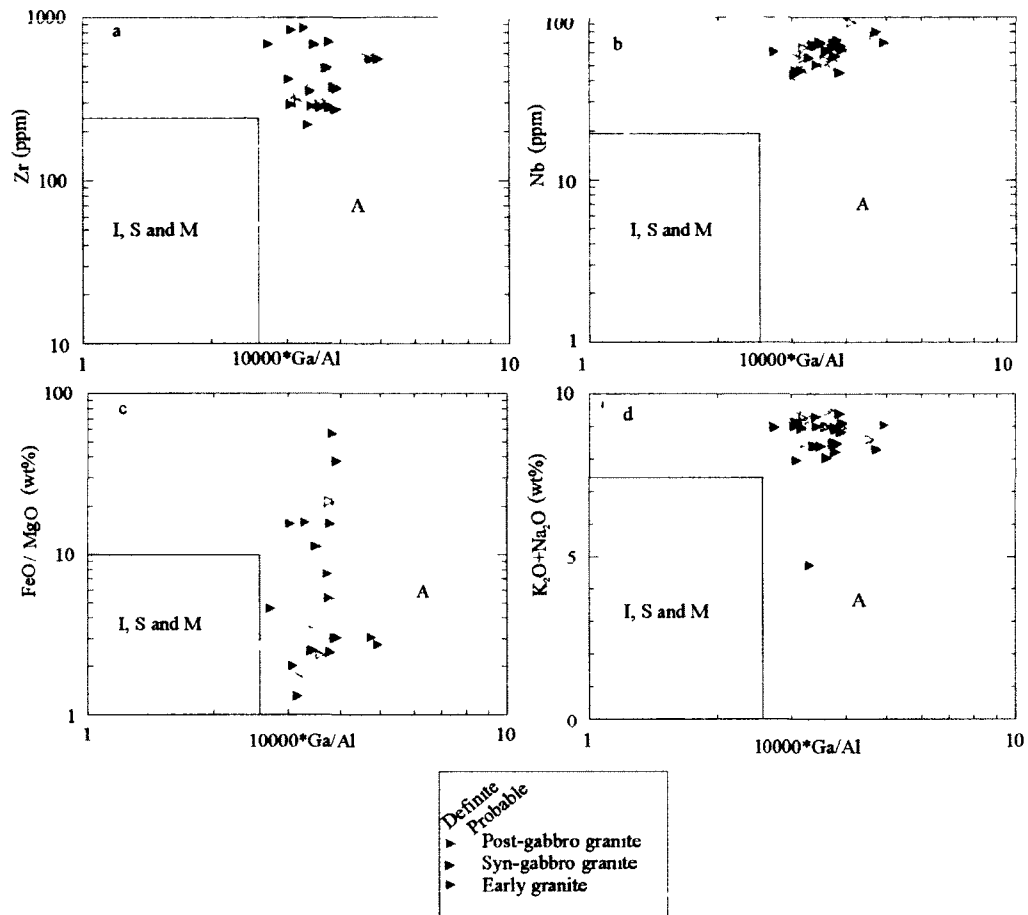
Figure 5-2: Elemental discrimination diagrams after Whalen (1987), showing the A-type nature of the Wentworth granites. I=granites derived from igneous protoliths, S= granites derived from sedimentary protoliths, M=granites derived from melting of subducted crust or overlying mantle, A= anorogenic granites.
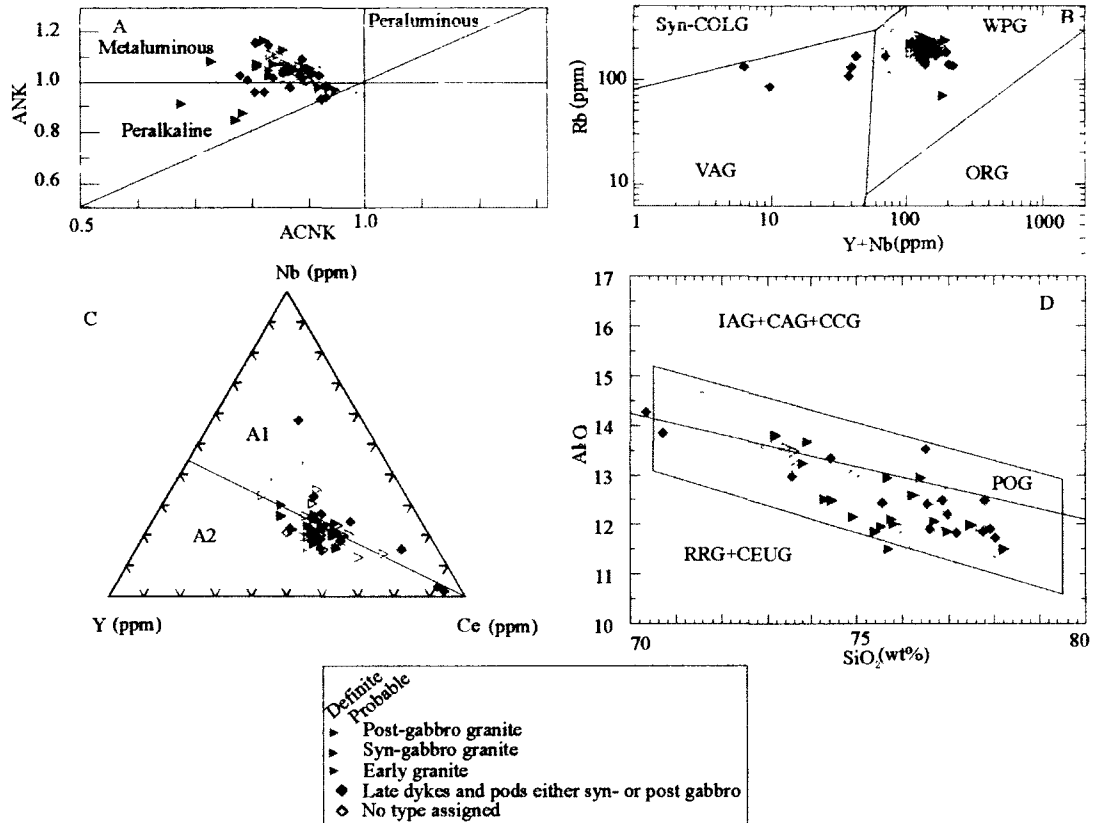
Figure 5-3: Classification diagrams for granitoid rocks showing the A-type affinity of the Wentworth granites. A) Alkalinity diagram (ANK= Al_2O_3/Na_2O+K_2O), ACNK= $Al_2O_3/(CaO+Na_2O+K_2O)$) after Maniar and Piccoli (1989). B) Tectonic discrimination diagram after Pearce (1984); syn-COLG= syn-collisional granites, WPG= within-plate granites, VAG= volcanic arc granites, ORG= orogenic granites. C) Tectonic discrimination diagram after Eby (1992); A1= rift-related anorogenic granites, A2= post-collisional (arc-related) anorogenic granites. D) Tectonic discrimination diagram after Maniar and Piccoli (1989); IAG= island arc granitoids, CAG= continental arc granitoids, CCG= continental collision granitoids, POG= post-orogenic granitoids, RRG= rift-related granitoids, CEUG= continental epeirogenic uplift granitoids.
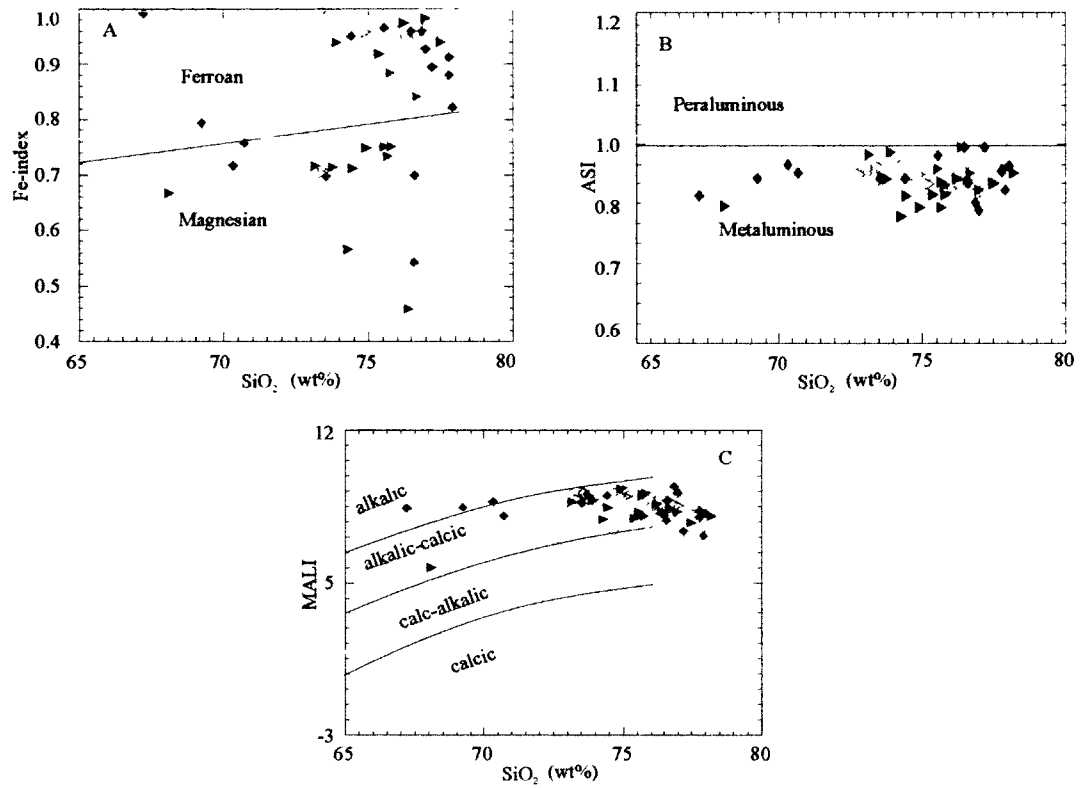
Figure 5-4: Geochemical classification diagrams after Frost et al. (2001) for the Wentworth Pluton granitoid rocks. A) Fe-index: FeO/(FeO+MgO). B) ASI (Aluminum Saturation Index): Al/(Ca-1.67P+Na+K), C) MALI (Modified alkali-lime index): $Na_2O+ K_2O-CaO$. Symbols as in Figure 5-3.
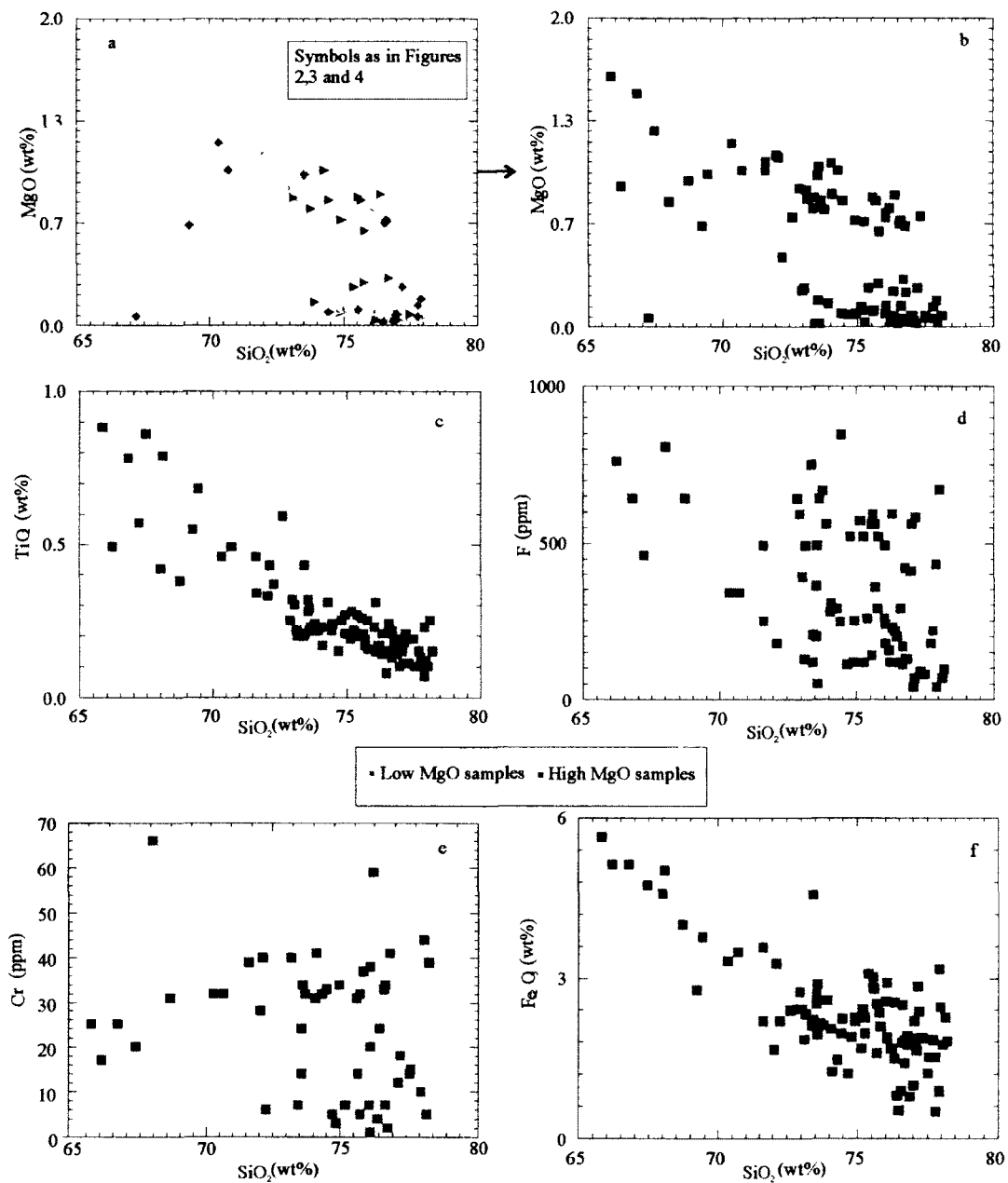
Figure 5-5: Geochemical trends in the Wentworth granites. Symbols in (a) are based on

relative age, whereas symbols in figures (b) to (f) are based on MgO abundance.

and pods (Fig 5-6b) Furthermore, fluorine seems to correlate positively with REEs for

granites of all relative ages except late granitic dykes and pods (Fig 5-6c) All

Wentworth granites show positive correlation of REEs with TiO_2 (Fig 5-6d) and even

stronger correlation of MREEs with Y (Fig 5-6e) Titanium shows a negative correlation

with SiO_2 and is in higher concentrations in the early Wentworth granites (Fig 5-6f)

Most of the granitic samples of all ages from the Wentworth Pluton present a

similar REE pattern, showing significant LREE enrichment of 100 to 700 times more

than the standard chondritic levels and flat HREE patterns with a strong Eu anomaly (Fig

5-7a) A few samples show different REE patterns One of these patterns shows strong

fractionation of both LREE and HREEs with a slight or even positive Eu anomaly (Fig

5-7b) Both samples that present such a pattern are from dykes and pods, either syn- or

post-gabbro Another pattern that has been observed is similar to the main REE pattern

but with a progressive enrichment in HREEs instead of the typical flat pattern (Fig 5-7c)

Samples of this REE pattern are from late dykes and pods and one possible Wentworth

early granite (sample 9820), all three samples are of the low-MgO group

The epsilon Nd values, calculated for 360 Ma, range from +1 15 to +3 60 (Table

S2) These data are compared with ε_{Nd} values recalculated to 360 Ma from Late

Neoproterozoic rocks of the region, which might represent either a source or contaminant

of the granitic magmas In a $f_{Sm/Nd}$ versus ε_{Nd} diagram ($f_{Sm/Nd}$ fractional difference in the

Sm/Nd ratio between the sample and the CHUR) (Fig 5-8a), the Wentworth granites

appear on the lower right quadrant together with the Wentworth gabbros The late

Neoproterozoic intermediate and felsic rocks plot on the lower left quadrant (Fig 5-8a)

Epsilon Nd values of the Wentworth Pluton granites do not correlate with MgO, however
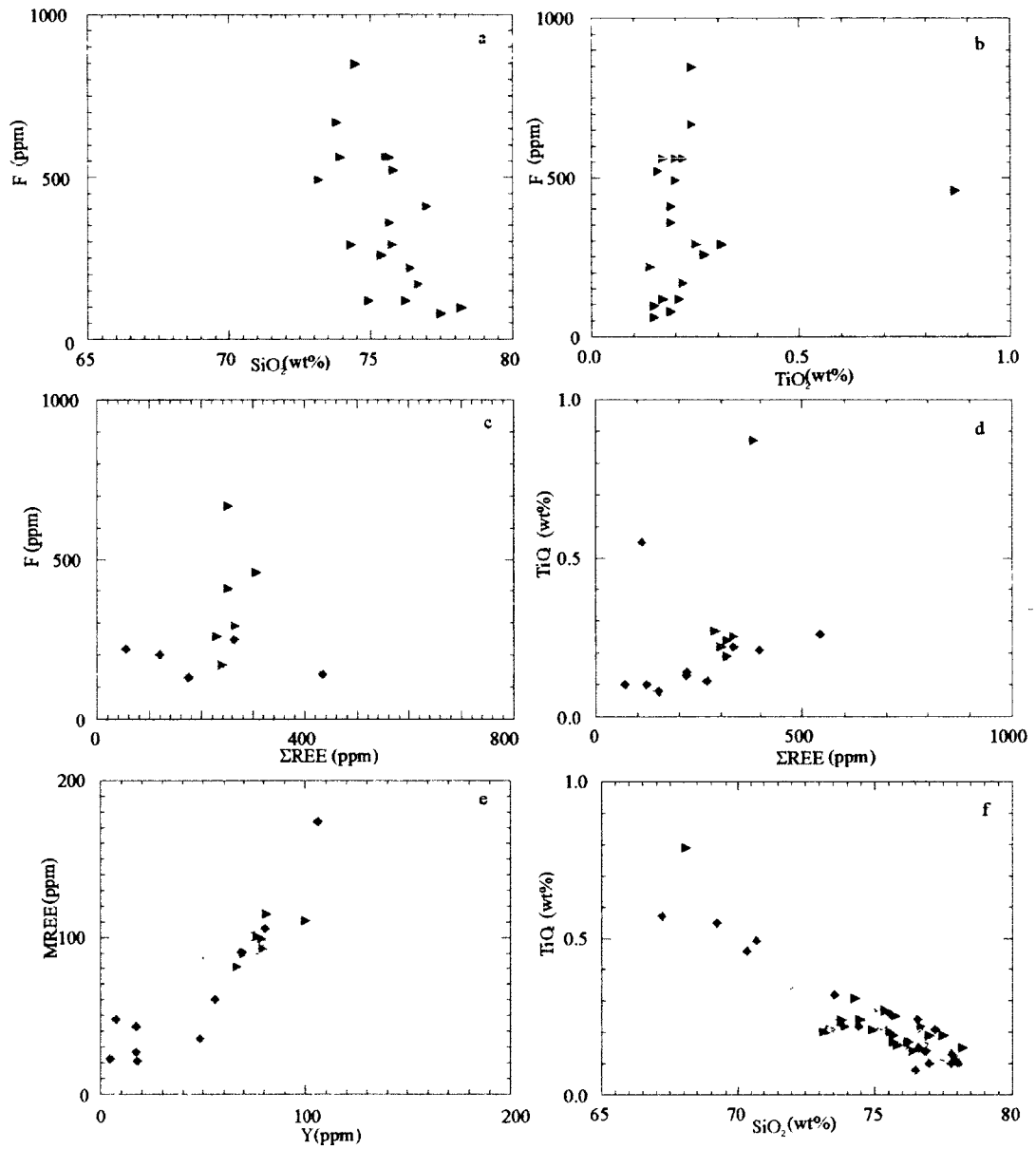
Figure 5-6: Selected geochemical plots for the Wentworth granites showing variation trends in trace elements. Symbols as in Figure 5-3.
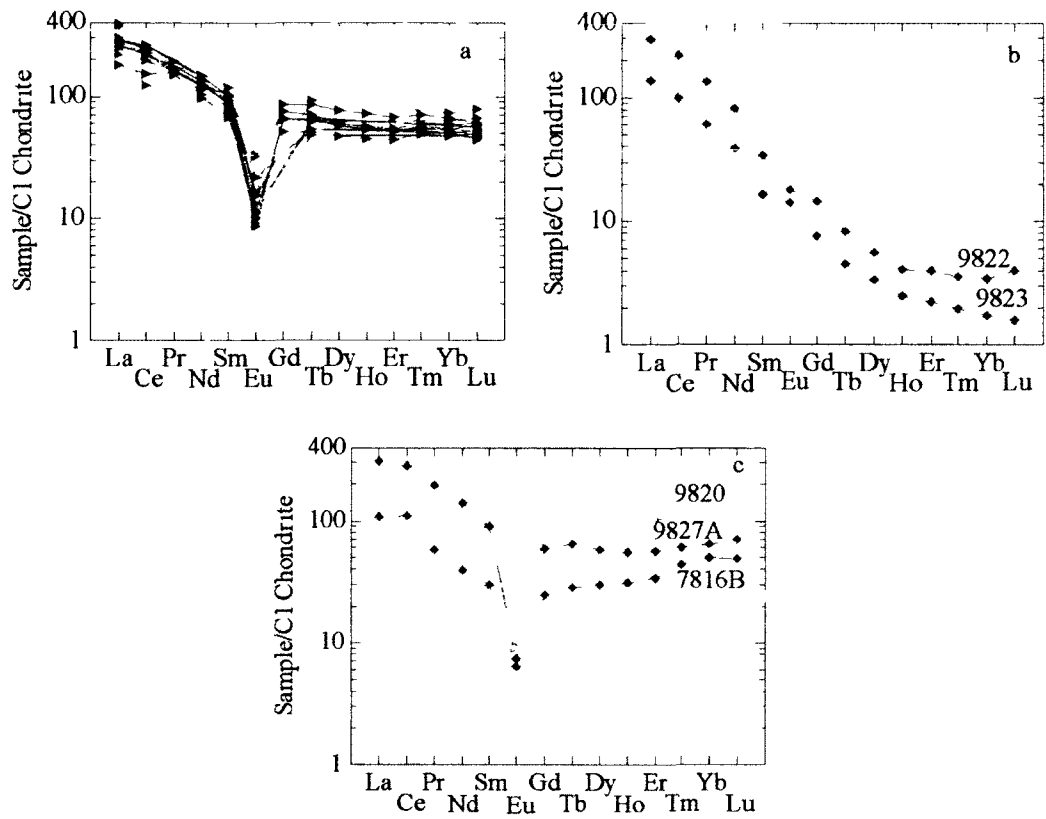
Figure 5-7: REE patterns for the Wentworth granites. (a) General REE pattern for most granitic samples; (b) two strongly REE fractionated samples from late granite dykes, (c) three low-Mg samples with a slight HREE enrichment. Symbols as in Figure 5-3.
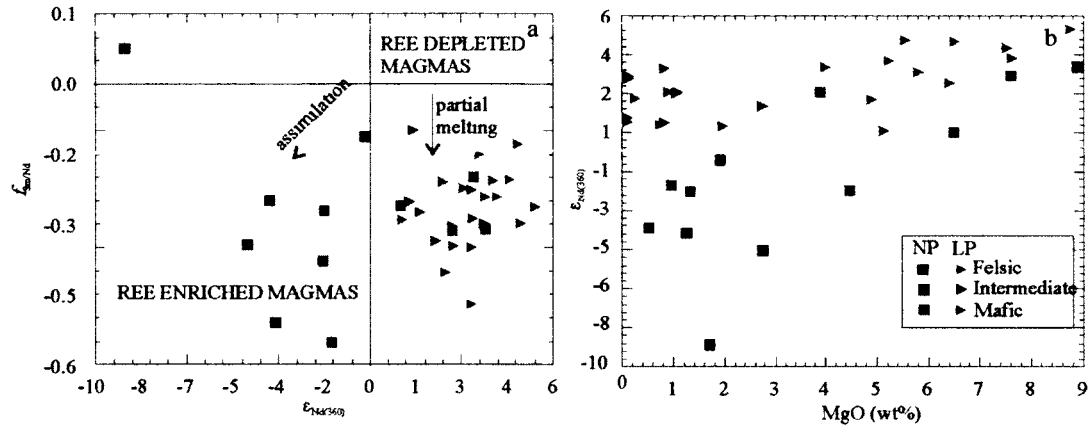
Figure 5-8: $f_{Sm/Nd}$ vs ε_{Nd} diagram (a) and ε_{Nd} vs MgO diagram (b) for Neoproterozoic

rocks of the Cobequid Highlands and Late Paleozoic rocks of the Wentworth Pluton.

NP= Neoproterozoic rocks, LP= Late Paleozoic rocks.

the Late Paleozoic and Late Neoproterozoic mafic rocks show two different trends The

Late Paleozoic mafic rocks show no variation in ε_{Nd} as MgO increases, whereas the Late

Neoproterozoic mafic rocks show a linear positive trend from low ε_{Nd} values, more

negative than those of more felsic Late Neoproterozoic rocks at low Mg content, to

higher values that are within the range of the Wentworth granites at high Mg content

(Fig 5-8b)

5.6. Discussion

In this section, first the noteworthy geochemical features of the Wentworth

granites are evaluated Second, the Sm-Nd isotope data are used to constrain the

petrogenetic origin of the granite magmas Then, this petrogenetic hypothesis is tested by

modeling two of the prominent features of the Wentworth granite the enrichment in REE

(Table 5-1) and the abundance of fluorine Finally, we consider the tectonic implications

of our petrogenetic model and its implications for the conditions under which A-type

granites similar to the Wentworth Pluton can form

5 6 1 Geochemical differences between the early and late granites

A distinct geochemical difference between the Wentworth granites of different

relative age is the abundance of fluorine In general, the Wentworth early granites have

higher amounts of F than the late (syn- and post-gabbro) granites (Fig 5-6a)

Furthermore, the same geochemical trend has been inferred from the geochemistry of

amphiboles in the Wentworth Pluton (Pe-Piper, 2007) The amphiboles from the

Wentworth early granites are richer in F than those present in the late granites This

implies that the parent magma was also rich in F, so that the element would be

incorporated in the mineral structure during amphibole crystallization (Martin, 2007)

94

The smaller amounts of fluorine in the syn- and post gabbro granites suggest that during the anatexis of the early granites by the heat provided by the gabbroic intrusion, fluorine was released during the breakdown of the amphiboles, and escaped as a volatile phase in the hydrothermal system that was developed after the pluton emplacement (Pe-Piper et al , 2004)

5 6 2 The origin of the high-Mg granitic group

The amounts of Mg measured in the Wentworth granites are within the range of other A-type granites described in the literature (Collins et al , 1982, Landenberger and Collins , 1996, Tollo et al , 1996, Whalen et al , 1996, Jung et al , 1998, Dall'agnol et al , 1999, Wu et al , 2002, Oliveira et al , 2009) However the published geochemical data for most A-type granitic suites resemble the low-Mg group of the Wentworth granites The correlation of Mg with Cr and Ti and their relative enrichment in intermediate rocks (Fig 5-5b-f) indicates the contribution of a mafic component that introduced these geochemical features to the granites by mixing Therefore the high-Mg group is interpreted to have formed by mixing of gabbro with initially low-Mg granites This implies that a gabbroic magma was present throughout the emplacement of the pluton and was not restricted to the ~357 Ma gabbro body

5 6 3 Nd isotope evidence for the source of the Wentworth granites

In general, crustal derived felsic rocks have low to negative ϵ_{Nd} values, in contrast to higher positive values in more primitive mafic rocks (Rollinson, 1993) The small $\epsilon_{Nd(360)}$ range of the Wentworth granites (1 15 to 3 6) (Table 5-2) implies their origin from an isotopically homogeneous source

There is no geochemical evidence for significant mixing of low-Mg granite with primitive gabbroic magma, which had $\varepsilon_{Nd(360)}$ of 0 9 to 5 37 High-Mg and low-Mg granites do not show a particular variation in $\varepsilon_{Nd(360)}$ (Fig 5-8b) Neither is there evidence for significant crustal contamination of the granitic magma by Neoproterozoic crust, most of which has $\varepsilon_{Nd(360)}$ of -0 6 to -5 (Fig 5-8a) (Zachariah et al , 1997) The high $\varepsilon_{Nd(360)}$ of the granites suggests derivation from mantle-derived rocks This might be either by extreme differentiation of a primitive mafic magma or by partial melting of mantle-derived intermediate rocks

The possibility of an origin through extreme fractionation of a mafic magma is unlikely for the Wentworth granites since the >5 km thickness of the Wentworth granites would require a very large amount of gabbro to be fractionated (Frost and Frost, 2010) Moreover, possible intermediate fractionation products such as tonalites are rare and those that are known show textural evidence for an origin by mixing of granite with gabbro (Pe-Piper et al , 1996)

Partial melting of mantle-derived rocks with relatively primitive isotopic signature, therefore appears to be the most likely source of the granitic magma (Fig 5-8a) Partial melting of intermediate rocks of tonalite to granodiorite composition will yield a granitic magma (Creaser et al , 1991, Douce, 1997, Frost and Frost, 2010) The strong negative Eu anomaly and lack of HREE fractionation in the Wentworth granites suggests partial melting in the stability field of plagioclase, with little or no involvement of garnet (Fig 5-7a) Of the 13 Nd isotope analyses available for Neoproterozoic rocks in the Cobequid Highlands, one gabbro and two quartz diorite enclaves have relatively primitive $\varepsilon_{Nd(360)}$ between 2 5 to 3 6 (equivalent to $\varepsilon_{Nd(600)}$ between 4 5 and 5 7), a range of

$\epsilon_{Nd(360)}$ similar to most Wentworth granites These enclaves are interpreted to be representative of mafic rocks underplating the lower crust during Neoproterozoic subduction If such underplated rocks included minor more silicic fractions of tonalitic composition, then partial melting of these intermediate rocks as a result of heat from Devono-Carboniferous gabbroic magmas would be a possible source of the Wentworth granites

5 6 4 Trace element patterns of granitic magmas derived from partial melting tonalite

The hypothesis that the Wentworth granite magma resulted from partial melting of Neoproterozoic tonalite bodies within a predominantly gabbroic underplated lower crust was tested by examining the concentrations of REEs Neoproterozoic gabbros and quartz diorites with primitive ϵ_{Nd} have similar rather flat REE patterns with 70-150 times chondrite enrichment (Fig 5-9a) A co-magmatic tonalite protolith is assumed to have similar REE abundance Batch melting modeling of varying degrees of partial melting of such tonalite with varying proportions of clinopyroxene, amphibole, plagioclase and K-feldspar show that the observed REE patterns in the Wentworth granite (Fig 5-7a) would be produced only by partial melting of a rock with predominant plagioclase (Fig 5-9b and Table 5-1) This suggests that rather than a tonalite, the source rock might be more leucocratic, closer in a composition to a trondhjemite or plagiogranite In that case, some of the enrichment in REE might have been a consequence of Neoproterozoic fractionation rather than Late Paleozoic partial melting

5 6 5 The origin of high fluorine content of the Wentworth early granites

The abundance of fluorine in the granites may also constrain the source Fluorine is present in basaltic magmas and correlates positively with K (Aoki et al , 1981)
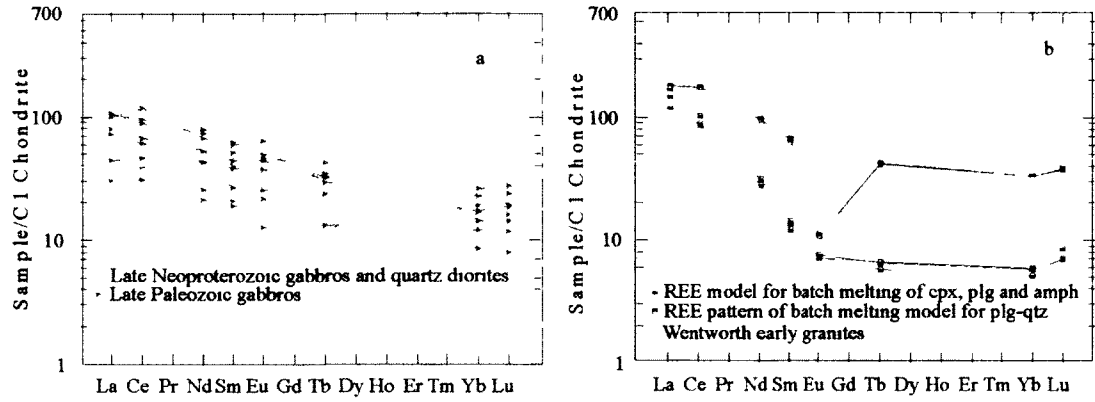
Figure 5-9 (a) REE patterns for Late Paleozoic and Neoproterozoic mafic rocks

(Pe-Piper and Piper, 1989, Pe-Piper, 1998), demonstrating the limited range of REE

amounts in these rocks (b) REE patterns of the Wentworth early granites compared to

the REE patterns derived from the batch partial melting model summarized in Table 5-1

Fractionation of hydrous basaltic magma, concentrates F in residual fluids together with K and Ba, which then crystallize out in amphiboles, principally pargasite The presence of pargasite in Neoproterozoic mafic rocks (Pe-Piper, 1988) is evidence for such F concentration in Neoproterozoic mafic magmas If this magma underplated gabbro and its differentiates at the base of the crust, this lower crust would be enriched in F

5 6 7 Tectonic implications of the petrogenetic model

The Wentworth granites represent a late Paleozoic felsic intrusion with limited fractionation, over Neoproterozoic predominantly juvenile crust formed during subduction The isotopic signature of the granites indicates a derivation through partial melting of juvenile Neoproterozoic intermediate to silicic rocks Therefore the protoliths should be felsic enough as to produce a granitic melt without further fractionation of the produced melt Crustal thinning and rise of asthenosphere in the late Devonian of the Magdalen Basin produced tholeitic mafic magmas that were the heat source for partial melting of these fertile intermediate to felsic rocks in the Neoproterozoic lower crust (Fig 5-10b)

Underplated mafic melts derived from the mantle wedge during subduction would underplate the lower crust to produce a section similar to that recognized in supra-subduction ophiolites (Fig 5-10a) The underplated crust in supra-subduction ophiolites consists principally of gabbro, but may include minor amounts of fractionates ranging from quartz diorite to plagiogranite (Bonev and Stampfli, 2009) These intermediate to felsic rocks thus inherit the primitive isotopic signature and incompatible elements from the mantle-derived mafic melts Such rocks include plagiogranites, a leucocratic variety of tonalite, however plagiogranite is always related to oceanic crust (Mirza and Sabah,

a) Neoproterozoic subduction

Granodiorite plutons and
volcanoes

Sea level

0

Avalonian
juvenile
crust

50

Lithosphere

Lithosphere

Trondhjemitic
fractionates

km

Oceanic
lithosphere

100

150

Asthenosphere

Gabbro magma
chambers

0   50   100   150   200   250   300

km
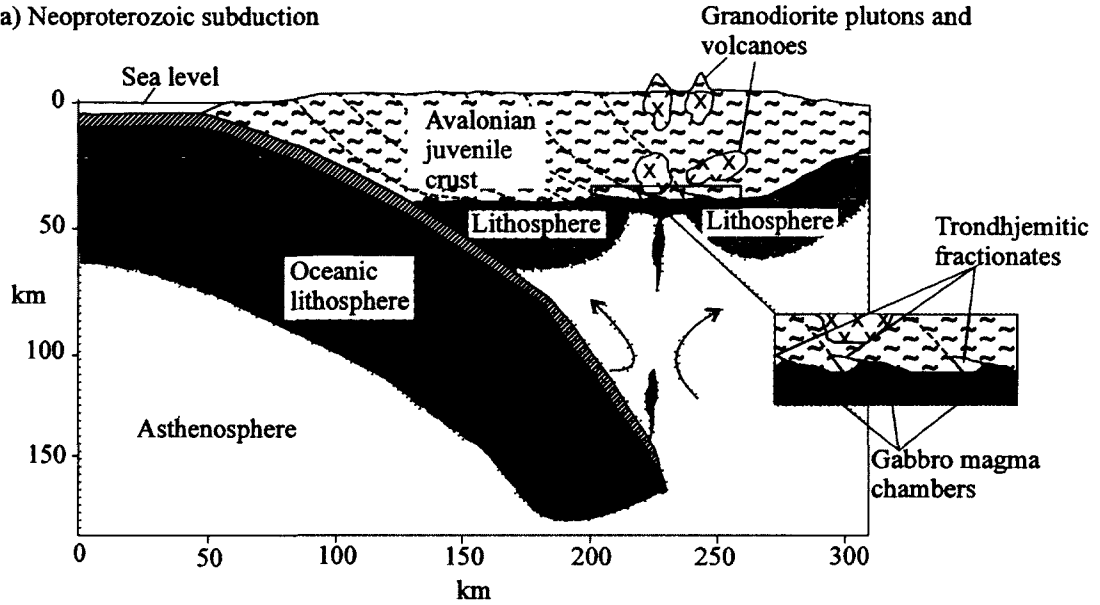
b) Late Paleozoic partial melting and underplating

Rockland
Brook Fault

Wentworth
Pluton

Horton basins   N

S

0

Avalon

Meguma

Gander Zone

50

Lithosphere

km

First stages of
underplating related
to the extension of
the Magdalen Basin

100

Heat

Asthenosphere

150

0   50   100   150   200   250   300

km

X X X / X X X / v v v	Neoproterozoic Plutons
v v v v v / v v v v v	Late Paleozoic volcanic rocks

(hatched)	Wentworth Granites
(black)	Wentworth Gabbro

Figure 5-10: Proposed petrogenetic model.

100

2007) A trondhjemite, on the other hand, can be of continental origin as well (Nilsen et

al, 2003) Furthermore a trondhjemite, which has biotite as a mafic mineral, could

produce a K-rich granitic magma, compared to a plagiogranite that contains amphibole

Moreover, a derivation from a trondhjemitic source with mostly sodic plagioclase

(oligoclase), could also account for the high sodium amounts in the Wentworth granites,

mineralogically reflected by the presence of sodic amphiboles

Several petrogenetic models have been suggested for the origin of the A-type

granites This study shows that partial melting of lower crustal underplated intermediate

rocks from an old episode of subduction gives distinctive A-type granites with a narrow

range of ε_{Nd} that reflects the ε_{Nd} in the earlier subduction system A range of tectonic

processes could produce the necessary heat source to cause partial melting In the case of

the Wentworth Pluton, the heat source appears to be upwelling asthenosphere It is

unknown, however, whether this upwelling resulted from crustal thinning by extension,

or from a slab detachment during final closure of the Rheic Ocean

5.7. Conclusions

The Wentworth pluton granites resemble other A-type granites described in the

literature (Collins et al, 1982, Landenberger and Collins, 1996, Tollo et al, 1996,

Whalen et al, 1996, Jung et al, 1998, Dall'agnol et al, 1999, Wu et al, 2002, Oliveira et

al, 2009) but are unusual in the bimodal distribution of Mg and Cr The early and late

granites differ in the abundance of fluorine, which is higher in the former

The isotopic data from the Wentworth granites present ε_{Nd} values similar to the

calculated $\varepsilon_{Nd(360)}$ from Neoproterozoic mafic rocks, such as gabbros and quartz diorites,

which represent the local Avalonian basement related to subduction The granites,

however, have significantly lower ε_{Nd} values than the late Paleozoic gabbros and basalts and at the same time, higher ε_{Nd} values than their Neoproterozoic equivalents The granites were derived from partial melting of a suitably silicic juvenile source in the predominantly gabbroic lower crust, formed during Neoproterozoic subduction

As noted by previous studies, the later gabbro remelted some of the early granites The only consistent geochemical difference between the early and late granites is the abundance of fluorine High-Mg granites show enrichment in Cr and Ti, which increases towards more intermediate compositions, indicating that this enrichment was the result of mixing with small amounts of gabbro High-Mg granites include rocks from all relative ages with respect to the ~357 gabbroic intrusion This implies that the mafic component was already present when the granitic magma was formed in the lower crust, supporting the hypothesis that A-type granites derive from partial melting of such rocks

Minor amounts of trondhjemite are inferred to have formed in the predominantly gabbroic juvenile lower crust developed during Neoproterozoic subduction Partial melting of this source, isotopically similar to the Neoproterozoic gabbros, was triggered by upwelling asthenospheric gabbroic magma in the latest Devonian, related to the extensional opening of the Magdalen Basin This magma provided the necessary high temperatures for anhydrous melting of small bodies on trondhjemite in the lower crust Partial melting of sodic plagioclase present in trondhjemite accounts for the REE enrichment in the Wentworth granites and the presence of sodic amphiboles, whereas the presence of biotite, a typical mafic mineral in trondhjemite, could also account for the high amounts of K in the granite magma Fluorine in the produced melt resulted from partial melting of amphibole, presumably pargasite

102

We suggest more generally that tectonic conditions that lead to partial melting of juvenile subduction-related lower crust is likely to result in A-type granite magmatism

5.8.Acknowledgements

5.9. CHAPTER 5: APPENDIX

All tables and supplementary data cited in chapter 5 can be found in this section

following similar format to the general style of peer-reviewed journals, as required for

manuscript submission

Table 5-1 Batch partial melting modeling for selected modal compositions of lower crustal source rock

Element	Starting composition (ppm) Neoproterozoic quartz diorite	Melt composition (ppm) for various assumed modal compositions, fraction of produced melt (F)= 0.3				Observed mean composition of Wentworth granites (ppm)
		50% cpx, 50% pl, 0% amp	20% cpx, 60% pl, 20% amp	15% cpx, 60% pl, 25% amp	35% qz, 62% pl, 3% Ksfp	
La	23.30	28 36	37 89	40 44	49 55	46.12
Ce	54.00	52 17	61 26	62 03	128 55	110.92
Nd	21.41	14 03	14 83	14 49	54 51	44.42
Sm	4.63	2 11	2 11	2 03	12 33	10.58
Eu	1.54	0 42	0 40	0 39	0 56	0.56
Tb	0.70	0 23	0 25	0 24	1 94	1.98
Yb	2.42	0 95	1 01	0 98	7 04	8.31
Lu	0.41	0 17	0 21	0 21	1 19	1.24

Notes Concentrations for these elements were calculated with the equation introduced by Wood and Fraser (1976) for batch melting Partition coefficients for the selected minerals are after Rollinson (1993) The sample selected as starting composition was chosen based on its isotopic similarities with the Wentworth granites However, only selected REEs were determined for that particular sample and therefore the modelled compositions do not cover the whole REE range, as determined for the Wentworth granites

Table 5-2 New Sm-Nd isotope analyses for selected granitic samples from the Wentworth Pluton (Data in this table also shown in Table S2)

Sample	SiO_2 (wt%)	$^{147}Sm/^{144}Nd$	$^{143}Nd/^{144}Nd$	$\varepsilon_{Nd(360)}$
4636	76.1	0.13378	0.51267	3.60
4641	70	0.12494	0.51260	2.52
5056	64.4	0.13313	0.51261	2.46
6419	76.7	0.14737	0.51268	3.15
6490	76.2	0.17041	0 51264	1.15
6518	73.1	0.10240	0.51258	3.13
7658	72.6	0.11487	0.51256	2.24
7710	75.9	0.13595	0.51266	3.19

Supplementary data Table S1 Whole-rock geochemical analyses of representative granitic rocks of the Wentworth Pluton

Sample	29-8-5	31-3-2	35-5-1	35-7-1	36-2-1		36-5-1	36-7-1	44-9-2	4614	4618	4623	4626	4630		4633	4634	4636	4640	4641	
Relative age	no type	late dykes and pods	post-gabbro probable	early granite definte	post-gabbro, probable		probable early granite	post-gabbro, probable	no type	syn-gabbro definte	syn-gabbro, definte	post-gabbro, probable	late dykes and pods	post-gabbro probable		post-gabbro, probable	post-gabbro, probable	early granite, definte	late dykes and pods	post-gabbro probable	
Source	Pe-Piper, 1996	Pe-Piper, 1996	Pe-Piper, 1996	Pe-Piper, 1996	Pe-Piper, 1996	new data	Pe-Piper, 1996	Pe-Piper 1996	Pe-Piper 1996	Pe-Piper 1996	Pe-Piper 1996	Pe-Piper 1996	Pe-Piper 1996	Pe-Piper 1996	new data	Pe-Piper, 1996	Pe-Piper, 1996	Pe-Piper, 1996	Pe-Piper, 1996	Pe-Piper, 1996	new data
Analysis	XRF-INAA	XRF	XRF	XRF-INAA	XRF-INAA	ICP-MS	XRF-INAA	XRF	XRF	XRF-INAA	XRF-INAA	XRF-INAA	XRF-INAA	XRF	ICP-MS	XRF	XRF-INAA	XRF-INAA	XRF-INAA	XRF	ICP-MS
Major elements (wt%)																					
SiO2	75 79	76 27	73 35	74 94	72 90		74 76	73 83	75 87	74 87	67 98	66 28	73 56	67 91		64 69	66 19	76 15	70 88	70 04	
TiO2	0 17	0 24	0 23	0 20	0 22		0 15	0 23	0 16	0 24	0 79	0 77	0 32	0 42		0 83	0 49	0 17	0 49	0 45	
Al2O3	12 09	12 37	13 10	11 86	13 76		11 79	13 13	11 78	12 55	12 90	14 52	12 95	14 80		14 63	15 02	11 58	13 87	14 25	
Fe2O3	1 68	0 98	2 14	2 79	1 85		1 85	2 04	1 90	2 25	5 01	5 07	2 51	4 57		5 87	5 12	2 53	3 49	3 48	
MnO	0 04	0 02	0 04	0 05	0 03		0 03	0 03	0 03	0 04	0 11	0 09	0 04	0 11		0 11	0 13	0 04	0 07	0 07	
MgO	0 77	0 67	0 82	0 83	0 89		0 73	1 06	0 64	0 82	2 27	1 50	0 98	0 91		1 52	0 91	0 82	1 01	1 05	
CaO	0 43	0 82	0 46	0 30	0 44		0 16	0 43	0 09	0 77	2 73	1 79	0 61	0 88		1 94	1 17	0 21	1 29	0 92	
Na2O	3 92	2 78	4 29	3 44	4 00		3 91	4 10	3 51	3 86	3 72	4 31	3 68	4 67		4 96	5 19	4 45	4 85	2 07	
K2O	4 56	5 55	5 11	4 77	5 55		4 88	4 79	4 83	5 32	4 20	4 71	5 31	5 63		4 92	5 71	4 65	4 39	5 36	
P2O5	0 03	0 03	0 03	0 03	0 03		0 03	0 05	0 02	0 03	0 14	0 18	0 05	0 05		0 21	0 06	0 01	0 11	0 10	
LOI	0 10	0 20	0 10	0 20	0 40		0 30	0 30	0 20	0 20	0 30	0 70	0 30	0 40		0 00	0 20	0 30	0 40	0 90	
Trace elements (ppm)																					
Ba	103	176	206	55	285	346 0	44	179	40	147	204	481	287	161	206 0	651	209	39	642	598	684 0
Rb	127	138	254	237	240	220 0	205	220	186	242	160	205	223	169	145 0	159	174	224	166	212	195 0
Sr	25	77	35	15	37	38 0	3	33	5	47	113	114	59	26	26 0	100	30	10	109	91	90 0
Y	70	92	85	114	60	44 1	96	116	66	93	90	79	86	83	75 4	82	95	90	48	53	43 6
Zr	142	643	292	548	212	231 0	306	308	303	710	827	453	325	850	1190 0	799	1087	552	295	324	396 0
Nb	37	46	54	81	23	27 9	62	55	45	57	46	39	45	41	65 8	36	76	69	23	20	24 3
Th	13	39	20	17	22		15	24	16	25	11	11	24	21		7	15	16	14	17	
Pb	7	88	25	21	17	15 0	8	15	13	b d	17	44	24	18	22 0	7	b d	3	8	41	27 0
Ga	21	23	25	30	20	18 0	23	22	24	25	21	24	24	29	27 0	26	31	30	19	19	18 0
Zn	46	57	58	161	32	29 0	43	27	36	49	128	95	51	123	115 0	119	111	131	51	72	60 0
Cu	4	30	6	4	b d	3 0	4	2	b d	b d	13	b d	b d	b d	7 0	b d	b d	b d	b d	b d	8 0
Ni	5	7	7	6	5	3 0	5	7	7	10	15	6	8	8	4 0	11	9	4	6	3	3 0
V	b d	9	4	2	21	< 5	b d	4	b d	1	81	40	10	5	< 5	31	5	2	15	15	11 0
Cr	59	33	32	31	21	< 20	38	31	41	33	66	25	24	26	< 20	27	17	32	32	34	< 20
Co	b d	b d	b d	b d	b d	< 1	b d	b d	b d	b d	b d	b d	b d	b d	< 1	b d	b d	b d	b d	b d	2 0
La	29	n d	n d	85	46	47 9	58	n d	n d	69	64	69	62	n d	160 0	64	106	71	41	n d	40 7
Ce	71	n d	n d	158	102	97 6	138	n d	n d	146	131	132	121	n d	329 0	130	202	152	76	n d	87 0
Pr	n d	n d	n d	n d	n d	10 7	n d	n d	n d	n d	n d	n d	n d	n d	36 8	n d	n d	n d	n d	n d	9 9
Nd	38	n d	n d	n d	n d	36 2	66	n d	n d	63	57	57	48	n d	134 0	63	86	68	33	n d	36 8
Sm	9 6	n d	n d	17 9	8 7	7 4	15 4	n d	n d	13 0	13 8	11 9	10 8	n d	23 5	13 5	16 3	15 3	7 9	n d	7 8
Eu	0 44	n d	n d	0 91	0 62	0 53	0 61	n d	n d	0 85	1 24	1 59	0 99	n d	1 40	2 40	1 68	0 58	1 47	n d	1 23
Gd	n d	n d	n d	n d	n d	6 8	n d	n d	n d	n d	n d	n d	n d	n d	19 3	n d	n d	n d	n d	n d	7 6
Tb	2 1	n d	n d	3 5	1 6	1 2	3 1	n d	n d	2 4	2 0	1 8	2 1	n d	2 9	2 0	2 3	2 3	1 1	n d	1 3
Dy	n d	n d	n d	n d	n d	7 4	n d	n d	n d	n d	n d	n d	n d	n d	15 7	n d	n d	n d	n d	n d	7 8
Ho	n d	n d	n d	n d	n d	1 6	n d	n d	n d	n d	n d	n d	n d	n d	3 1	n d	n d	n d	n d	n d	1 6
Er	n d	n d	n d	n d	n d	4 7	n d	n d	n d	n d	n d	n d	n d	n d	8 9	n d	n d	n d	n d	n d	4 7
Tm	n d	n d	n d	n d	n d	0 76	n d	n d	n d	n d	n d	n d	n d	n d	1 45	n d	n d	n d	n d	n d	0 76
Yb	6 9	n d	n d	12 4	5 8	5 2	10 1	n d	n d	9 9	9 1	7 2	8 8	n d	9 6	7 7	10 2	10 7	4 6	n d	5 1
Lu	1 09	n d	n d	1 99	0 85	0 74	1 28	n d	n d	1 54	1 47	1 12	1 34	n d	1 50	1 14	1 62	1 67	0 73	n d	0 72
Co	1	n d	n d	1	2		b d	n d	n d	n d	n d	n d	n d	n d		n d	n d	n d	4	n d	
Cr	42	n d	n d	26	19		b d	n d	n d	n d	n d	n d	n d	n d		n d	n d	n d	0	n d	
Cs	n d	n d	n d	n d	n d	4 6	2 2	n d	n d	n d	n d	n d	n d	n d	3 4	n d	n d	n d	2 4	n d	5 2
Hf	6 1	n d	n d	20 5	7 9	6 8	13 9	n d	n d	n d	n d	n d	n d	n d	20 4	n d	n d	n d	9 7	n d	8 8
Sb	b d	n d	n d	b d	b d	< 0 2	b d	n d	n d	n d	n d	n d	n d	n d	< 0 2	n d	n d	n d	0 0	n d	< 0 2
Sc	2	n d	n d	1	3	n d	1	n d	n d	n d	n d	n d	n d	n d	n d	n d	n d	n d	7	n d	n d
Ta	2 4	n d	n d	7 0	2 6	2 7	6 3	n d	n d	n d	n d	n d	n d	n d	3 2	n d	n d	n d	1 9	n d	2 1
Be	n d	n d	n d	n d	n d	n d	n d	n d	n d	n d	n d	n d	n d	n d	n d	n d	n d	n d	n d	n d	n d
Cd	n d	n d	n d	n d	n d	< 0 5	n d	n d	n d	n d	n d	n d	n d	n d	< 0 5	n d	n d	n d	n d	n d	b d
S	n d	n d	n d	n d	n d	b d	n d	n d	n d	n d	n d	n d	n d	n d	b d	n d	n d	n d	n d	n d	b d
Ge	n d	n d	n d	n d	n d	1 4	n d	n d	n d	n d	n d	n d	n d	n d	2 0	n d	n d	n d	n d	n d	n d
Th	17	n d	n d	26	29	25 8	21	n d	n d	24	14	16	25	n d	17 9	11	18	20	20	n d	19 2
U	b d	n d	b d	b d	b d	5 1	4 1	n d	n d	6 1	3 3	2 8	4 4	n d	3 8	n d	4 4	n d	4 6	n d	4 6

Note n d not determined, b d below detection limit XRF analyses for major and trace elements and INAA analyses for REEs and certain trace elements were done at the Regional Geochemical Center, Saint Mary's University, Halifax ICP-MS analyses were done by Activation Laboratories Ltd in Toronto, according to their code 4Lithoresearch and code 4B1 packages. Code 4Lithoresearch combines Fusion ICP for major elements and ICP/MS for trace elements, whereas code 4B1 includes Digestion ICP for certain trace elements (Ni, Cu, Zn, Ag)

107

108

Sample	4642	4646	4646	4648	4648	4650	4652	4654	4656	4660	4660	4663	4663	4664	4664	4665	4846	4644	4644	4652	4652	5056	5056
Relative age	post gabbro probable	post gabbro probable		early granite, probable		early granite, cut by gbr	early granite probable	post gabbro, definite	late dykes and pods	post gabbro probable		post gabbro, probable		early granite, probable		early granite definite	post gabbro, probable	early granite, probable		early granite, probable		syn-gabbro definite	
Source	Pe-Piper 1996	Pe-Piper 1996	new data	Pe-Piper 1996	new data	Pe-Piper 1996	Pe-Piper 1996	Pe-Piper 1996	Pe-Piper 1996	Pe-Piper 1996	new data	Pe-Piper 1996	new data	Pe-Piper 1996	new data	Pe-Piper 1996	Pe-Piper 1996	Pe-Piper 1996	new data	Pe-Piper 1996	new data	Pe-Piper 1996	new data
Analysis	XRF	XRF	ICP MS	XRF	ICP-MS	XRF-INAA	XRF	XRF-INAA	XRF-INAA	XRF	ICP MS	XRF	ICP MS	XRF	ICP MS	XRF INAA	XRF	XRF	ICP-MS	XRF	ICP-MS	XRF	ICP-MS
Major elements (wt%)																							
SiO2	71 78	74 10		73 62		73 03	73 52	76 07	76 34	75 38		72 49		76 40		76 01	74 10	74 11		73 52		64 43	
TiO2	0 43	0 17		0 21		0 20	0 20	0 14	0 15	0 20		0 25		0 15		0 16	0 17	0 24		0 20		0 86	
Al2O3	13 55	13 78		13 58		13 75	13 61	12 87	11 88	12 34		13 43		11 95		12 03	13 78	13 29		13 81		15 80	
Fe2O3	3 27	1 25		2 22		2 33	2 10	0 80	1 77	2 25		2 40		1 90		2 09	1 25	2 11		2 10		5 37	
MnO	0 06	0 03		0 05		0 06	0 06	0 02	0 03	0 04		0 05		0 04		0 04	0 03	0 03		0 06		0 07	
MgO	1 10	0 96		0 84		0 83	0 77	0 85	0 69	0 68		0 90		0 71		0 62	0 98	0 76		0 77		1 05	
CaO	0 74	0 74		0 52		0 57	0 64	0 43	0 16	0 18		0 74		0 34		0 20	0 74	0 50		0 64		2 62	
Na2O	3 59	4 30		3 95		3 84	4 05	3 77	3 31	3 99		4 09		4 05		4 16	4 30	4 07		4 05		3 44	
K2O	4 94	4 74		5 21		5 14	5 21	4 58	5 32	5 06		5 04		4 91		4 93	4 74	5 26		5 21		5 47	
P2O5	0 10	0 04		0 04		0 05	0 04	0 03	0 01	0 02		0 06		0 01		0 02	0 04	0 03		0 04		0 20	
LOI	0 60	0 20		0 20		0 20	0 20	0 60	0 00	0 20		0 60		0 50		0 10	0 20	0 20		0 20		0 60	
Trace elements (ppm)																							
Ba	555	376	445 0	168	223 0	204	248	133	57	113	142 0	190	254 0	52	57 0	37	376	212	277 0	248	316 0	669	752 0
Rb	210	139	119 0	272	254 0	240	258	205	206	179	162 0	252	230 0	203	171 0	189	139	260	228 0	258	232 0	176	161 0
Sr	88	119	112 0	34	37 0	39	37	55	11	9	100	51	54 0	8	9 0	5	119	44	43 0	37	38 0	148	150 0
Y	50	26	155	84	69 9	84	88	82	78	60	51 7	84	75 1	51	40 2	95	26	82	66 3	88	77 0	93	80 8
Zr	250	97	100 0	268	328 0	286	268	218	276	369	436 0	306	403 0	311	375 0	364	97	253	355 0	269	274 0	579	679 0
Nb	19	14	14 6	49	68 9	51	51	67	46	44	47 7	47	63 7	57	69 4	63	14	52	66 4	51	64 6	50	61 1
Th	29	31		33		21	27	31	19	12		26		25		27	31	24		27		19	
Pb	23	b d	15 0	22	18 0	8	17	119	11	b d	21 0	13	22 0	136	105 0	43	b d	14	16 0	17	18 0	30	28 0
Ga	19	15	14 0	24	23 0	25	21	23	25	24	24 0	20	21 0	26	22 0	25	15	26	24 0	21	23 0	23	23 0
Zn	50	24	17 0	37	28 0	32	34	33	40	90	97 0	60	57 0	62	61 0	114	24	48	45 0	34	25 0	88	62 0
Cu	b d	b d	14 0	b d	4 0	b d	b d	17	b d	b d	4 0	b d	5 0	b d	8 0	b d	b d	b d	5 0	b d	3 0	10	7 0
Ni	9	7	5 0	4	3 0	9	8	8	7	6	3 0	8	4 0	10	6 0	7	7	7	3 0	8	3 0	6	6 0
V	6	7	8 0	4	< 5	1	1	4	b d	b d	< 5	8	8 0	b d	< 5	b d	7	7	6 0	1	< 5	49	45 0
Cr	40	41	< 20	24	< 20	40	27	24	34	21	< 20	24	< 20	49	20 0	37	41	26	< 20	27	< 20	12	< 20
Co	b d	b d	< 1	b d	< 1	b d	b d	b d	b d	b d	< 1	b d	1 0	b d	< 1	b d	b d	b d	1 0	b d	< 1	b d	37 0
La	38	n d	58 2	n d	67 4	88	n d	60	57	n d	40 9	n d	92 7	n d	39 3	66	n d	n d	60 8	n d	81 7	n d	67 6
Ce	67	n d	83 0	n d	157 0	136	n d	75	82	n d	135 0	n d	176 0	n d	97 8	136	n d	n d	142 0	n d	144 0	n d	159 0
Pr	0 0	n d	5 5	n d	15 7	n d	n d	n d	n d	n d	13 2	n d	19 2	n d	10 5	n d	n d	n d	14 0	n d	18 5	n d	18 1
Nd	31	n d	16 0	n d	53 8	62	n d	44	54	n d	49 9	n d	62 1	n d	39 3	63	n d	n d	48 5	n d	64 7	n d	68 4
Sm	7 2	n d	2 9	n d	11 7	14 2	n d	11 2	14 0	n d	11 6	n d	12 3	n d	8 6	14 2	n d	n d	10 3	n d	13 8	n d	15 6
Eu	1 24	n d	0 51	n d	0 78	0 96	n d	0 53	0 54	n d	0 88	n d	0 83	n d	0 49	0 89	n d	n d	0 67	n d	0 79	n d	1 88
Gd	n d	n d	2 8	n d	11 2	n d	n d	n d	n d	n d	10 7	n d	12 3	n d	7 8	n d	n d	n d	10 5	n d	13 3	n d	15 3
Tb	1 0	n d	0 5	n d	2 1	2 0	n d	1 8	2 3	n d	1 9	n d	2 2	n d	1 4	2 5	n d	n d	1 9	n d	2 4	n d	2 6
Dy	n d	n d	2 7	n d	12 8	n d	n d	n d	n d	n d	11 4	n d	13 5	n d	8 5	n d	n d	n d	11 8	n d	14 2	n d	15 5
Ho	n d	n d	0 6	n d	2 7	n d	n d	n d	n d	n d	2 3	n d	2 8	n d	1 8	n d	n d	n d	2 5	n d	2 9	n d	3 1
Er	n d	n d	1 7	n d	7 7	n d	n d	n d	n d	n d	6 4	n d	8 0	n d	5 1	n d	n d	n d	7 3	n d	8 2	n d	8 6
Tm	n d	n d	0 27	n d	1 28	n d	n d	n d	n d	n d	1 05	n d	1 32	n d	0 86	n d	n d	n d	1 25	n d	1 33	n d	1 33
Yb	4 3	n d	2 0	n d	8 1	n d	n d	7 9	8 0	n d	7 0	n d	8 4	n d	5 7	9 7	n d	n d	8 4	n d	8 4	n d	8 5
Lu	0 67	n d	0 30	n d	1 15	1 31	n d	1 19	1 20	n d	0 95	n d	1 12	n d	0 80	1 43	n d	n d	1 11	n d	1 18	n d	1 16
Co	4	n d		n d		2	n d	1	1	n d		n d		n d		n d	n d	n d		n d		n d	
Cr	b d	n d		n d		b d	n d	n d	n d	n d		n d		n d		n d	n d	n d		n d		n d	
Cs	4 7	n d	1 9	n d	6 0	5 6	n d	2 1	1 8	n d	1 5	n d	4 0	n d	3 3	n d	n d	n d	3 7	n d	5 4	n d	6 0
Hf	8 3	n d	2 8	n d	8 6	10 5	n d	9 4	12 4	n d	11 5	n d	10 2	n d	10 9	n d	n d	n d	9 8	n d	7 0	n d	14 2
Sb	b d	n d	< 0 2	n d	< 0 2	b d	n d	n d	n d	n d	< 0 2	n d	< 0 2	n d	< 0 2	n d	n d	n d	< 0 2	n d	< 0 2	n d	< 0 2
Sc	6	n d	n d	n d	n d	3	n d	2	1	n d	n d	n d	n d	n d	n d	n d	n d	n d	n d	n d	n d	n d	n d
Ta	1 8	n d	1 4	n d	4 6	4 5	n d	5 2	2 3	n d	2 7	n d	4 3	n d	4 7	n d	n d	n d	5 5	n d	4 9	n d	3 7
Be	n d	n d	n d	n d	n d	n d	n d	n d	n d	n d	n d	n d	n d	n d	n d	n d	n d	n d	n d	n d	n d	n d	n d
Cd	n d	n d	< 0 5	n d	< 0 5	n d	n d	n d	n d	n d	< 0 5	n d	< 0 5	n d	< 0 5	n d	n d	n d	< 0 5	n d	< 0 5	n d	< 0 5
S	n d	n d	b d	n d	b d	n d	n d	n d	n d	n d	b d	n d	b d	n d	0 0	n d	n d	n d	b d	n d	b d	n d	b d
Ge	n d	n d	1 5	n d	1 9	n d	n d	n d	n d	n d	1 9	n d	1 7	n d	1 0	n d	n d	n d	1 7	n d	1 9	n d	1 5
Th	23	n d	31 8	n d	30 5	28	n d	32	17	n d	16 5	n d	31 0	n d	15 9	18	n d	n d	25 5	n d	26 8	n d	18 9
U	4 0	n d	2 2	n d	5 9	5 4	n d	9 6	4 8	n d	6 2	n d	3 7	n d	5 4	n d	n d	n d	5 3	n d	4 6		

Note n d not determined b d below detection limit XRF analyses for major and trace elements and INAA analyses for REEs and certain trace elements were done at the Regional Geochemical Center Saint Mary's University Halifax ICP-MS analyses were done by Activation Laboratories Ltd in Toronto according to their code 4Lithoresearch and code 4B1 packages Code 4Lithoresearch combines Fusion ICP for major elements and ICP/MS for trace elements whereas code 4B1 includes Digestion ICP for certain trace elements (Ni Cu Zn Ag)

Supplementary data Table S1 Whole rock geochemical analyses of representative granitic rocks of the Wentworth Pluton

Sample	5060		8518	6588	6590	6591		6688	6902		6971		7814		4615	4629	4631	4632	4645	4651	4657	4658	
Relative age	post gabbro probable		post gabbro probable	early granite definite	syn-gabbro probable	late fine-grained granite dyke		early granite probable	early granite probable		early granite probable		early granite cut by gbr		syn-gabbro definite	late dykes and pods	post gabbro probable	post-gabbro probable	post gabbro probable	post gabbro probable	syn-gabbro definite	syn-gabbro probable	
Source	Pe-Piper 1996	new data	Pe-Piper 1996	Pe-Piper 1996	Pe-Piper 1996	Pe-Piper 1996	new data	Pe-Piper 1996	Pe-Piper 1996	new data	Pe-Piper 1996	new data	Pe-Piper 1996	new data	Pe-Piper 1996	Pe-Piper 1996	Pe-Piper 1996	Pe-Piper 1996	Pe-Piper 1996	Pe-Piper 1996	Pe-Piper 1996	Pe-Piper 1996	new data
Analysis	XRF	ICP-MS	XRF INAA	XRF-INAA	XRF-INAA	XRF	ICP-MS	XRF ICP-MS	XRF	ICP-MS	XRF INAA	ICP-MS	XRF-INAA	ICP-MS	XRF-INAA	XRF	XRF	XRF	XRF	XRF	XRF	XRF	ICP-MS
Major elements (wt%)																							
SiO$_2$	76.62		73.09	75.18	76.42	74.02		78.03	77.74		76.83		76.65		74.49	69.95	68.29	65.86	71.21	73.48	75.81	77.33	
TiO$_2$	0.15		0.43	0.19	0.23	0.22		0.25	0.07		0.18		0.19		0.31	0.46	0.38	0.88	0.34	0.22	0.21	0.11	
Al$_2$O$_3$	11.80		11.74	12.84	10.34	13.27		11.42	12.25		11.53		11.80		12.55	14.19	14.68	14.29	14.50	13.45	12.32	11.54	
Fe$_2$O$_3$	1.79		4.54	1.58	3.11	1.94		2.26	0.89		2.18		1.87		1.46	3.30	3.97	5.63	2.18	1.94	2.30	1.87	
MnO	0.02		0.10	0.02	0.01	0.03		0.07	0.02		0.05		0.03		0.04	0.06	0.07	0.12	0.06	0.03	0.04	0.03	
MgO	0.00		0.02	0.00	0.00	0.09		0.07	0.00		0.07		0.03		1.01	1.16	0.94	1.62	1.00	1.04	0.70	0.72	
CaO	0.10		0.56	0.42	0.23	0.56		0.28	0.32		0.29		0.53		1.37	0.93	0.49	2.04	1.04	0.34	0.31	0.15	
Na$_2$O	3.02		4.25	3.55	2.49	3.90		4.58	3.92		3.77		3.37		3.21	4.41	4.69	4.67	4.06	4.28	3.57	3.42	
K$_2$O	5.09		4.82	5.54	5.21	5.37		2.92	4.57		4.81		5.07		5.77	4.90	5.85	4.60	4.95	5.03	5.92	4.74	
P$_2$O$_5$	0.01		0.02	0.02	0.03	0.03		0.03	0.01		0.02		0.02		0.05	0.09	0.03	0.25	0.08	0.04	0.02	0.01	
LOI	0.00		0.20	0.00	0.00	0.30		0.19	0.33		0.35		0.32		0.30	0.30	1.00	0.20	0.10	0.50	0.00	0.00	
Trace elements (ppm)																							
Ba	47	880	12	123	38	173	2480	23	49	1080	60	550	b d	680	187	468	140	640	570	158	125	24	470
Rb	201	173.0	170	229	180	192	176.0	95	279	242.0	246	205.0	174	166.0	214	217	194	152	143	211	169	197	194.0
Sr	7	8.0	12	16	18	31	33.0	18	8	8.0	14	13.0	33	22.0	84	76	20	116	152	30	13	9	11.0
Y	57	48.2	102	85	189	75	68.4	137	79	59.2	107	79.8	88	76.4	98	77	63	64	38	124	85	63	54.2
Zr	276	267.0	2136	292	1280	294	331.0	1011	143	138.0	608	569.0	262	280.0	1009	452	911	460	198	298	370	371	416.0
Nb	71	71.2	77	47	96	48	56.2	84	65	64.0	85	88.4	60	72.0	47	41	34	34	20	58	45	73	93.0
Th	16		21	25	27	28		17	27		19		17		25	23	18	21	21	19	15	15	
Pb	20	21.0	14	19	26	16	19.0	13	18	24.0	8	11.0	16	18.0	18	22	28	15	21	0	9	34	41.0
Ga	22	22.0	34	21	20	21	19.0	22	25	21.0	33	29.0	27	24.0	21	22	26	24	18	23	25	26	25.0
Zn	47	58.0	138	16	135	53	53.0	52	46	17.0	122	107.0	40	32.0	39	61	106	78	36	27	70	55	52.0
Cu	6	16.0	22	b d	10	b d	3.0	b d	14	14.0	15	9.0	6	5.0	b d	b d	b d	b d	b d	b d	b d	5	17.0
Ni	b d	2.0	b d	b d	5	b d	3.0	5	b d	2.0	b d	7.0	4	2.0	7	5	8	9	6	9		b d	3.0
V	b d	<5	b d	b d	30	7	<5	b d	b d	<5	b d	<5	b d	<5	14	15	2	39	16	4		b d	<5
Cr	19	<20	7	5	10	0	<20	5	b d	<20	b d	<20	12	<20	32	32	31	25	39	34		32	<20
Co	b d	47.0	b d	b d	b d	b d	73.0	b d	b d	98.0	b d	76.0	b d	78.0	b d	b d	b d	b d	b d	b d	b d	b d	<1
La	n d	315	232	92	109	n d	67.3	104	n.d	25.8	54	48.2	n.d	59.0	n d	n d	n.d	n d	n d	n d	n d	n d	23.9
Ce	n d	834	437	130	225	n d	136.0	208	n d	49.0	117	122.0	122	120.0	n d	n d	n d	n d	n d	n d	n d	n d	55.5
Pr	n d	9.0	n d	n d	n d	n d	16.0	n d	n d	7.1	n d	13.7	n d	15.5	n d	n d	n d	n d	n d	n d	n d	n d	6.9
Nd	n d	33.6	176	70	103	n d	55.3	96	n d	24.7	56	52.9	n d	58.5	n d	n d	n d	n d	n d	n d	n d	n d	25.2
Sm	n d	8.2	30.1	13.0	22.3	n d	11.7	20.0	n d	7.1	12.7	13.8	n d	13.7	n d	n d	n d	n d	n d	n d	n d	n d	7.5
Eu	n d	0.34	1.44	0.76	0.65	n.d	0.50	1.17	n d	0.07	0.62	0.65	n d	0.50	n d	n d	n d	n d	n d	n d	n d	n d	0.07
Gd	n d	8.0	n d	n d	n d	n d	11.0	n d	n d	7.8	n d	14.0	n d	13.4	n d	n d	n d	n d	n d	n d	n d	n d	8.3
Tb	n d	1.5	3.3	1.9	4.0	n d	2.0	3.3	n d	1.6	2.4	2.6	n d	2.4	n d	n d	n d	n d	n.d	n d	n d	n d	1.7
Dy	n d	9.6	n d	n d	n d	n d	12.3	n d	n d	10.5	n d	15.8	n d	14.6	n d	n d	n d	n d	n d	n d	n d	n d	10.5
Ho	n d	2.1	n d	n d	n d	n d	2.6	n d	n d	2.2	n d	3.2	n d	3.0	n d	n d	n d	n d	n d	n d	n d	n d	2.2
Er	n d	5.9	n d	n d	n d	n d	7.6	n.d	n d	6.5	n d	9.2	n d	8.4	n d	n d	n d	n d	n d	n d	n d	n d	6.4
Tm	n d	0.98	n d	n d	n d	n.d	1.29	n d	n d	1.13	n d	1.60	n d	1.40	n d	n d	n d	n d	n d	n d	n d	n d	1.06
Yb	n d	6.5	13.4	8.1	17.3	n d	8.4	14.1	n d	7.5	10.3	10.3	n.d	8.8	n d	n d	n d	n d	n d	n d	n d	n d	7.1
Lu	n d	0.90	2.10	1.24	2.69	n d	1.18	2.09	n d	0.98	1.57	1.43	n.d	1.22	n d	n d	n d	n d	n d	n d	n d	n d	0.93
Co	n d		n d	n d	n d	n.d		n d	n d		n d		n d		n.d	n d	n.d	n d	n d	n d	n d		
Cr	n d		n d	n d	n d	n d		n d	n d		n d		n d		n.d	n d	n d	n d	n d	n d	n d		
Cs	n d	2.3	n d	n d	n d	n d	1.9	n d	n d	3.1	n d	2.3	n d	1.3	n d	n d	n d	n d	n d	n d	n d	n d	2.3
Hf	n d	8.9	n d	n d	n d	n d	9.4	n d	n d	5.7	n d	14.9	n d	8.9	n d	n d	n d	n d	n d	n d	n.d	n d	12.8
Sb	n d	<0.2	n d	n d	n d	n d	<0.2	n.d.	n d	<0.2	n d	<0.2	n d	<0.2	n d	n d	n d	n d	n d	n d	n d	n d	<0.2
Sc	n d	n d	n d	n d	n d	n d	n d	n d	n d	n d	n d	n d	n d	n d	n d	n d	n d	n d	n d	n d	n d	n d	n d
Ta	n d	5.9	n d	n d	n d	n d	5.5	n d	n d	7.1	n d	8.3	n d	5.1	n d	n d	n d	n d	n d	n d	n d	n d	4.8
Be	n d	n d	n d	n d	n d	n d	n d	n d	n d	n d	n d	n d	n d	n d	n d	n d	n d	n d	n d	n d	n d	n d	n d
Cd	n d	<0.5	n d	n d	n d	n d	<0.5	n d	n d	<0.5	n d	<0.5	n d	<0.5	n d	n d	n d	n d	n d	n d	n d	n d	<0.5
S	n d	b d	n d	n d	n d	n d	b d	n d	n d	b d	n d	b d	n d	b d	n d	n d	n d	n d	n d	n d	n d	n d	b d
Ge	n d	1.9	n d	n d	n d	n d	1.7	n d	n d	1.7	n d	1.9	n d	2.2	n d	n d	n d	n d	n d	n d	n d	n d	1.7
Th	n d	18.2	17	23	26	n d	25.3	18	n d	30.8	22	19.8	n d	18.7	n d	n d	n d	n d	n d	n d	n d	n d	17.6
U	n d	4.4	3.5	6.0	38.4	n d	5.9	5.0	n d				n d	4.5	n d	n d	n d	n d	n d	n d	n d	n d	4.4

Note n d not determined b d below detection limit XRF analyses for major and trace elements and INAA analyses for REEs and certain trace elements were done at the Regional Geochemical Center Saint Mary's University, Halifax ICP-MS analyses were done by Activation Laboratories Ltd in Toronto according to their code 4Lithoresearch and code 4B1 packages Code 4Lithoresearch combines Fusion ICP for major elements and ICP/MS for trace elements whereas code 4B1 includes Digestion ICP for certain trace elements (Ni, Cu, Zn, Ag)

Supplementary data Table S1 Whole-rock geochemical analyses of representative granitic rocks of the Wentworth Pluton

Sample	4862B	6533	6370	6373	6419	6490	6686	6808	6970	5067	6110	6484	7359		7360		7372		7373		7374		7419	7514
Relative age	post-gabbro, probable	late dykes and pods	late dykes and pods	post-gabbro, probable	syn-gabbro definite	post-gabbro, probable	early granite definite	post-gabbro, probable	syn-gabbro definite	syn-gabbro, probable	syn-gabbro, definite	syn-gabbro, definite	late dykes and pods		late dykes and pods		post-gabbro granite		post gabbro granite		syn-gabbro granite		early granite,	early granite, probable
Source	Pe-Piper 1996	Pe-Piper 1996	Pe-Piper 1996	Pe-Piper 1996	Pe-Piper 1996	Pe-Piper 1996	Pe-Piper 1996	Pe-Piper 1996	Pe-Piper 1996	Pe-Piper 1996	Pe-Piper 1996	Pe-Piper 1996	Pe-Piper 1996	new data	Pe-Piper 1996	new data	Pe-Piper 1996	new data	Pe-Piper 1996	new data	Pe-Piper 1996	new data	Pe-Piper 1996	Pe-Piper 1996
Analysis	XRF	XRF	XRF	XRF	XRF	XRF	XRF	XRF	XRF	XRF	XRF	XRF	XRF	ICP-MS	XRF	ICP-MS	XRF	ICP-MS	XRF	ICP-MS	XRF	ICP-MS	XRF	XRF
Major elements (wt%)																								
SiO$_2$	72 14	76 35	77 87	67 24	76 79	76 21	73 59	73 58	74 67	77 06	75 40	77 24	76 63		77 53		76 20		75 72		75 44		75 08	73 67
TiO$_2$	0 33	0 11	0 10	0 57	0 18	0 17	0 29	0 22	0 27	0 15	0 21	0 19	0 14		0 10		0 22		0 25		0 27		0 22	0 15
Al$_2$O$_3$	14 37	11 98	11 72	13 57	11 13	12 59	13 49	13 60	12 93	11 35	11 50	11 95	12 45		11 99		12 09		11 96		11 96		12 83	14 45
Fe$_2$O$_3$	1 65	1 62	1 75	7 69	2 82	1 67	2 88	2 57	2 18	1 78	2 78	1 21	0 77		0 49		1 82		2 35		3 08		1 94	1 18
MnO	0 05	0 03	0 01	0 17	0 05	0 03	0 07	0 02	0 04	0 02	0 06	0 02	0 01		0 01		0 04		0 05		0 03		0 04	0 03
MgO	1 11	0 00	0 00	0 06	0 02	0 04	0 02	0 15	0 09	0 00	0 11	0 07	0 03		0 06		0 31		0 28		0 25		0 03	0 09
CaO	1 11	0 19	0 26	1 27	0 18	0 45	0 63	0 45	0 34	0 25	0 54	0 79	0 24		0 51		0 30		0 71		0 73		0 50	1 08
Na$_2$O	4 69	3 57	3 71	4 53	3 75	3 50	5 24	4 07	3 69	2 79	4 38	3 32	2 33		3 68		3 63		3 78		2 89		3 50	4 37
K$_2$O	4 61	5 15	4 38	4 98	4 59	5 31	3 75	4 87	5 39	5 11	4 70	4 85	7 06		4 80		4 81		4 69		5 49		5 58	3 61
P$_2$O$_5$	0 07	0 00	0 01	0 06	0 01	0 02	0 02	0 02	0 03	0 01	0 03	0 03	0 02		0 02		0 03		0 03		0 03		0 02	0 04
LOI	0,20	0 40	0 29	0 13	0 40	0 28	0 29	0 74	0 55	0 10	0 35	0 40	0 29		0 36		0 46		0 29		0 32		0 26	0,30
Trace elements (ppm)																								
Ba	650	b d	b d	157	52	128	579	209	257	45	40	109	452	620 0	77	134 0	72	129 0	87	126 0	170	310 0	230	1092
Rb	83	296	180	136	257	170	146	221	240	201	187	188	181	169 0	136	130 0	190	178 0	180	171 0	210	189 0	249	85
Sr	162	18	16	18	13	21	29	29	36	10	7	46	108	110 0	36	38 0	34	36 0	50	53 0	23			122
Y	31	97	112	144	89	71	115	66	70	87	162	70	21	17 4	21	17 7	88	79 3	90	78 5	113	100 0	79	19
Zr	196	262	271	981	722	271	625	414	372	282	564	279	69	810 0	69	930 0	434	492 0	420	482 0	633	688 0	333	89
Nb	19	92	87	74	106	66	62	44	61	61	85	68	22	26 3	20	22 4	69	68 0	57	64 0	58	68 7	56	12
Th	6	28	22	11	21	14	18	25	18	19	20	12	16		24		18		15		22		21	11
Pb	3	34	8	14	29	12	7	43	5	23	18	65	25	24 0	14	13 0	10	14 0	11	10 0	17	19 0	15	16
Ga	12	26	27	39	34	26	26	22	27	22	30	24	23	17 0	15	13 0	32	24 0	29	24 0	26	22 0	21	15
Zn	90	90	45	309	181	77	82	63	52	42	148	50	10	10 0	b d	5 0	34	37 0	61	62 0	49	50 0	61	9
Cu	b d	b d	5	27	40	23	17	31	8	b d	5	19	10	1 0	12	7 0	38	33 0	13	3 0	15	4 0	20	b d
Ni	6	5	77	b d	25	b d	b d	b d	b d	b d	b d	b d	b d	3 0	b d	3 0	b d	4 0	b d	6 0	b d	6 0	b d	b d
V	15	7	b d	b d	13	b d	b d	b d	b d	b d	b d	18	7	< 5	5	< 5	12	9 0	17	11 0	17	12 0	b d	11
Cr	28	b d	44	b d	18	b d	b d	b d	b d	39	14	14	b d	< 20	b d	< 20	7	< 20	10	< 20	8	< 20	b d	5
Co	b d	b d	b d	b d	b d	b d	b d	b d	b d	b d	b d	b d	b d	75 0	b d	98 0	b d	107 0	0	83 0	0	81 0	b d	b d
La	n d	n d	n d	n d	n d	n d	n d	n d	n d	n d	n d	n d	n d	34 4	n d	10 8	n d	51 4	n d	60 9	n d	43 0	n d	n d
Ce	n d	n d	n d	n d	n d	n d	n d	n d	n d	n d	n d	n d	n d	127 0	n d	29 3	n d	121 0	n d	136 0	n d	92 1	n d	n d
Pr	n d	n d	n d	n d	n d	n d	n d	n d	n d	n d	n d	n d	n d	8 7	n d	3 4	n d	14 0	n d	15 8	n d	14 7	n d	n d
Nd	n d	n d	n d	n d	n d	n d	n d	n d	n d	n d	n d	n d	n d	29 2	n d	11 7	n d	52 1	n d	58 2	n d	57 9	n d	n d
Sm	n d	n d	n d	n d	n d	n d	n d	n d	n d	n d	n d	n d	n d	5 5	n d	3 1	n d	12 6	n d	13 0	n d	15 7	n d	n d
Eu	n d	n d	n d	n d	n d	n d	n d	n d	n d	n d	n d	n d	n d	0 86	n d	0 17	n d	0 57	n d	0 66	n d	0 90	n d	n d
Gd	n d	n d	n d	n d	n d	n d	n d	n d	n d	n d	n d	n d	n d	4 4	n d	3 0	n d	13 1	n d	13 3	n d	17 5	n d	n d
Tb	n d	n d	n d	n d	n d	n d	n d	n d	n d	n d	n d	n d	n d	0 7	n d	0 5	n d	2 4	n d	2 4	n d	3 2	n d	n d
Dy	n d	n d	n d	n d	n d	n d	n d	n d	n d	n d	n d	n d	n d	3 7	n d	3 2	n d	15 0	n d	14 4	n d	19 6	n d	n d
Ho	n d	n d	n d	n d	n d	n d	n d	n d	n d	n d	n d	n d	n d	0 7	n d	0 6	n d	3 2	n d	3 0	n d	4 1	n d	n d
Er	n d	n d	n d	n d	n d	n d	n d	n d	n d	n d	n d	n d	n d	2 1	n d	1 8	n d	9 0	n d	8 6	n d	11 2	n d	n d
Tm	n d	n d	n d	n d	n d	n d	n d	n d	n d	n d	n d	n d	n d	0 36	n d	0 33	n d	1 55	n d	1 44	n d	1 81	n d	n d
Yb	n d	n d	n d	n d	n d	n d	n d	n d	n d	n d	n d	n d	n d	2 7	n d	2 5	n d	10 1	n d	9 2	n d	11 3	n d	n d
Lu	n d	n d	n d	n d	n d	n d	n d	n d	n d	n d	n d	n d	n d	0 36	n d	0 38	n d	1 38	n d	1 29	n d	1 53	n d	n d
Co	n d	n d	n d	n d	n d	n d	n d	n d	n d	n d	n d	n d	n d		n d		n d		n d		n d		n d	n d
Cr	n d	n d	n d	n d	n d	n d	n d	n d	n d	n d	n d	n d	n d		n d		n d		n d		n d		n d	n d
Cs	n d	n d	n d	n d	n d	n d	n d	n d	n d	n d	n d	n d	n d	2 5	n d	1 7	n d	1 3	n d	1 8	n d	3 4	n d	n d
Hf	n d	n d	n d	n d	n d	n d	n d	n d	n d	n d	n d	n d	n d	2 7	n d	3 6	n d	11 7	n d	11 0	n d	15 0	n d	n d
Sb	n d	n d	n d	n d	n d	n d	n d	n d	n d	n d	n d	n d	n d	< 0 2	n d	< 0 2	n d	< 0 2	n d	< 0 2	n d	< 0 2	n d	n d
Sc	n d	n d	n d	n d	n d	n d	n d	n d	n d	n d	n d	n d	n d	n d	n d	n d	n d	n d	n d	n d	n d	n d	n d	n d
Ta	n d	n d	n d	n d	n d	n d	n d	n d	n d	n d	n d	n d	n d	3 7	n d	6 4	n d	7 2	n d	5 5	n d	6 2	n d	n d
Be	n d	n d	n d	n d	n d	n d	n d	n d	n d	n d	n d	n d	n d	n d	n d	n d	n d	n d	n d	n d	n d	n d	n d	n d
Cd	n d	n d	n d	n d	n d	n d	n d	n d	n d	n d	n d	n d	n d	< 0 5	n d	< 0 5	n d	< 0 5	n d	< 0 5	n d	< 0 5	n d	n d
S	n d	n d	n d	n d	n d	n d	n d	n d	n d	n d	n d	n d	n d	0 0	n d	b d	n d	b d	n d	b d	n d	b d	n d	n d
Ge	n d	n d	n d	n d	n d	n d	n d	n d	n d	n d	n d	n d	n d	1 4	n d	1 2	n d	1 7	< 5	1 7	n d	1 8	n d	n d
Th	n d	n d	n d	n d	n d	n d	n d	n d	n d	n d	n d	n d	n d	14 8	n d	23 5	n d	19 5	n d	17 3	n d	20 1	n d	n d
U	n d	n d	n d	n d	n d	n d	n d	n d	n d	n d	n d	n d	n d	2 4	n d	2 2	n d	4 3	n d	4 4	n d	5 1	n d	n d

Note n d not determined, b d below detection limit XRF analyses for major and trace elements and INAA analyses for REEs and certain trace elements were done at the Regional Geochemical Center, Saint Mary's University, Halifax ICP-MS analyses were done by Activation Laboratories Ltd in Toronto, according to their code 4Lithoresearch and code 4B1 packages Code 4Lithoresearch combines Fusion ICP for major elements and ICP/MS for trace elements, whereas code 4B1 includes Digestion ICP for certain trace elements (Ni, Cu, Zn, Ag)

110

Supplementary data Table S1 Whole rock geochemical analyses of representative granitic rocks of the Wentworth Pluton

Sample	7629	7658	7630		7710	7704	7816B		8001	8002	8005	8010	8061	8083A	8083B	8084	8085	8202	8203		8204	9819	9820	9821
Relative age	post gabbro probable	post-gabbro, probable	late dykes and pods		post-gabbro probable	early granite definite	late, fine-grained granite		early granite probable	early granite probable	early granite, probable	early granite, probable	early granite probable	early granite probable	early granite probable	early granite probable	no data	post gabbro probabl	late fine-grained granite		no data	early granite, probable	early granite, probable	early granite, probable
Source	Pe-Piper 1996	Pe-Piper 1996	Pe-Piper 1996	new data	Pe-Piper 1996	Pe-Piper 1996	Pe-Piper 1996	new data	Pe-Piper 1996	Pe-Piper 1996	Pe-Piper 1996	Pe-Piper 1996	Pe-Piper 1996	Pe-Piper 1996	Pe-Piper 1996	Pe-Piper 1996	Pe-Piper 1996	Pe-Piper 1996	Pe-Piper, 1996	new data	Pe-Piper 1996	new data	new data	new data
Analysis	XRF	XRF	XRF	ICP-MS	XRF	XRF-INAA	XRF	ICP-MS	XRF	XRF	XRF	XRF	XRF	XRF	XRF	XRF	XRF	XRF	XRF	ICP-MS	XRF	ICP-MS	ICP-MS	ICP-MS
Major elements (wt%)																								
SiO$_2$	76.55	72.62	72.76		75.85	83.35	76.05		74.32	76.26	76.33	75.76	74.63	76.22	76.30	76.56	72.40	76.84	75.74		71.96	73.09	79.36	66.44
TiO$_2$	0.19	0.32	0.30		0.23	0.15	0.08		0.25	0.21	0.31	0.21	0.19	0.14	0.13	0.10	0.28	0.15	0.26		0.37	0.58	0.07	0.84
Al$_2$O$_3$	12.21	13.60	13.87		11.91	7.97	13.43		13.01	11.56	11.61	11.50	12.78	12.55	12.41	11.74	13.09	12.60	12.47		14.95	13.29	10.60	13.62
Fe$_2$O$_3$	1.73	2.72	2.39		2.54	2.08	0.52		1.99	2.53	2.91	2.47	1.88	1.49	1.40	1.49	2.66	1.75	3.02		2.19	2.41	1.97	4.85
MnO	0.04	0.08	0.05		0.04	0.07	0.02		0.02	0.05	0.04	0.03	0.03	0.02	0.01	0.02	0.04	0.03	0.03		0.06	0.08	0.01	0.07
MgO	0.22	0.24	0.25		0.09	0.12	0.02		0.08	0.23	0.14	0.14	0.13	0.07	0.06	0.06	0.17	0.04	0.10		0.45	0.71	0.11	1.25
CaO	0.48	0.90	0.97		0.40	1.17	0.75		0.45	0.50	0.43	0.41	0.45	0.44	0.34	0.47	0.51	0.23	0.38		1.19	1.98	0.10	3.16
Na$_2$O	3.47	3.72	3.80		3.91	2.48	4.60		3.96	3.75	3.90	3.70	3.69	3.81	3.65	3.66	4.14	3.71	3.37		4.27	4.20	5.95	3.52
K$_2$O	4.77	5.24	5.17		4.77	2.25	3.93		5.37	4.80	4.67	4.64	5.74	5.14	5.20	4.66	5.12	4.38	4.67		4.06	4.17	0.04	4.74
P$_2$O$_5$	0.04	0.07	0.06		0.02	0.02	0.01		0.03	0.02	0.03	0.02	0.01	0.01	0.01	0.01	0.03	0.00	0.01		0.08	0.13	0.01	0.16
LOI	0.52	0.57	0.53		0.29	0.47	0.32		0.40	0.52	0.30	0.50	0.56	0.30	0.59	0.29	0.10	0.18	0.65		0.65	0.34	0.22	0.46
Trace elements (ppm)																								
Ba	185	365	383	395.0	76	157	0	167.0	329	93	192	83	299	274	222	291	991	25	260	700	735.0	561.0	24.0	325.0
Rb	181	253	201	182.0	203	70	148	140.0	257	202	221	228	287	284	203	366	191	169	203	170.0	124.0	108.0	<1	74.0
Sr	37	65	66	65.0	16	58	77	66.0	42	39	31	29	33	29	30	17	35	13	25	23.0	163.0	124.0	44.0	189.0
Y	72	82	73	60.2	88	130	60	48.7	76	82	122	98	67	52	41	75	58	52	120	106.0	43.0	52.2	136.0	74.3
Zr	245	383	407	394.0	699	867	62	67.0	326	614	843	586	218	232	218	174	553	323	650	696.0	224.0	596.0	630.0	348.0
Nb	47	47	44	51.4	57	56	122	159.0	53	72	67	75	41	35	34	92	90	96	86	61.2	37.0	28.6	112.0	42.3
Th	16	29	26		18	18	35		22	18	16	23	29	31	25	56	29	30	18.0					
Pb	37	29	90	94.0	15	49	31	32.0	11	8	8	31	29	28	34	56	77	16	19	14.0	19.0	6.0	5.0	14.0
Ga	21	24	22	20.0	31	14	29	26.0	26	28	27	29	25	26	25	26	23	29	29	29.0	23.0	18.0	28.0	25.0
Zn	62	81	82	56.0	112	59	46	26.0	43	76	50	74	56	27	33	19	41	66	48	50.0	30.0	27.0	49.0	52.0
Cu	5	6	15	4.0	11	28	7	6.0	4	3	6	14	5	3	2	8	10	11	9	5.0	14.0	17.0	33.0	22.0
Ni	b d	b d	b c	4.0	b d	b d	9	1.0	5	2	b d	b d	6	5	8	20	20	20	19	3.0	22.0	10.0	3.0	12.0
V	10	11	10	7.0	6	25	b d	<5	10	16	16	b d	8	5	3	2	b d	5	7	<5	80	24.0	6.0	75.0
Cr	b d	b d	b c	<20	7	b d	b d	<20	3	b d	1	7	7	4	2	15	14	12	12	<20	60	<20	<20	200
Co	b d	b d	b c	67.0	b d	b d	b d	82.0	b d	b d	b d	b d	b d	n d	n d	n d	n d	n d	<1		4.0	1.0	8.0	80
La	n d	n d	n d	72.9	n d	n d	n d	25.6	17	9	85	38	24	38	5	38	33	32	91	105.0	38.0	67.5	37.3	43.1
Ce	n d	n d	n d	137.0	n d	n d	n d	67.6	119	147	155	200	108	85	55	n d	78	116		142.0	66.0	89.7	142.0	101.0
Pr	n d	n d	n d	15.7	n d	n d	n d	5.5	n d	n d	n d	n d	n d	n d	n d	n d	n d	n d	27.3	n d	15.8	11.2	12.6	
Nd	n d	n d	n d	53.2	n d	n d	n d	18.2	55	66	68	69	51	39	23	31	36	31	66	105.0	19.0	57.4	43.3	49.8
Sm	n d	n d	n d	10.9	n d	n d	n d	4.6	n d	n d	n d	n d	n d	n d	n d	n d	n d	n d	23.2	n d	11.7	13.3	12.5	
Eu	n d	n d	n d	1.03	n d	n d	n d	0.37	n d	n d	n d	n d	n d	n d	n d	n d	n d	n d	1.19	n d	1.39	0.53	1.30	
Gd	n d	n d	n d	10.4	n d	n d	n d	5.1	n d	n d	n d	n d	n d	n d	n d	n d	n d	n d	23.1	n d	10.4	15.6	12.9	
Tb	n d	n d	n d	1.8	n d	n d	n d	1.1	n d	n d	n d	n d	n d	n d	n d	n d	n d	n d	3.8	n d	1.6	3.7	2.4	
Dy	n d	n d	n d	11.1	n d	n d	n d	7.6	n d	n d	n d	n d	n d	n d	n d	n d	n d	n d	21.8	n d	10.3	25.0	14.3	
Ho	n d	n d	n d	2.3	n d	n d	n d	1.8	n d	n d	n d	n d	n d	n d	n d	n d	n d	n d	4.3	n d	2.0	5.7	2.8	
Er	n d	n d	n d	6.4	n d	n d	n d	5.7	n d	n d	n d	n d	n d	n d	n d	n d	n d	n d	11.7	n d	5.5	17.1	7.8	
Tm	n d	n d	n d	1.07	n d	n d	n d	1.12	n d	n d	n d	n d	n d	n d	n d	n d	n d	n d	1.81	n d	0.81	2.82	1.12	
Yb	n d	n d	n d	6.9	n d	n d	n d	8.4	n d	n d	n d	n d	n d	n d	n d	n d	n d	n d	10.9	n d	5.1	19.5	6.9	
Lu	n d	n d	n d	0.95	n d	n d	n d	1.24	n d	n d	n d	n d	n d	n d	n d	n d	n d	n d	1.50	n d	0.82	1.95	6.9	
Co	n d	n d	n d		n d	n d	n d		72	81	115	101	94	89	76	n d	n d	n d	n d		n d			
Cr	n d	n d	n d		n d	n d	n d		n d	n d	n d	n d	n d	n d	n d	n d	n d	n d	n d		n d			
Cs	n d	n d	n d	1.8	n d	n d	n d	2.4	n d	n d	n d	n d	n d	n d	n d	n d	n d	n d	2.1	n d	0.7	0.2	0.3	
Hf	n d	n d	n d	9.1	n d	n d	n d	3.7	n d	n d	n d	n d	n d	n d	n d	n d	n d	n d	14.2	n d	13.7	26.7	9.1	
Sb	n d	n d	n d	<0.2	n d	n d	n d	<0.2	n d	n d	n d	n d	n d	n d	n d	n d	n d	n d	<0.2	n d	<0.2	<0.2	<0.2	
Sc	n d	n d	n d	n d	n d	n d	n d	n d	16	8	11	11	16	15	15	14	13	19	n d	n d	18.0	7.0	<1	10.0
Ta	n d	n d	n d	4.3	n d	n d	n d	20.2	n d	n d	n d	n d	n d	n d	n d	n d	n d	n d	4.9	0.0	1.8	11.8	2.5	
Be	n d	n d	n d	n d	n d	n d	n d	n d	n d	n d	n d	n d	n d	n d	n d	n d	n d	n d	n d	n d	2.0	10.0	2.0	
Cd	n d	n d	n d	<0.5	n d	n d	n d	<0.5	n d	n d	n d	n d	n d	n d	n d	n d	n d	n d	<0.5	n d	<0.5		<0.5	
S	n d	n d	n d	0.0	n d	n d	n d	b d	n d	n d	n d	n d	n d	n d	n d	n d	n d	n d	b d	n d	b d	0.0	0.0	
Ge	n d	n d	n d	1.4	n d	n d	n d	1.9	n d	n d	n d	n d	n d	n d	n d	n d	n d	n d	2.0	n d	1.4	2.1	1.8	
Th	n d	n d	n d	30.2	n d	n d	n d	38.5	n d	n d	n d	n d	n d	n d	n d	n d	n d	n d	17.0	n d	12.1	31.6	3.4	
U	n d	n d	n d	5.6	13	18	110	13.1	80	70	60	70	100	80	80	90	60	50	70		3.9	4.0	1.7	0.8

Note n d not determined b d below detection limit XRF analyses for major and trace elements and INAA analyses for REEs and certain trace elements were done at the Regional Geochemical Center, Saint Mary's University, Halifax ICP-MS analyses were done by Activation Laboratories Ltd in Toronto according to their code 4Lithoresearch and code 4B1 packages Code 4Lithoresearch combines Fusion ICP for major elements and ICP/MS for trace elements whereas code 4B1 includes Digestion ICP for certain trace elements (Ni, Cu, Zn Ag)

Supplementary data Table S1 Whole rock geochemical analyses of representative granitic rocks of the Wentworth Pluton

Sample	9822	9823	9824	9827A	9827B	9830	9831	9832
Relative age	late dykes and pods	late dykes and pods	late dykes and pods	late fine-grained granite dyke	late fine-grained granite dyke	early granite, probable	early granite, probable	early granite, probable
Source	new data	new data	new data	new data	new data	new data	new data	new data
Analysis	ICP-MS	ICP-MS	ICP-MS	ICP-MS	ICP-MS	ICP-MS	ICP-MS	ICP-MS
Major elements (wt%)								
SiO_2	77 69	77 19	69 19	77 23	78 23	69 33	78 38	73 63
TiO_2	0 11	0 10	0 55	0 21	0 13	0 68	0 12	0 27
Al_2O_3	11 87	12 23	15 31	11 84	11 92	13 94	11 37	12 36
Fe_2O_3	0 87	0 99	2 77	2 37	1 51	3 75	2 46	2 35
MnO	0 00	b d	0 03	0 02	0 02	0 05	0 00	0 06
MgO	0 17	0 07	0 65	0 25	0 13	0 99	0 04	0 11
CaO	1 11	0 38	1 58	0 57	0 44	2 44	0 14	0 30
Na_2O	2 53	2 34	3 27	3 86	3 40	3 76	3 90	3 92
K_2O	5 37	6 95	6 51	3 70	4 90	4 76	4 11	4 91
P_2O_5	0 01	0 01	0 08	0 02	0 02	0 13	b d	0 03
LOI	0 11	0 08	0 19	0 26	0 13	0 47	0 02	0 06
Trace elements (ppm)								
Ba	462 0	291 0	795 0	113 0	64 0	376 0	60 0	212 0
Rb	85 0	133 0	107 0	152 0	226 0	58 0	153 0	214 0
Sr	137 0	100 0	213 0	63 0	36 0	141 0	21 0	30 0
Y	7 2	4 3	17 2	80 3	55 9	53 5	112 0	78 4
Zr	147 0	74 0	233 0	503 0	273 0	357 0	541 0	501 0
Nb	2 7	2 1	21 2	57 7	56 4	33 8	66 4	52 1
Th								
Pb	20 0	17 0	19 0	4 0	6 0	23 0	27 0	20 0
Ga	19 0	17 0	22 0	32 0	31 0	22 0	30 0	24 0
Zn	14 0	10 0	31 0	20 0	17 0	33 0	34 0	75 0
Cu	13 0	23 0	10 0	16 0	10 0	8 0	42 0	14 0
Ni	7 0	6 0	8 0	6 0	5 0	8 0	5 0	3 0
V	10 0	8 0	49 0	11 0	7 0	54 0	< 5	15 0
Cr	< 20	< 20	< 20	< 20	< 20	< 20	< 20	< 20
Co	1 0	3 0	6 0	3 0	2 0	22 0	< 1	1 0
La	69 6	32 5	26 4	73 2	33 2	35 1	47 2	52 5
Ce	135 0	60 5	48 6	175 0	97 2	78 9	123 0	129 0
Pr	12 6	5 8	5 0	18 7	9 4	10 0	14 9	13 6
Nd	38 0	17 8	17 3	64 8	33 3	39 6	57 6	49 5
Sm	5 1	2 5	3 3	13 9	8 4	9 9	16 5	11 7
Eu	1 04	0 81	1 72	0 43	0 33	1 32	0 38	0 57
Gd	2 9	1 6	3 0	12 2	8 0	10 1	17 0	11 3
Tb	0 3	0 2	0 5	2 4	1 7	1 8	3 5	2 3
Dy	1 4	0 8	2 9	14 8	10 9	10 6	21 6	14 3
Ho	0 2	0 1	0 6	3 1	2 3	2 1	4 6	3 0
Er	0 7	0 4	1 7	9 4	6 9	5 6	13 1	8 7
Tm	0 09	0 05	0 24	1 54	1 16	0 79	2 10	1 35
Yb	0 6	0 3	1 6	10 9	8 3	4 9	14 2	8 9
Lu	0 10	0 04	0 26	1 77	1 45	0 76	2 32	1 35
Co								
Cr								
Cs	0 4	0 3	1 0	2 3	2 4	0 1	0 6	3 1
Hf	5 3	2 7	6 6	13 0	8 5	9 4	15 8	13 0
Sb	< 0 2	< 0 2	< 0 2	< 0 2	< 0 2	< 0 2	< 0 2	< 0 2
Sc	< 1	< 1	3 0	2 0	1 0	7 0	< 1	2 0
Ta	0 2	0 1	1 7	6 6	5 8	1 6	6 3	4 7
Be	1 0	< 1	2 0	12 0	10 0	1 0	11 0	5 0
Cd	< 0 5	< 0 5	< 0 5	< 0 5	< 0 5	< 0 5	< 0 5	0 6
S	b d	0 0	0 0	b d	b d	0 1	0 0	b d
Ge	1 3	1 1	1 3	2 3	2 1	1 5	2 2	1 6
Th	32 1	25 4	10 4	25 5	19 7	3 9	16 9	21 7
U	1 5	1 2	1 2	5 2	4 4	1 0	5 3	4 1

Note n d not determined, b d below detection limit XRF analyses for major and trace elements and INAA analyses for REEs and certain trace elements were done at the Regional Geochemical Center, Saint Mary's University, Halifax ICP-MS analyses were done by Activation Laboratories Ltd in Toronto, according to their code 4Lithoresearch and code 4B1 packages Code 4Lithoresearch combines Fusion ICP for major elements and ICP/MS for trace elements, whereas code 4B1 includes Digestion ICP for certain trace elements (Ni, Cu, Zn, Ag)

Supplementary data Table S2 Sm-Nd isotope data for Wentworth Pluton, equivalent volcanic, and possible Neoproterozoic source rocks

Sample	SiO_2 (wt%)	$^{147}Sm/^{144}Nd$	$^{143}Nd/^{144}Nd$	$\varepsilon_{Nd(360)}$	Reference
Neoproterozoic rocks of the Cobequid Highlands					
Jeffers block					
812B	61.8	0 14300	0 51231	-3.93	Pe-Piper and Piper, 1998
449	73.2	0 09504	0 51221	-3.68	Pe-Piper and Piper, 1998
1347	43.3	0 13170	0 51267	3.62	Pe-Piper and Piper, 1998
1950	48.3	0 15230	0 51270	3.25	Pe-Piper and Piper, 1998
3709	54 2	0 13100	0 51261	2.48	Pe-Piper and Piper 1998
2106	63 9	0 16790	0 51254	-0.59	Pe-Piper and Piper, 1998
2865A	68.5	0 20228	0 51219	-9.00	Pe-Piper and Piper, 1998
3500	65 5	0 12568	0 51223	-4.70	Pe-Piper and Piper, 1998
Bass River Block					
3150	47.5	0 13890	0 51240	-1.99	Pe-Piper and Piper, 1998
3135	50.4	0 14080	0 51254	0.66	Pe-Piper and Piper, 1998
3171	71.1	0 08710	0 51229	-1.75	Pe-Piper and Piper, 1998
4152	73 1	0 11665	0 51129	-22.64	Pe-Piper and Piper, 1998
4156	70 1	0 11900	0 51235	-2.05	Pe-Piper and Piper, 1998
Late paleozoic rocks of the Cobequid Highlands					
Fountain Lake Group basalts					
4200	49.7	0 15030	0 51264	2.17	Pe-Piper and Piper, 1998
4232	46.9	0 14020	0 51278	5.37	Pe-Piper and Piper, 1998
5095	59.8	0 12700	0 51257	1.88	Pe-Piper and Piper, 1998
5010	61 6	0 14230	0 51256	0.98	Pe-Piper and Piper, 1998
3919	46.5	0 15120	0 51276	4.48	Pe-Piper and Piper, 1998
4601	48.0	0 16130	0 51273	3.43	Pe-Piper and Piper, 1998
50-3-5	47 1	0 15360	0 51274	3.98	Pe-Piper and Piper, 1998
6061	46 1	0 15060	0 51273	3.92	Pe-Piper and Piper, 1998
6069	6069	0 14760	0 51267	2.88	Pe-Piper and Piper, 1998
7723	45.9	0 16510	0 51281	4.81	Pe-Piper and Piper, 1998
Wentworth and Wyvern gabbros					
5053	47.2	0 13410	0 51274	4.87	Pe-Piper and Piper, 1998
2214	52 1	0 13529	0 51253	0.72	Pe-Piper and Piper, 1998
6387	46.9	0 14440	0 51270	3.62	Pe-Piper and Piper, 1998
6761	46 8	0 14410	0 51272	4.02	Pe-Piper and Piper, 1998
Late dykes					
7361	46.9	0 15280	0 51269	3.04	Pe-Piper and Piper, 1998
7081	43.4	0 14434	0 51263	2.25	Pe-Piper and Piper, 1998
4649	44 8	0 13935	0 51271	4.05	Pe-Piper and Piper, 1998
6357	47.3	0 15844	0 51269	2.78	Pe-Piper and Piper, 1998
Wentworth pluton granites					
4636	76.1	0 13378	0 51267	3.60	new data
4641	70	0 12494	0 51260	2.52	new data
5056	64.4	0 13313	0 51261	2.46	new data
6419	76 7	0 14737	0 51268	3.15	new data
6490	76 2	0 17041	0 51264	1.15	new data
6518	73 1	0 10240	0 51258	3.13	new data
7658	72 6	0 11487	0 51256	2.24	new data
7710	75.9	0 13595	0 51266	3.19	new data
7814	76.7	0 13820	0 51257	1.36	Pe-Piper and Piper 1998
35-7-1	74 9	n d	0 51261	~1.1	Pe-Piper and Piper 1998
36-5-1	74 8	n d	0 51261	~1.0	Pe-Piper and Piper, 1998
36-2-1	72 9	n d	0 51262	~2.5	Pe-Piper and Piper 1998
7290	76.3	0 12480	0 51263	3.15	Pe-Piper and Piper 1998
6074	70.7	0 13690	0 51261	2.21	Pe-Piper and Piper, 1998

113

CHAPTER 6: DISCUSSION

The most important points discussed in the previous chapters are summarized in this part of the thesis. Geochemical and mineralogical evidence from both studies are presented here unified, and compared with the existing literature as to provide the complete sequence of geological processes that formed the Wentworth granites and are responsible for their distinct geochemical character.

6 1 From Neoproterozoic to Late Paleozoic derivation of parent magma

Samarium-Neodymium isotope data from the Wentworth A-type granites suggest that they are derived from partial melting of a juvenile lower crust, with limited contamination by more evolved crustal material. Furthermore, the limited range of ε_{Nd} values of these granites (1 1 to 3 6) indicates an origin from an isotopically homogeneous source.

During Neoproterozoic subduction, the oldest rocks of the Avalonian juvenile crust were formed, represented in the surface by the arc sequences of the plutonic and volcanic rocks from the Jeffers Block (Pe-Piper and Piper, 1989) Compared to these rocks, the Wentworth granites present more isotopic similarities with the mafic lithologies rather that the felsic ones (Table S2) On the other hand, the Late Paleozoic gabbros and basalts have more primitive isotopic characteristics than their Neoproterozoic equivalents (Table S2) These indicate that the Wentworth Pluton was formed by melts derived from a source in the lower crust rather than Neoproterozoic crustal rocks

Rising of the asthenosphere from the mantle wedge, during subduction, resulted in the underplating of primitive melts in the base of the crust The presence of pargasite in Neoproterozoic mafic rocks (Pe-Piper, 1988) is evidence for F concentration in Neoproterozoic mafic magmas (Aoki et al , 1981) If this magma underplated gabbro at the base of the crust, this lower crust would also be enriched in F

Underplating of mafic magmas in the base of the Avalonian juvenile, F-enriched crust, created a crustal section similar to that recognized in supra-subduction ophiolites This section consists of gabbro and minor amounts of its trondhjemitic fractionates These felsic products would, thus, inherit the primitive isotopic signature of their gabbroic source

During Late Paleozoic, underplating of mafic melts during the extension of the Magdalen Basin (Marillier and Reid, 1990) and the synchronous extrusion of primitive flood basalts of substantial thickness (Dessureau et al , 2000) imply upwelling of the asthenosphere This provided the necessary high temperatures for anhydrous melting of the lower crust, during Late Paleozoic Frost and Frost (2010) argued that partial melting of a tonalitic to granodioritic source-rock could give rise to A-type granitic magmas The hypothesis that partial melting of the trondhjemitic fractionates is the source of the parent magma of the Wentworth granites, was tested in this study through geochemical modeling This geochemical model was based on the REE abundances of a produced melt, derived from batch partial melting (Wood and Fraser, 1976) of lower crustal lithologies (Table 5-1) As feldspar-dominated rocks, trondhjemites would give rise to a REE-enriched granitic magma with limited further fractionation Furthermore the high amounts of sodic plagioclase (oligoclase) (Nilsen et al , 2003), the presence of biotite and

fluorine would result in the production of an alkaline F-rich melt This melt would also present the relatively primitive isotopic characteristics, passed on from their mantle-derived source rocks

6 2 Latest Devonian Magma evolution and emplacement of the early Wentworth granites

The emplacement of the granitic parent magma in Late Paleozoic was almost synchronous with the gabbroic underplating beneath the Gulf of St Lawrence, related to the extension of the Magdalen Basin (Marillier and Verhoef, 1989) and with mafic intrusions in the Cobequid Highlands (Pe-Piper et al , 2004, Murphy et al , 2011) Furthermore, continental flood basalts were extruded from the Cobequid Shear Zone before and after the emplacement of the granites (Dessureau et al , 2000) Mixing of the granitic magma with pristine gabbro is inferred by a striking, bimodal distribution of Mg and co-variation of Cr and Ti in the Wentworth granites The fact that both low-Mg and high-Mg granites are F-enriched confirms that a mafic contribution was present from the onset of the plutonism

The Rockland Brook Fault was the major fault of the Cobequid Shear Zone during the Late Paleozoic (Miller et al , 1995) and the close spatial relationship between this fault and the Wentworth Pluton indicates that it was the major pathway for magma (Piper et al , 1993) The abundance of fluorine in the parent magma kept the REEs and rare metals in solution for prolonged periods by increasing the solubility of REE phosphates such as monazite and xenotime (Keppler, 1993) The high sodium amount in the parent granitic melt resulted in the formation of primary sodic amphiboles such as

116

arfvedsonite, ferrorichterite and katophorite, in which fluorine incorporated as well (Pe-Piper, 2007) The removal of fluorine from the magma during amphibole crystallization led to the fractionation of allanite and zircon with small amounts of Y, Hf and HREE

6 3 Early Carboniferous (Tournaisian) Gabbroic intrusion and formation of the Wentworth late granites

Geochronological data indicate that the gabbroic part of the Wentworth pluton is younger than the granites (Doig et al, 1996, Pe-Piper, 2004, Murphy et al, 2011) and it has been demonstrated that the gabbro remelted the early granites of the Wentworth Pluton (Koukouvelas et al, 2002) This later intrusion provided the necessary high temperatures for the crystallization of chevkinite-Ce, rather than allanite, in the late granites After the crystallization of allanite and chevkinite, the granitic magma became enriched in the middle and heavy REEs and thus hingganite-(Y) crystallized during late magmatic stages

During the anatexis of the early granites, the breakdown of the sodic amphiboles resulted in fluorine release (Pe-Piper, 2007, Schonenberger et al, 2006)) Furthermore, reheating of pyrite, present in the granites, resulted in its decomposition to hematite with release of SO_4 as a volatile phase (Bhargava et al, 2009) Fluorine and sulfur escaped the magma through the hydrothermal system which was developed after the emplacement of the late granites, mobilizing the LREE and HREE respectively (Rolland et al, 2003) Anatexis led to the late granitic magma being depleted in F (Koukouvelas et al, 2002)

6 4 Early Carboniferous (Tournaisian to Visean) Hydrothermal alteration of the granites

After the emplacement of the gabbro and the formation of the late Wentworth granites, the developed hydrothermal system circulated the REEs and rare metals by complexing with fluorine and sulfur Fluorine complexes with HREEs are more stable compared to those with LREE, which can be mobilized with sulfur (Rolland et al , 2003) This resulted in the formation of a variety of REE-rich hydrothermal minerals hosted in the Wentworth granites and the paragenetic sequence based on textural relationships allows an interpretation of the evolution of the hydrothermal fluids Such evidence include REE-rich epidote overgrowths (Figs 4-4) and 4-7a and b), patches of fersmite surrounding a corroded grain of samarskite (Figs 4-12c and d), hydroxylbastnasite-(Ce) forming along the rim of allanite-(Ce) (Fig 4-17), and grains of aeschynite-Y engulfing grains of titanite which itself alters to titania mineral (Fig 4-14)

The presence of late-magmatic hingganite-(Y) indicates that the magma was HREE-enriched during the late magmatic stages, so that these residual elements would also enrich the hydrothermal fluids Therefore, Y, Nb and HREEs were the first to achieve saturation in the fluids, forming samarskite-(Y) early in the paragenesis of secondary minerals, leaving, thus, the fluids with the more incompatible LREEs, complexed with sulfur This preferential complexing lead to the precipitation of a sequence of LREE-minerals after the formation of the Y-HREE-minerals Fersmite resulted from the alteration of samarskite-(Y) from these LREE fluids, whereas the hydrothermal alteration of magmatic allanite-(Ce) resulted in the formation of REE-rich hydrothermal epidote

A regional hydrothermal event occurred at the end of Visean (at 320-315 Ma), forty million years after the pluton emplacement This event resulted in circulation of carbon and sulfur-rich fluids (Wright, 1975) Such a composition of fluids could also promote REE (Rolland et al , 2003) and Ti mobility (Parnell, 2004) It is possible at that point that presence of carbonate ions in the fluids lead to the formation of the youngest mineral in the secondary mineral paragenesis, fluorine-bearing hydroxylbastnasite-(Ce) after allanite-(Ce) However, the La/Nd ratios suggest low concentrations of carbon (Rolland et al , 2003) and therefore the formation of this mineral is not necessarily related to this hydrothermal event but could be related to an earlier one, related to the granite emplacement This late event, however, is the only known event that could be related to Ti-mobility and therefore it is taken to be related to the breakdown of titanite to titania mineral and the formation of aeschynite-(Y)

It is, therefore, clear that the mineralogy and geochemistry of the Wentworth granites is the result of a complex magmatic history, and reflects several stages in both the generation of the parent magma and the evolution and emplacement of the granites The evolution of the Cobequid Shear Zone was a major factor that controlled the geochemical character of the Wentworth pluton a) providing the main pathway for alkaline-mantle-derived melts from the lower crust through the Rockland Brook Fault which was the major fault during Late Paleozoic and b) providing the necessary conditions for the development and circulation of hydrothermal fluids, in the area, for over a period of tens of millions of years

CHAPTER 7: CONCLUSIONS

The first question in this study was whether the early and late granites of the Wentworth Pluton have the same source and what was that source To address this question, all granites have been derived from the same source which has relatively homogeneous isotopic characteristics This source was juvenile Neoproterozoic trondhjemites, present in the lower crust as fractionation products of underplated gabbro, similar to those observed in supra-subduction ophiolitic sequences Melting of these rocks produced the parent granitic melt with limited contamination by more evolved Neoproterozoic upper crustal rocks Melting of this source was triggered by heat provided during the upwelling of the asthenosphere, combined with thinning of the crust, related to the synchronous extension of the Magdalen Basin in the Late Paleozoic This study introduces a new petrogenetic model for A-type granites which involves partial melting of a lower crust related to a pre-existing subduction system.

The later gabbroic intrusion caused anatexis of the early granites and released fluorine due to amphibole breakdown and sulfur by oxidation of pyrite Both elements escaped in the hydrothermal system, and thus, the late granitic magma was depleted in these elements Part of the granitic magma assimilated minor amounts of gabbro, resulting in a distinct group of granites with high Mg, Ti and Cr

The observed REE enrichment is genetically related to the Wentworth granites The parent magma was saturated in REEs as a result of its initial enrichment in F from the lower crust The presence of fluorine in the parent magma kept Zr in solution for prolonged periods and along with it, rare metals like Y, Th and Nb The crystallization of

chevkinite-(Ce), in the late granites, is a result of the heat provided by the intrusion of the later gabbro rather than a change in alkalinity of the granitic magma

The release of F and S to the hydrothermal system during the anatexis of the early granites played an important role in introducing the REEs and rare metals in the hydrothermal system. Fluorine and sulfur mobilized, by preferential complexing, the HREEs and LREEs, respectively Yttrium, along with the middle and heavy REE were the first metals to precipitate from these fluids, in the form of samarskite-(Y), causing a relative LREE enrichment in the fluid that was influenced by the presence of sulfur LREEs then precipitated, forming post-magmatic REE-rich epidote, fersmite and most probably hydroxylbastnasite-(Ce) Carbonate and sulfide-rich fluids were involved in a late regional phase of hydrothermal circulation at 320-315 Ma and may have been responsible for Ti and REE enrichment aeschynite-(Y) and titanite alteration to titania mineral could be related to this event The key factor in creating this unique, mainly hydrothermal, REE-enriched system was the magmatically-triggered anatectic processes

However, it is still unclear whether the distinct alkalinity of the Wentworth Pluton is a result of the proposed petrogenetic model or if this applies to other felsic intrusions in the shear zone Furthermore, additional work is needed on the extent of REE and rare metal enrichment to other coeval granitic plutons in the Cobequid Shear Zone Further work on the geochemistry and mineralogy of the other Late Paleozoic plutons in the region would be a significant step to better understand the regional magmatic system by testing the hypotheses applied for the Wentworth Pluton This could provide great improvement on both the existing petrogenetic models on A-type granites and on the understanding of the origin of REE magmatic enrichment

CHAPTER 8: REFERENCES

Abraham, A P G, Spooner E T C, 1995 Late Achaean regional deformation and structural controls on gold-quartz vein mineralization in the northwestern Slave Province, N W T, Canada Canadian Journal of Earth Sciences 32, 1132-1154

Aoki, K., Ishiwaka, K., Kanisawa, S, 1981 Fluorine geochemistry of basaltic rocks from continental and oceanic regions and petrogenetic application Contributions to Mineralogy and Petrology 76, 53-59

Armbruster, T, Bonazzi P, Akasaka, M, Bermanec, V, Chopin, C, Gieré, R, Heuss-Assbichler, S, Liebscher, A, Menchetti ,S, Pan, Y, Pasero, M, 2006 Recommended nomenclature of epidote-group minerals European Journal of Mineralogy 28, 551-567

Aurisicchio, C, De Vito, C, Ferrini, V, Orlandi, P, 2001 Nb-Ta oxide minerals from miarolitic pegmatites of the Baveno pink granite, NW Italy Mineralogical Magazine 65, 509-522

Bhargava, S K., Garg, A, Subasinghe, N D, 2009 In situ high-temperature phase transformation studies of pyrite Fuel 88, 988-993

Bonev, N, Stampfli, G, 2009 Gabbro, plagiogranite and associated dykes in the supra-subduction zone Evros ophiolites, NE Greece Geological Magazine 146, 72-91

Calder, J H, 1998 The Carboniferous evolution of Nova Scotia Geological Society of London, Special Publication 143, 261-302

Clark, J R , Williams-Jones, A E , 2004 Rutile as a potential indicator mineral for

metamorphosed metallic ore deposits Diversification of Mineral

Exploration of Quebec, final report, project SC2

Clarke, D B , MacDonald, M A , Tate, M C , 1997 Late Devonian mafic-felsic

magmatism in the Meguma Zone, Nova Scotia, in the nature of magmatism

in the Appalachian orogen, Geological Society of America Memoir 191,

107-127

Creaser, R A , Prince, R C , Wormald, R J , 1991 A-type granites revisited assessment

of a residual source model Geology 19, 163-166

Collins,,W J , Beams, S D , White, A J R , Chappell, B W , 1982 Nature and origin of

A-type granites with particular reference to Southeastern Australia

Contributions to Mineralogy and Petrology 80, 189–200

Dall'Agnol, R , Scaillet, B , Pichavant, M , 1999 An experimental study of a lower

Proterozoic A-type granite from the eastern Amazonian Craton, Brazil

Journal of Petrology 40, 1673-1698

Dessureau, G , Piper, D J W , Pe-Piper, G , 2000 Geochemical evolution of earliest

Carboniferous continental tholeiitic basalts along a crustal-scale shear zone

southwestern Maritimes Basin, eastern Canada Lithos 50, 27-50

Doig, R , Murphy, J B , Pe-Piper, G , Piper D J W , 1996 U-Pb geochronology of the late

Paleozoic plutons, Cobequid Highlands, Nova Scotia, Canada Evidence for

late Devonian emplacement adjacent to the Meguma-Avalon terrane

boundary in the Canadian Appalachians Geological Journal 31, 179-188

Donohoe, H V , Wallace, P I , 1982 Geological map of the Cobequid Highlands, Nova

    Scotia Scale 1 50000 Nova Scotia Department of Mines and Energy

Douce, A E , 1997 Generation of metaluminous A-type granites by low-pressure melting

    of calc-alkaline granitoids Geology 25, 743-746

Dunning, G R , Barr, S M , Giles, P S , McGregor, D C , Pe-Piper, G , Piper, D J W ,

    2002 Chronology of Devonian to early Carboniferous rifting and igneous

    activity in southern Magdalen Basin based on U-Pb (zircon) dating

    Canadian Journal of Earth Sciences 39, 1219-1237

Drake, M J , Weill, D F , 1972 New rare earth elements standards for electron

    microprobe analysis Chemical Geology 10, 179-181

Eby, G N , 1992 Chemical subdivision of the A-type granitoids petrogenetic and

    tectonic implications Geology 20, 641-644

Ercit, T S , 2005 Identification and alteration trends of granitic-pegmatite-hosted

    (Y,REE,U,Th)-(Nb,Ta,Ti) oxide minerals a statistical approach Canadian

    Mineralogist 43, 1291-1303

Ewing, R C , 1975 The crystal chemistry of complex niobium and tantalum oxides IV

    The metamict state discussion American Mineralogist 60, 728-733

Forster, H J , 2000 Cerite-(Ce) and thorian synchysite-(Ce) from the Niederbobritzsch

    granite, Erzgebirge, Germany Implications for the differential mobility of

    the LREE and Th during alteration Canadian Mineralogist 38, 67-79

Frost, C D , Frost, B R , 2010 On ferroan (A-type) granitoids their compositional

    variability and modes of origin Journal of Petrology 52, 39-53

Frost, B R , Barnes, C G , Collins, W J , Argulus, R J , Ellis, D J , Frost, C D , 2001 A geochemical classification for granitic rocks Journal of Petrology 42, 2033-2048

Gower, D P , 1988 Geology and genesis of uranium mineralization in subaerial felsic volcanic rocks of the Byers Brook Formation and the comagmatic Hart Lake granite, Wentworth area, Cobequid Highlands, Nova Scotia MSc Thesis, Memorial University of Newfoundland

Hibbard, J , Waldron, J W F , 2009 Truncation and translation of Appalachian promontories mid-Paleozoic strike-slip tectonics and basin initiation Geology 37, 487–490

Holtstam, D , Andersson, U B , 2007 The REE minerals of the Bastnas-type deposits, south-central Sweden Canadian Mineralogist 45, 1073-1114

Irvine, T N , Baragar, W R A , 1971 A guide to the chemical classification of the common rocks Canadian Journal of Earth Sciences 8, 523–548

Jiang, N , 2006 Hydrothermal alteration of chevkinite-(Ce) in the Shuiquangou syenitic intrusion, northern China Chemical Geology 227, 100-112

Jung, S , Mezger, K , Hoernes, S , 1998 Petrology and geochemistry of syn- to post-collisional metaluminous A-type granites—a major and trace element and Nd–Sr–Pb–O-isotope study from the Proterozoic Damara Belt, Namibia Lithos 45, 147-175

Keppler, H , 1993 Influence of fluorine on the enrichment of high field strength trace elements in granitic rocks Contributions to Mineralogy and Petrology 114, 479-488

Krauskopf, K B , Bird D K., 2003 Introduction to geochemistry, third edition Published

    by McGraw-Hill Science Engineering

Koukouvelas, I , Pe-Piper, G , Piper, D J W , 1996 Pluton emplacement by wall-rock

    thrusting, hanging wall translation and extensional collapse latest Devonian

    plutons of the Cobequid Fault Zone, Nova Scotia, Canada Geological

    Magazine 133,285-298

Koukouvelas, I , Pe-Piper, G , Piper, D J W , 2002 The role of dextral transpressional

    faulting in the evolution of an early Carboniferous mafic-felsic plutonic and

    volcanic complex Cobequid Highlands, Nova Scotia, Canada

    Tectonophysics 348, 219-246

Koukouvelas, I , Pe-Piper, G , Piper, D J W , 2006 The relationship between length and

    width of plutons, within the crystal-scale Cobequid Shear Zone, northern

    Appalachians, Canada Earth Sciences 95, 963-976

Kuiper, K F , Deino, A , Hilgen, F J , Krijgsman, W , Renne, P R , Wijbrans, J R , 2008

    Synchronizing rock clocks of earth history Science 320, 500-504

Landenberger, B , Collins, W J , 1996 Derivation of A-type granites from a dehydrated

    charnockitic lower crust evidence from the Chaelundi Complex, Eastern

    Australia Journal of Petrology 37, 145-170

Liferovich, R P , Mitchell, R H , 2005 Composition and paragenesis of Na-, Nb- and Zr-

    bearing titanite from Khibina, Russia and crystal-structure data from

    synthetic analogues Canadian Mineralogist 43, 795-812

Loiselle, M C , Wones, D , 1979 Characteristics and origin of anorogenic granites

    Geological Society of America, Abstracts with Programs 11, 468

126

Macdonald, R , Belkin, H E , 2002 Compositional variation in minerals of the

chevkinite-group Mineralogical Magazine 66, 1075-1098

Macdonald, R , Marshall, A S , Dawson, J B , Hinton, R W , Hill P G , 2002

Chevkinite-group minerals from salic volcanic rocks of the East African

Rift Mineralogical Magazine 66, 287-299

MacHattie, T G , 2009 Magmatism, alteration and polymetallic mineralization in late

Devonian to early Carboniferous felsic volcanic and plutonic rocks of the

eastern Cobequid Highlands Nova Scotia Department of Natural Resources,

Mineral Resources Branch, Report of Activities, 65-75

Maniar, P D , Piccoli, P M , 1989 Tectonic discrimination of granitoids Geological

Society of America Bulletin 101, 635-643

Marillier, F , Verhoef, J , 1989 Crustal thickness under the Gulf of St Lawrence,

northern Appalachians, from gravity and deep seismic data Canadian

Journal of Earth Sciences 26, 1517-1532

Marillier, F , Reid, I , 1990 Crustal underplating beneath the Carboniferous Magdalen

Basin (Eastern Canada) evidence from seismic reflection and refraction, in

Pinet, B , Bois, C (Eds),The Potential of Deep Seismic Profiling for

Hydrocarbon Exploration Éditions Technip, Paris, pp 209-218

Meintzer, R E , Mitchell, R S , 1988 The epigene alteration of allanite Canadian

Mineralogist 26, 945-955

Miller, B V , Nance, R D , Murphy, J B , 1995 Kinematics of the Rockland Brook

fault, Nova Scotia implications for the interaction of the Meguma and

Avalon terranes, Journal of Geodynamics 19, 253-270

Mirza, T A , Sabah, A I , 2007 Origin of plagiogranites in the Mawat ophiolite complex,

Kurdistan region, NE Iraq Journal of Kirkuk University-Scientific Studies

2, no 1

Murphy, J B 2002 Geochemistry of the Neoproterozoic metasedimentary Gamble Brook

Formation, Avalon Terrane, Nova Scotia evidence for a rifted-arc

environment along the west Gondwanan margin of Rodinia Journal of

Geology 110, 407–419

Murphy, J B , Nance, R D , 2002 Nd-Sm isotopic systematics as tectonic tracers an

example from West Avalonia, Canadian Appalachians Earth Science Reviews 59,

77–100

Murphy, J B , Waldron, J W F , Kontak, D J , Pe-Piper, G , Piper, D J W , 2011 Minas

Fault Zone Late Paleozoic history of an intra-continental orogenic

transform fault in the Canadian Appalachians Journal of Structural Geology

33, 312-328

Nance, R D , Murphy, J B , Keppie, J D , 2002 A Cordilleran model for the evolution of

Avalonia Tectonophysics 352, 11-31

Nilsen, O , Bjørn, S , Roberts, D , Corfu, F , 2003 U-Pb geochronology and

geochemistry of trondhjemites and a norite pluton from the SW Trondheim

Region, central Caledonides Norges Geologiske Undersøkelse Bulletin 441,

5-16

Oliveira, D C , Dall'Agnol, R , Mesquita Barros, C E , Oliveira, M A , 2009 Geology,

geochemistry and magmatic evolution of the Paleoproterozoic, anorogenic

oxidized A-type Redenção granite of the Jamon suite, eastern Amazonian

Craton, Brazil Canadian Mineralogist 97, 1441-1468

Orris, G , Grauch R I , 2002 Rare earth element mines, deposits, and occurrences U S

Geological Survey, Open-file report 02-189

Parnell, J , 2004 Titanium mobilization by hydrocarbon fluids related to sill intrusion in

a sedimentary sequence, Scotland Ore Geology Reviews 24, 155-167

Pearce, J A., Harris, N W , Tindle, A G , 1984 Trace element discrimination diagrams

for the tectonic interpretation of granitic rocks Journal of Petrology 25,

956-983

Pe-Piper, G , 1988 Calcic amphiboles of mafic rocks of the Jeffers Brook plutonic

complex, Nova Scotia, Canada American Mineralogist 73, 993-1006

Pe-Piper, G , 1998 The Devonian- Carboniferous Wentworth plutonic complex (Folly

Lake and Hart Lake-Byers Lake plutons) of the central Cobequid Highlands,

Nova Scotia Geological Survey of Canada, open file report 3373

Pe-Piper, G, 2007 Relationship of amphibole composition to host-rock geochemistry

the A-type gabbro-granite Wentworth pluton, Cobequid Shear Zone, eastern

Canada European Journal of Mineralogy 19, 29-38

Pe-Piper, G , Murphy, J B 1989 Petrology of the Late Proterozoic Folly River

Formation, Cobequid Highlands, Nova Scotia a continental rift within a

volcanic arc environment Atlantic Geology 25, 143–151

Pe-Piper, G , Piper, D J W , 1989 The upper Hadrynian Jeffers Group, Cobequid

Highlands, Avalon zone of Nova Scotia A back-arc volcanic complex

Geological Society of America Bulletin 101, 364-376

Pe-Piper, G , Piper, D J W , 1998 Geochemical evolution of Devonian-Carboniferous

igneous rocks of the Magdalen basin, Eastern Canada Pb and Nd isotope

evidence for mantle and lower crustal sources Canadian Journal of Earth

Sciences 35, 201-221

Pe-Piper, G , Piper, D J W ,2002 A synopsis of the geology of the Cobequid Highlands,

Nova Scotia Atlantic Geology 38,145-160

Pe-Piper, G , Piper, D J W 2005 Bedrock Geological Map of the Wentworth Area

(parts of NTS sheets 11E/05, 11E/06, 11E/11 and 11E/12), Cobequid

Highlands, Nova Scotia, scale 1 50 000 Nova Scotia Department of Natural

Resources, Mineral Resources Branch, open file map, OFM ME 2005-116

Pe-Piper, G , Piper, D J W , Clerk, S B , 1991 Persistent mafic igneous activity in an A-

type granite pluton, Cobequid Highlands, Nova Scotia Canadian Journal of

Earth Sciences 28, 1058-1072

Pe-Piper, G , Zeeman, M , Piper, D J W , 1996 Magmatic relationships between the

mafic and felsic phases of the Folly Lake pluton, Cobequid Highlands, Nova

Scotia, in Current Research 1996-D, Geological Survey of Canada, 27-33

Pe-Piper, G , Reynolds, P H, Nearing, J , Piper, D J W , 2004 Early Carboniferous

deformation and mineralization in the Cobequid Shear Zone, Nova Scotia

an ^{40}Ar/^{39}Ar geochronology study Canadian Journal of Earth Sciences 41,

1425-1436

Piper, D J W , Pe-Piper, G , Loncarevic, B D , 1993 Devonian-Carboniferous igneous

intrusions, and their deformation, Cobequid Highlands, Nova Scotia

Atlantic Geology 29, 219-232

Piper, D J W , Dessureau, G , Pe-Piper, G , 1999 Occurrence of early Carboniferous

high-Zr rhyolites, Cobequid Highlands, Nova Scotia Temperature effect of

a contemporaneous mafic magma Canadian Mineralogist 37, 619-634

Rabbia, O M , Hernández, L B , French, D H , King, R W , Ayers J C , 2009 The El

Teniente porphyry Cu-Mo deposit from a hydrothermal rutile perspective

Mineralium Deposita 44, 849-866

Ridolfi, F , Renzulli, A , MacDonald, R , Upton, B G J , 2006 Peralkaline syenite

autoliths from Kilombe volcano, Kenya Rift Valley evidence for

subvolcanic interaction with carbonatitic fluids Lithos 91, 373-392

Rolland, Y , Cox S , Boullier, A , Pennacchioni, G , Mancktelow, N , 2003 Rare earth

and trace element mobility in mid-crustal shear zones insights from the

Mont Blanc Massif (Western Alps) Earth and Planetary Science Letters

214, 203-219

Rollinson, H R , 1993 Using geochemical data evaluation, presentation, interpretation

Longman, UK [Co-published by J Wiley & Sons Inc in the USA]

Rubatto, D , Muntener, O , Barnhoorn, A , Gregory, C , 2008 Dissolution-reprecipitation

of zircon at low-temperature, high-pressure conditions (Lanzo Massif,

Italy) American Mineralogist 93, 1519-1529

Rubin, J N , Henry, C D , Price, J G , 1989 Hydrothermal zircons and zircons

overgrowths, Sierra Blanca Peaks, Texas American Mineralogist 74, 865-

869

Saveleva, V B , Karmanov, N S , 2008 REE minerals of alkaline metasomatic rocks in

the Main Sayan Fault Geology of Ore Deposits 50, 681-696

Scaillet, B , Macdonald, R , 2001 Phase relations of peralkaline silicic magmas and

petrogenetic implications Journal of Petrology 42, 825-845

Schmitt, A K., Trumbull, R B , Dulski, P , Emmermann, R , 2002 Zr-Nb-REE

mineralization in peralkaline granites from the Amis Complex, Brandberg

(Namibia) Evidence for magmatic pre-enrichment from melt inclusions

Economic Geology 97, 399-413

Schonenberger, J , Marks, M , Wagner, T , Markl, G , 2006 Fluid-rock interaction in

autoliths of agpaitic nepheline syenites in the Ilímaussaq intrusion, South

Greenland Lithos 91, 331-351

Seifert, W , Rhede, D , Forster, H -J ,Thomas, R , 2009 Accessory minerals as

fingerprints for the thermal history and geochronology of the Caledonian

Rumburk granite Neues Jahrbuch für Mineralogie Abhandlungen 186, 215-

233

Škoda, R , Novák, M , 2007 Y, REE, Nb, Ta, Ti-oxide (AB_2O_6) minerals from REL-

REE euxenite-subtype pegmatites of the Třebíč Pluton, Czech Republic,

substitutions and fractionation trends Lithos 95, 43-57

Tilley, D B , Eggleton, R A , 2005 Titanite low-temperature alteration and Ti mobility

Clays and Clay Minerals 53, 100-107

Tollo, R P , Aleinikoff, J N , Bartholomew, M J , Rankin, D W , 1996 Neoproterozoic A-

type granitoids of the central and southern Appalachians intraplate

magmatism associated with episodic rifting of the Rodinian supercontinent

Precambrian Research 128, 3-38

Tomaschek, F , Kennedy, A K., Villa, I M , Lagos, M , Ballhaus, C , 2003 Zircons from

Syros, Cyclades, Greece-Recrystallization and mobilization of zircon during

high-pressure metamorphism Journal of Petrology 44, 1977-2003

Troll, V R , Sachs, P M , Schmincke, H U , Sumita, M , 2003 The REE-Ti mineral

chevkinite in comenditic magmas from Gran Canaria, Spain a SYXRF-

probe study Contributions to Mineralogy and Petrology 145, 730–741

Uher, P , Ondrejka, M , Konečný, P , 2009 Magmatic and post-magmatic YREE-Th

phosphate, silicate and Nb-Ta-Y-REE oxide minerals in A-type metagranite

an example from the Turčok massif, western Carpathians, Slovakia

Mineralogical Magazine 73, 1009-1025

Vazquez, J A , Reid, M R , 2004 Probing the accumulation history of the voluminous

Toba magma Science 305, 991-994

Vlach, S R F , Gualda, G A R , 2007 Allanite and chevkinite in A-type granites and

syenites of the Graciosa Province, southern Brazil Lithos 97, 98-121

Wang, R C , Wang, D Z , Zhao, G T , Lu, J J , Chen ,X M , Xu S J , 2001 Accessory

mineral record of magma-fluid interaction in the Laoshan I- and A-type

granitic complex, eastern China Physics and Chemistry of the Earth 26,

835-849

Whalen, J B , Currie, K L , Chappell, B W , 1987 A-type granites geochemical

characteristics, discrimination and petrogenesis Contributions to

Mineralogy and Petrology 95, 407-419

Whalen, J B , Jenner, J A , Longstaffe, F J , Robert, F , Gariépy, C , 1996 Geochemical

and isotopic (O, Nd, Pb and Sr) constraints on A-type granite petrogenesis

based on the Topsails igneous suite, Newfoundland Appalachians Journal of Petrology 97, 1463-1489

Whitney, D L , Evans B W , 2010 Abbreviations for names of rock-forming minerals American Mineralogist 95, 185-187

Wood, S A , Ricketts, A , 2000 Allanite-(Ce) from the Eocene Casto granite, Idaho Response to hydrothermal alteration The Canadian Mineralogist 38, 81-100

Wood, B J , Fraser, D G , 1976 Elementary thermodynamics for geologists Oxford University Press, London, 303p

Wright, J D , 1975 Iron deposits of Nova Scotia Nova Scotia Department of Natural Resources, Economic Geology Series 75 (1), 154

Wu, F , Sun, D , Li, H , Jahn, B , Wilde, S , 2002 A-type granites in northeastern China age and geochemical constraints on their petrogenesis Chemical Geology 187, 143-173

Zachariah, J K , Balakrishnan, S , Rajamani, V , 1997 Significance of Sm-Nd isotopr sustematics in crustal genesis A case of Archean metabasalts of the eastern Dharwar Craton Procambrian Indian Academic Sciences, 106, 361-367